

**Charles University
Faculty of Medicine in Hradec Králové**

**15th INTERNATIONAL MEDICAL
POSTGRADUATE CONFERENCE**



**New Frontiers in the Research
of Ph.D. Students**

Conference of Medical Schools



**Hradec Králové
November 22 – 23, 2018**

**Charles University
Faculty of Medicine in Hradec Králové**



**15th INTERNATIONAL MEDICAL
POSTGRADUATE CONFERENCE**

New Frontiers in the Research of Ph.D. Students

Conference of Medical Schools

November 22 – 23, 2018

Organized by
Charles University, Faculty of Medicine in Hradec Králové

Supported by
Specific Research Projekt no. 260400

Under the Auspices of His Magnificence
Rector of the Charles University
Tomáš Zima

Hradec Králové
Educational Centre of the Faculty of Medicine
Location: University Hospital

Table of content

General Information	5
Dean's Welcome	7
Programme Overview	8
Scientific Programme	9
Evaluation Committee	12
Presentations	14
Author's Index	127

Organizing Committee

Miroslav Červinka
Jiří Mandáček

Editor:
Miroslav Červinka

Technical Assistance:
Petra Malá

The publication has undergone neither linguistic editing nor proof reading.
It is printed from the author's e-mail correspondence.

GENERAL INFORMATION

Venue:

Educational Centre (Výukové centrum)
Charles University, Faculty of Medicine
University Hospital (Fakultní nemocnice) Hradec Králové

Conference Office:

The conference office is to be set up for information and registration at the Educational Centre in the area of the University Hospital at the following opening hours:

Thursday, November 22, 10:00 – 17:20

Friday, November 23, 9:00 – 15:40

Official Language:

English

Presentation Time:

Lecture 15 min

Discussion 5 min

Accommodation of Participants:

Hotel U Královny Elišky
Malé náměstí 117/10
500 03 Hradec Králové 3

WELCOME



Dear participants of this conference, dear friends and colleagues,

It is my great pleasure to welcome you to the 15th International Medical Postgraduate Conference held in the Educational Center of the Faculty of Medicine of Charles University in Hradec Králové on November 22 – 23, 2018.

One of the main objectives of this event is to facilitate the exchange of knowledge and information not only for young researchers, but for all of us. Personal contacts allow us to compare our acquired experience, and to sort and specify the huge flow of information from many sources. This year's conference programme covers many different aspects of medical science and, as always, we are hoping to create an interactive meeting by fostering discussions and debates between participants across all medical fields and disciplines.

Thirty-two students from different European countries nominated by their Universities are taking part in this conference and I am honoured and delighted by their presence.

During the two days of the competition, an international panel of experts will assess the scientific level of the submitted works, their presentation, as well as the ability of students to defend their views and respond to the arguments of others.

The competitors judged the best by the panel of experts will receive a financial award. From my point of view, however, every one, all participants, should be considered as winners, because active participation in an international conference is the most important thing and therefore a victory for them.

Finally I would like to complete my welcome address by another important announcement. International conferences are not only a chance to compare our scientific results and clinical skills but an occasion to meet all together as well. That's why, in addition to the outstanding scientific programme, allow me to invite you, all the participants, to the social events of this conference.

I sincerely hope you will all enjoy the scientific meeting and your short time in our beautiful city as much as possible!

Prof. Jiří Mandáček, M.D., Ph.D.,

dean of the Faculty

PROGRAMME OVERVIEW

Thursday – November 22, 2018

10:00 – 10:30	Meeting of the Evaluation Committee	Seminar room 4
10:30 – 11:00	Opening of the Conference	Main Lecture Hall
11:00 – 12:40	Presentations I (1-5)	Main Lecture Hall
12:40 – 13:40	Lunch	Seminar room 1
13:40 – 15:20	Presentations II (6 – 10)	Main Lecture Hall
15:20 – 15:40	Coffee break	Seminar room 1
15:40 – 17:20	Presentations III (11 – 15)	Main Lecture Hall
20:00 – 22:00	Social dinner	Hotel U Královny Elišky

Friday – November 23, 2018

9:00 – 11:00	Presentations IV (16 – 21)	Main Lecture Hall
11:00 – 11:20	Coffee break	Seminar room 1
11:20 – 13:00	Presentations V (22 – 26)	Main Lecture Hall
13:00 – 14:00	Lunch	Seminar room 1
14:00 – 15:40	Presentations VI (27–31)	Main Lecture Hall
15:40 – 16:40	Meeting of Evaluation Committee	Seminar room 4
19:30 – 22:00	Social evening, Awards, Closing ceremony	Medical Library – Portico Hall

SCIENTIFIC PROGRAMME

THURSDAY, NOVEMBER 22

Part I

Chairperson: Jan Čáp

- 11:00 **Babić A. (Zagreb, Croatia):** Cognitive and Metabolic Effects of Oral Galactose in Streptozotocin-induced Rat Model of Sporadic Alzheimer's Disease
- 11:20 **Baldwin L. (Hull, United Kingdom):** Development of a Gut-on-a-chip Model for the Study of Inflammatory Bowel Diseases
- 11:40 **Boudriot E. (Dresden, Germany):** The Role of Ve-cadherin Expression in Triple Negative Breast Cancer Cells for Lymphatic and Vascular Extravasation
- 12:00 **Branco P. (Porto, Portugal):** Brain Mapping with Resting-state FMRI: A Novel Approach to Presurgical Planning
- 12:20 **Cesneková D. (Martin, Slovak Republic):** Fluoxetine Monotherapy and Augmentation Treatment in Adolescent Depression – our Clinical Experience.

Part II

Chairperson: Stanislav Mičuda

- 13:40 **Fulová M. (Bratislava, Slovak Republic):** Legionella SPP. in the Hospital's Water System - Infection Risk and Prevention
- 14:00 **Janovičová E. (Bratislava, Slovak Republic):** Deoxyribonuclease Activity in Animal Model of Sepsis
- 14:20 **Kakhniashvili T. (Tbilisi, Georgia):** Serum Vascular Endothelial Growth Factor in the Course of Microangiopathy in Obstructive Sleep Apnea Comorbid Type 2 Diabetes Patients
- 14:40 **Kántás B. (Pécs, Hungary):** Examination of Somatostatin 4 Receptor Agonists in Mouse Models of Neuropathic Pain, Anxiety and Depression-like Behavior
- 15:00 **Kaňtoch A. (Krakow, Poland):** Mortality Risk Factors among Institutionalized Geriatric Population

SCIENTIFIC PROGRAMME

Part III

Chairperson: Emil Rudolf

- 15:40 **Koucký V. (Prague, Czech Republic):** Dysfunction of HPV16-specific CD8+ T Cells Infiltrating Oropharyngeal Cancer in Relation to the Expression of TIM-3 and PD-1
- 16:00 **Kovács Á. (Pécs, Hungary):** Age Dependent Neuronal Activation of Stress Centers in Acute and Chronic Stress Models in the Rat
- 16:20 **Nadareishvili I. (Tbilisi, Georgia):** Complementary and Alternative Medicine Practice and Healthcare Integration in Georgia
- 16:40 **Nová Z. (Martin, Slovak Republic):** Exogenous Surfactant and Pulmonary Homeostasis in an Animal Model of LPS-induced Acute Lung Injury
- 17:00 **Obermayer G. (Vienna, Austria):** Natural IgM Antibodies Protect from Microvesicle-driven Thrombosis.

FRIDAY, NOVEMBER 23

Part IV

Chairperson: Jan Laco

- 9:00 **Pálek R. (Plzeň, Czech Republic):** Reconstruction of Portal Vein by Different Types of Allogeneous Venous Grafts in Experimental Model of Pancreaticoduodenectomy
- 9:20 **Antunes I. (Porto, Portugal):** Emergence of Multidrug Cross-resistance between Agricultural and Human Antifungals in Clinically Relevant Species of *Aspergillus* and *Candida*
- 9:40 **Rejlová K. (Prague, Czech Republic):** Low Hox Gene Expression in PML-RARA-positive Leukemia Results from Suppressed Histone Demethylation
- 10:00 **Rickett N. (Liverpool, United Kingdom):** Determinants of Patient Survival Following Acute Ebola Virus Infection
- 10:20 **Riedel K. (Dresden, Germany):** Sex Differences in Adrenergic Vessel Tone - A Role of Estrogen
- 10:40 **Rosendorf J. (Plzeň, Czech Republic):** Fortification of Anastomosis on Gastrointestinal Tract with Nanomaterials

SCIENTIFIC PROGRAMME

Part V

Chairperson: Petr Hejna

- 11:20 **Skořepa P. (Hradec Králové, Czech Republic):** Influence of Specific Parenteral Nutrition on Selected Metabolic Markers and their Consequences
- 11:40 **Stojková P. (Hradec Králové, Czech Republic):** HU Protein Plays an Important Role in Virulence of Francisella Tularensis
- 12:00 **Šilhán D. (Prague, Czech Republic):** Brief and Easy Visual Parietal Atrophy Score (PAS) on Brain Magnetic Resonance Imaging in Early-onset Alzheimer's Disease
- 12:20 **Škrott Z. (Olomouc, Czech Republic):** Alcohol-abuse Drug Disulfiram Targets Cancer via p97 Segregase Adaptor NPL4
- 12:40 **Štark T. (Brno, Czech Republic):** Peripubertal Cannabidiol Treatment Prevents Molecular and Behavioral Changes in Neurodevelopmental Model of Schizophrenia

Part VI

Chairperson: Milan Kaška

- 14:00 **Ůbachs J. (Maastricht, the Netherlands):** Gut Microbiota Composition and Short-chain Fatty Acid Levels in Human Cancer Cachexia: A Pilot Study
- 14:20 **van der Kroft G. (Maastricht, the Netherlands):** “Radiomics” Features in Body Composition Imaging Associated with Muscle Wasting and Poor Survival after Pancreatic Cancer Resection
- 14:40 **Wenzina J. (Vienna, Austria):** Inhibition of P38 RE-expresses E-cadherin and Prevents Vascular Invasion in Melanoma
- 15:00 **Wilkinson H. (Hull, United Kingdom):** A Mechanistic Role for CXCR2-Mediated Cellular Senescence in Diabetic Wound Repair
- 15:20 **Praňnická A. (Hradec Králové, Czech Republic):** Alternation of Bile Acid Homeostasis by Iron Overload in Rats

EVALUATION COMMITTEE

Chairperson: **Miroslav Červinka**

Dean Emeritus
Charles University, Faculty of Medicine
Hradec Králové, the Czech Republic

Members: **Margarethe Geiger**

Head of Department of Vascular Biology and Thrombosis
Research Centre of Physiology and Pharmacology
Medical University of Vienna, Austria

John Greenman

Professor of Tumour Immunology
Head of School of Biological, Biomedical and Environmental Sciences
University of Hull, the United Kingdom

Gabor Kovacs

Professor Emeritus
A Regular Member of the Hungarian Academy of Sciences
Chairman of the Doctoral Council of the Hungarian Academy of Sciences
Faculty of Medicine, University of Pécs, Hungary

Zdravko Lacković

Professor of Pharmacology
Council of the Croatian Agency for Science and Higher Education Deputy Dean
for Ph.D. Programme and Director of Ph.D. Programme
'Biomedicine and Health Sciences' President of ORPHEUS
EC Member of AMSE - Association of Medical Schools in Europe University
of Zagreb Medical School, Croatia

Thorsten Liebers

Head of Representative Office for Construction and Laboratory Affairs
Faculty Administration
Faculty of Medicine Carl Gustav Carus, Dresden, Germany

Deolinda Lima

Professor of Molecular Cell Biology, Histology and Embryology
Director of Experimental Biology Department
Director of Department for Research and Graduate Studies
Faculty of Medicine, University of Porto, Portugal

EVALUATION COMMITTEE

Peter Soeters

Professor Emeritus of Surgery (Gastroenterology and Clinical Nutrition)
Former President of the International Association for Surgical Metabolism
and Nutrition (IASMEN)

Chairman of the European Society of Parenteral and Enteral Nutrition
(ESPEN)

Maastricht University Medical Centre, the Netherlands

EMERGENCE OF MULTIDRUG CROSS-RESISTANCE BETWEEN AGRICULTURAL AND HUMAN ANTIFUNGALS IN CLINICALLY RELEVANT SPECIES OF *ASPERGILLUS* AND *CANDIDA*.

Isabel Cristina Santos Silva de Faria Ramos Antunes

Microbiology, Department of Pathology, Faculty of Medicine of the University of Porto

Tutor: Acácio Agostinho Gonçalves Rodrigues

Introduction

The spectrum of human pathogens and infectious diseases is continuously changing through evolution and changes in the way human populations interact with the surrounding environment. Modern agriculture - large scale, industrialized and fungicide dependent - was one of the turning points in the history of infectious diseases. Over the last three decades, clinically important fungi have become more prevalent, mostly due to medical advances that allow the survival of an increasing number of immunocompromised patients. Fungicides with similar chemical structure and mode of action to those used in medicine are also widely used in agriculture. Thus, a few years ago a critical problem emerged – the development of cross-resistance between agricultural and human antifungals in clinically relevant species of *Aspergillus* and *Candida*.

Aim

To provide insights whether the acquisition of resistance can arise from nature and impact on human health.

Methods

The epidemiological landscape of fungal invasive infections (IFI) is changing. Therefore, a national multicentric surveillance study was carried out. From this study important clinical and demographic data were obtained as well as information regarding the *in vitro* susceptibility profile of yeast isolates.

From this newly assembled collection, we determined its *in vitro* susceptibility to the most frequently used agricultural fungicides. Susceptible isolates of *C. albicans*, *C. parapsilosis* and *C. glabrata* to both clinical and agricultural antifungals were selected; an *in vitro* induction assay was started with one of the most frequently used fungicide in Portugal, Prochloraz (PCZ), at sub-inhibitory concentrations. Afterwards, the induced molecular resistance mechanisms were unveiled. The following work recreated a similar approach with another clinical relevant fungal pathogen – *A. fumigatus*. Two clinical and one environmental isolate were daily incubated with sub-inhibitory concentrations of PCZ.

Results

Candida albicans remains the most frequent agent of IFI but the prevalence of non-*albicans* keeps increasing. The overall susceptibility rates ranged from 84 to 98% to azoles and 74 to 97% to echinocandins. During the 90 days of induction, minimal inhibitory concentration (MIC) values

were continuously evaluated and after 10 days all *Candida* species revealed a 32 to 64 times higher MIC value to the inducer fungicide. *C. glabrata* was the only species developing cross-resistance to clinical azoles after 60 days of exposure to the agricultural fungicide. After screening the most common azole resistance mechanisms, we found that PCZ selective pressure triggered an upregulation of the ATP Binding Cassette multidrug transporter genes and the transcription factor, *PDR1*. Single point mutation previously associated with azole resistance was described in *PDR1* while in *ERG11* gene several synonymous single nucleotide polymorphisms were found (**Figure 1**). Regarding *A. fumigatus* induction assays, the 3 isolates developed a progressive increment of PCZ MIC value comparatively to the initially determined value. Concerning the clinical azoles, cross-resistance was developed for all isolates. Besides the emergence of cross-resistance, we found that PCZ exposure caused marked morphological colony changes, both macroscopically (**Figure 2**) and microscopically (**Figure 3**), revealing the progressive nonappearance of conidiation during the assay.

Discussion

From the epidemiological study we obtained information about clinical and demographic data and about cryptic species such as *C. parapsilosis* and *C. glabrata* complex, along with the resistance rate to clinical antifungals. From the 240 fungemia episodes we have calculated an incidence of 2.4 per 1.000 admissions, being 86% nosocomial (2.1/1.000). In fact, in most surveillance studies, healthcare-associated fungemia in hospitalized patients remains the main source of infection, frequently representing more than 80% of the cases (1,2). *C. albicans* remained the leading agent of fungemia; however, in agreement with findings in Europe the proportion of non-*C. albicans* is rising (3). We did not find any isolate of the sibling species of *C. glabrata*, *C. nicavariensis* or *C. bracarensis*; only *C. glabrata* sensu stricto was found. The same occurred in similar studies from Mediterranean countries and Brazil (4, 5-7). The susceptibility testing results were interpreted by two distinct protocols, CLSI and EUCAST, and the overall susceptibility rates ranged from 74 to 97% for echinocandins and from 84% to 98% for azoles. It is noteworthy that resistance rates discrepancies between protocols were found with *C. albicans* and *C. glabrata* for echinocandins and with *C. parapsilosis* and *C. tropicalis* for azoles.

The induction assays with *Candida* species showed that cross-resistance emerged following the selective pressure of PCZ but only for *C. glabrata*. So we considered that a specific genetic event should be responsible for such cross-resistance, not only because it was a permanent susceptible-to-resistant phenotype alteration but also because *C. glabrata* is a haploid cell and for that reason cells might be more prone to genetic modifications. We screened the most common azole resistance associated genes, namely: *CDR1*, *PDH1*, *YOR1*, *SNQ2*, *PDR1* and *ERG11*. In contrast to several other studies reporting genetic alterations responsible for azole resistance, to the best of our knowledge, this was the first time that genes like *YOR1* and *PDH1* have such an upregulation, 66.8 and 45.5 fold overexpressed, respectively. All the other genes were also upregulated but to a smaller extent while no *ERG11* contribution was verified. Can this particular genetic context of resistance only arise from a fungicide azole selective pressure? These results provide possible explanations for the worldwide increasing prevalence of *C. glabrata* and its poor clinical outcome. Following the induction assays with *A. fumigatus* we found that besides the emergence of cross-resistance, PCZ exposure also caused marked morphological colony changes, both macro and microscopically. Although these pigmentation changes had already been

described as a consequence of azole exposure, yet no clear explanation is given of such phenomena besides one report by Varansi and colleagues suggesting that it possible may be due to the fact that azoles bind to a phytochrome-like regulatory molecule, inhibiting the initiation and development of conidiophores in *Aspergillus* species (8).

Conclusions

Our studies suggest that the use of fungicides in nature may cause serious problems in the medical field – the potential of saprophyte fungi to suffer the selective pressure of fungicides with very similar mode of action to those antifungals used to treat humans and develop cross-resistance and then compromise clinical efficacy of medical drugs.

Summary

This work highlights the occurrence of antifungal cross-resistance between agriculture and medicine involving two relevant species of *Aspergillus* and *Candida*. Both pathogenic fungi showed that agricultural fungicides are capable of inducing cross-resistance to medical antifungals.

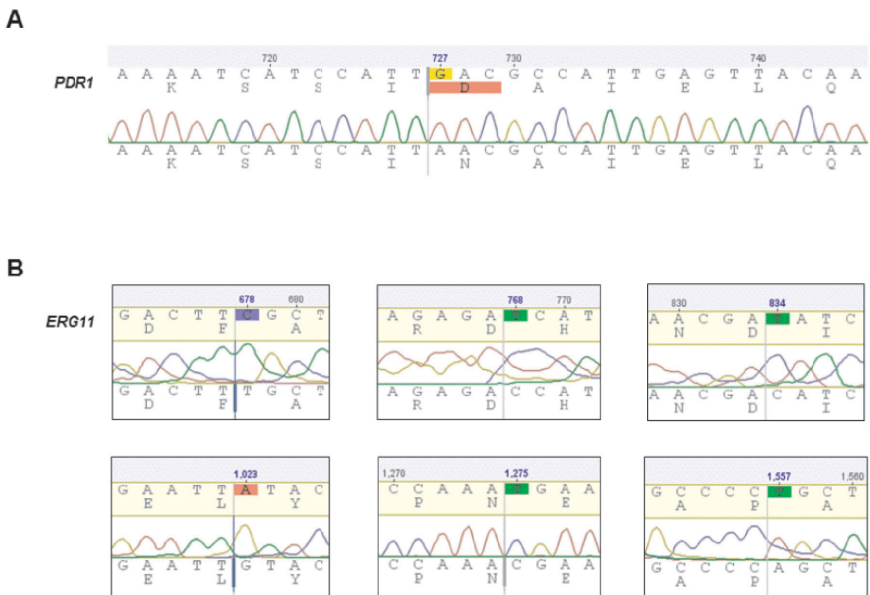


Figure 1. Single Nucleotide Polymorphisms (SNPs) found in *Candida glabrata* *PDR1* and *ERG11* genes. **(A)** *PDR1* missense mutation G727A results in the amino acid change D243N. **(B)** Several synonymous SNPs throughout the *ERG11* gene.

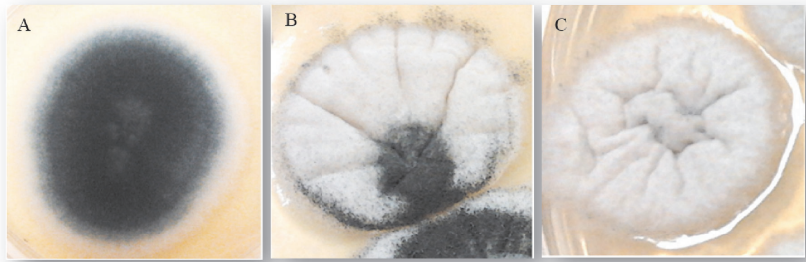


Figure 2. Photographs of Sabouraud dextrose agar plates showing macroscopic morphological changes of colonies of *A. fumigatus* following exposure to subinhibitory concentration of PCZ. **A.** Initial morphological aspect (control). **B.** After fifteen days. **C.** After thirty days.

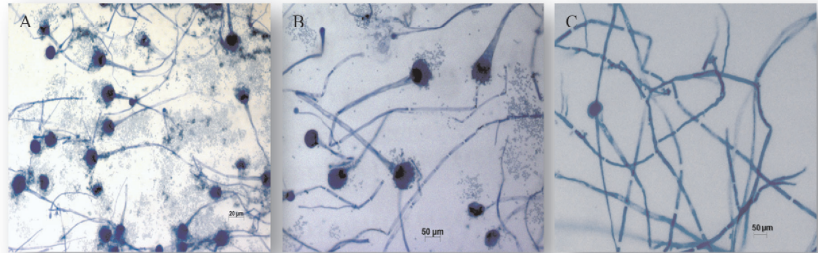


Figure 3. Photomicrographs of *A. fumigatus* colonies using the cellotape flag technique preparation with lactophenol cotton blue staining. Microscopic morphological changes in the development of conidiation of *A. fumigatus* following exposure to subinhibitory concentration of PCZ. **A.** Initial morphological aspect (control). **B.** After fifteen days. **C.** After thirty days.

References

1. Asmundsdottir LR, Erlendsdottir H, Gottfredsson M: Nationwide study of candidemia, antifungal use, and antifungal drug resistance in Iceland, 2000 to 2011. *Journal of clinical microbiology* 2013, 51(3):841-848.
2. Das I, Nightingale P, Patel M, Jumaa P: Epidemiology, clinical characteristics, and outcome of candidemia: experience in a tertiary referral center in the UK. *International journal of infectious diseases : IJID : official publication of the International Society for Infectious Diseases* 2011, 15(11):e759-763.
3. Arendrup MC: Epidemiology of invasive candidiasis. *Current opinion in critical care* 2010, 16(5):445-452
4. Peman J, Canton E, Quindos G, Eraso E, Alcoba J, Guinea J, Merino P, Ruiz-Perez-de-Pipaon MT, Perez-del-Molino L, Linares-Sicilia MJ *et al*: Epidemiology, species distribution

- and in vitro antifungal susceptibility of fungaemia in a Spanish multicentre prospective survey. *The Journal of antimicrobial chemotherapy* 2012, 67(5):1181-1187.
5. Bonfietti LX, Szeszs MW, Chang MR, Martins MA, Pukinskas SR, Nunes MO, Pereira GH, Paniago AM, Purisco SU, Melhem MS: Ten-year study of species distribution and antifungal susceptibilities of *Candida* bloodstream isolates at a Brazilian tertiary hospital. *Mycopathologia* 2012, 174(5-6):389-396.
 6. Tosun I, Akyuz Z, Guler NC, Gulmez D, Bayramoglu G, Kaklikkaya N, Arikan-Akdagli S, Aydin F: Distribution, virulence attributes and antifungal susceptibility patterns of *Candida parapsilosis* complex strains isolated from clinical samples. *Medical mycology* 2013, 51(5):483-492.
 7. Esposto MC, Prigitano A, Romeo O, Criseo G, Trovato L, Tullio V, Fadda ME, Tortorano AM, Group FW: Looking for *Candida nivariensis* and *C. bracarensis* among a large Italian collection of *C. glabrata* isolates: results of the FIMUA working group. *Mycoses* 2013, 56(3):394-396.
 8. Varanasi NL, Baskaran I, Alangaden GJ, Chandrasekar PH, Manavathu EK: Novel effect of voriconazole on conidiation of *Aspergillus* species. *International journal of antimicrobial agents* 2004, 23(1):72-79.

COGNITIVE AND METABOLIC EFFECTS OF ORAL GALACTOSE IN STREPTOZOTOCIN-INDUCED RAT MODEL OF SPORADIC ALZHEIMER'S DISEASE

Ana Babić Perhoč

Department of Pharmacology, University of Zagreb School of Medicine and Research Centre of Excellence for Fundamental Clinical and Translational Neuroscience, Croatian Institute for Brain Research, Zagreb, Croatia

Co-authors: A. Knezović, J. Osmanović Barilar, R. Bagarić, V. Farkaš, M. Šalković-Petrišić

Tutor: Melita Šalković-Petrišić

Introduction

Sporadic Alzheimer's disease (sAD) is associated with dysfunction of the brain insulin receptor signaling (1) and decreased glucose metabolism and energy in the brain (2) which have become new targets in sAD therapeutic strategy. D-galactose, a C-4-epimer of D-glucose, could be considered as an alternative source of energy but can also stimulate secretion of glucagon-like peptide 1 (GLP-1) (3), an incretin which stimulates insulin release and has its own neuroprotective activity (4). Our preliminary research in a streptozotocin-induced (STZ-icv) rat model of sAD demonstrated that one month of oral galactose treatment initiated immediately after STZ-icv administration successfully prevented the development of STZ-icv induced cognitive deficits (5). With this research we aimed to explore if oral galactose treatment could improve already developed cognitive deficit in the STZ-icv rat model and which mechanisms might be involved.

Methods

Two-month oral galactose treatment (200 mg/kg/day) was initiated 1 month (Exp 1/early sAD stage) and 4 months (Exp 2/medium sAD stage) after STZ/buffer-icv injection (3 mg/kg) in 3-months old male Wistar rats (10 animals per group). Cognitive performance was tested by Morris Water Maze (MWM) and Passive Avoidance (PA) test. The level of GLP-1 (active/total), insulin, glucose and galactose was measured by ELISA immunoassay in plasma and cerebrospinal fluid (CSF). Brain glucose metabolism was measured *in vivo* by [18F]-fluorodeoxyglucose positron emission tomography (FDG-PET) scanning (6). Data was analyzed by Kruskal-Wallis, followed by Mann-Whitney U test ($p < 0.05$).

Results

STZ-treated animals showed cognitive decline in both experiments compared to their respective control (-85% PA, +93% MWM/Exp1 (Figure 1); -78% PA, +71% MWM/Exp 2; $p < 0.05$), while galactose treatment successfully improved cognitive deficit only in Exp 1 (+349% PA, -36% MWM; $p < 0.05$). FDG-PET scan indicated a time-dependent mild decrement in glucose metabolism in the brain of STZ-treated rats compared to the controls in both experiments (-3% Exp 1; -12% Exp 2) which was increased (+14% Exp 1; +38% Exp 2) by oral galactose treatment in STZ-icv rats (Figure 2). The level of active GLP-1 was found decreased in plasma of STZ-treated rats

compared to the controls only in Exp 1 (-51%, $p < 0.05$) which was normalized by galactose treatment (+70%, $p < 0.05$) (Figure 3). Compared to the untreated controls, galactose-treated control rats demonstrated decreased levels of active GLP-1 in plasma (-80%, $p < 0.05$) and total GLP-1 in CSF (-31%, $p < 0.05$) in Exp 1 only. Plasma and CSF insulin levels were remained unchanged regardless the treatment in both experiments.

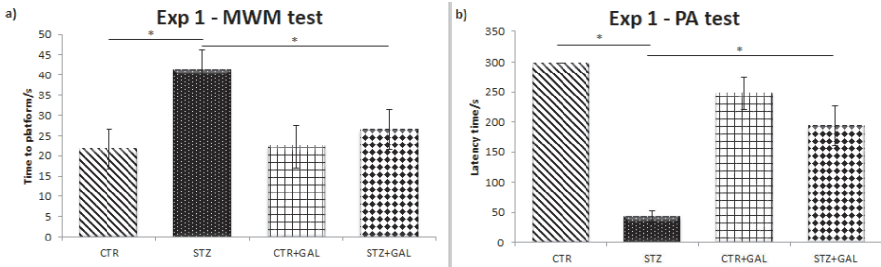


Figure 1. Oral galactose treatment normalizes cognitive deficits induced by intracerebroventricular administration of streptozotocin. Oral galactose treatment (200 mg/kg/day in a drink ad libitum) started 1 month after the STZ-icv injection and lasted 2 months. Cognitive performance was measured at the end of galactose treatment. a) Each bar represents mean \pm SEM of the time spent to reach the platform in the probe trial of MWM test (day 6) (* $p < 0.05$) N = 10 per group. (b) Each bar represents post-shock latency time measured by Passive Avoidance (PA) test. Values are expressed as mean \pm SEM. N = 10 per group. Data were analysed by non-parametric Kruskal-Wallis one-way ANOVA test followed by a Mann Whitney U test (* $p < 0.05$). CTR = control animals (buffer-icv treatment); STZ = streptozotocin-icv-treated animals; CTR+GAL = control animals treated (buffer-icv treatment) with 2-month oral galactose treatment; STZ+GAL = streptozotocin-icv-treated animals treated with 2-month oral galactose treatment.

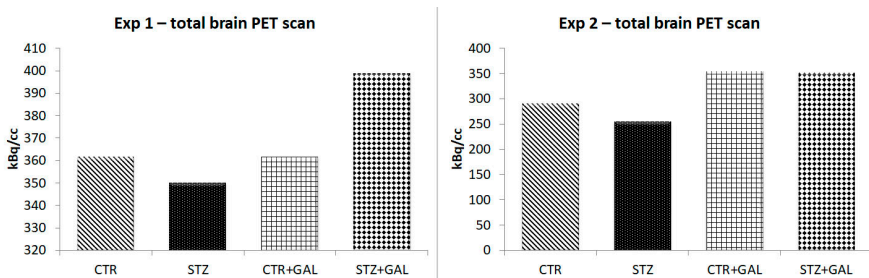


Figure 2. Glucose uptake using FDG as a radiotracer in streptozotocin-treated animals subjected to chronic oral galactose treatment. Regions of interest were selected and analyzed by PMOD software for indication of glucose uptake/metabolism rate. The bars represent calculated kBq/cc for total brain. N = 2 animals per group. CTR = control animals (buffer-icv treatment); STZ = streptozotocin-icv-treated animals; CTR+GAL = control animals treated (buffer-icv treatment) with 2-month oral galactose treatment; STZ+GAL = streptozotocin-icv-treated animals treated with 2-month oral galactose treatment.

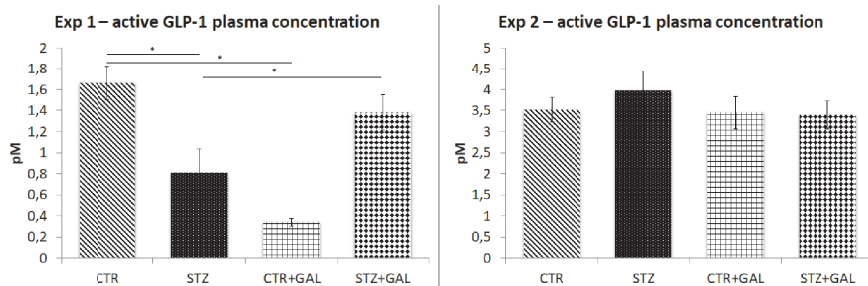


Figure 3. Active glucagon-like peptide-1 concentration in plasma after chronic galactose treatment. Active GLP-1 levels were measured by ELISA immunoassay. Values are expressed as mean \pm SEM. N = 10 per group. Data were analysed by non-parametric Kruskal-Wallis one-way ANOVA test followed by a Mann Whitney U test (* $p < 0.05$). CTR = control animals (buffer-icv treatment); STZ = streptozotocin-icv-treated animals; CTR+GAL = control animals treated (buffer-icv treatment) with 2-month oral galactose treatment; STZ+GAL = streptozotocin-icv-treated animals treated with 2-month oral galactose treatment.

Discussion and Conclusion

Our preliminary results indicate that 2-month oral galactose treatment has a potential to normalize previously developed cognitive deficits in a STZ-icv rat model in early but not in medium-stage of experimental sAD. The mechanism of this cognitive improvement in early sAD stage might be the stimulation of GLP-1-mediated effects, as shown by increments in total/active GLP-1 plasma levels found previously decreased only in early stage of sAD in the STZ-icv rat model. Since oral galactose-induced improvement in brain glucose metabolism in the STZ-icv rat model was manifested both in early and medium stage of diseases, this mechanism is likely a minor contributor to the beneficial effects of oral galactose on cognitive impairment.

Acknowledgement: Supported by the Croatian Science Foundation; HRZZ-IP-09-2014-4639.

Summary

Oral galactose treatment normalizes previously developed cognitive deficits in early-stage, but not in medium-stage experimental sporadic Alzheimer's disease induced by intracerebroventricular streptozotocin administration.

References

1. De La Monte SM, Tong M. Brain metabolic dysfunction at the core of Alzheimer's disease. *Biochem Pharmacol.* 2014; 88, 548–59.
2. Baker LD, Cross DJ, Minoshima S, Belongia D, Watson GS, Craft S. Insulin resistance and Alzheimer-like reductions in regional cerebral glucose metabolism for cognitively normal adults with prediabetes or early type 2 diabetes. *Arch Neurol.* 2011; 68, 51–7.
3. Baggio LL, Drucker DJ. Biology of Incretins: GLP-1 and GIP. *Gastroenterology.* 2007; 132, 2131–57.
4. Salcedo I, Tweedie D, Li Y, Greig NH. Neuroprotective and neurotrophic actions of glucagon-like peptide-1: An emerging opportunity to treat neurodegenerative and cerebrovascular disorders. *Br J Pharmacol.* 2012; 166, 1586–99.
5. Salkovic-Petrisic M, Osmanovic-Barilar J, Knezovic A, Hoyer S, Mosetter K, Reutter W. Long-term oral galactose treatment prevents cognitive deficits in male Wistar rats treated intracerebroventricularly with streptozotocin. *Neuropharmacology.* 2014; 77, 68–80.
6. Sempere Roldan P, Chereul E, Dietzel O, Magnier L, Pautrot C, Rbah L, et al. Raytest ClearPET™, a new generation small animal PET scanner. *Nucl Instruments Methods Phys Res Sect A Accel Spectrometers, Detect Assoc Equip.* 2007; 571, 498–501.

DEVELOPMENT OF A GUT-ON-A-CHIP MODEL FOR THE STUDY OF INFLAMMATORY BOWEL DISEASES

Lydia Baldwin

Faculty of Life Sciences (Biomedical science), University of Hull

Co-authors: A. Iles, J. Greenman, N. Pamme, C.E. Dyer

Tutor: C.E. Dyer

Co-tutors: J. Greenman, N. Pamme

Introduction

Inflammatory bowel diseases (IBD) are chronic conditions characterised by inflammation of the gut wall arising from an uncontrolled immune response and leading to damage of the epithelial barrier lining the intestinal wall. IBD is currently not curable. Furthermore, the role of the gut microbiome in disease progression and the wider systemic and neural effects is poorly defined. Improved human-relevant laboratory models are therefore required to support further understanding of the disease¹. Established models either involve animal testing or use cell lines which provide limited information and are often poorly represent the *in vivo* environment. An alternative for current models is the use of microfluidics and organ-on-chip technology to culture cell lines in a 3D culture under flow conditions². Here we describe the design, manufacture and initial characterisation of a dual-flow microfluidic chip device to model the gut and the blood brain barrier for the investigation of the effect of IBD on the intestinal and neural systems.

Aim

To design, fabricate and characterise a dual-flow microfluidic device which can model both the gut and the blood-brain barrier providing improved clinical and physiological relevance over existing models. To ascertain whether the effects of gut inflammation on the blood-brain-barrier (BBB) can be modelled on chip.

Methods

A dual channel chip was designed, with two independent flow streams separated by a semi-permeable membrane, which allows for the co-culture of cell lines either side of the membrane (Figure 1). CACO2 cells, a colonic cell line, were seeded on the device to model the gut on-chip and cultured for up to 96 h with an applied flow rate of 4 μ L/min (0.4 dyne/cm²). Cell viability and barrier integrity were analysed using Trans-Endothelial Electrical Resistance (TEER) measurements. The effluent was tested for biomarkers of cell viability and function, such as cell death using lactate dehydrogenase (LDH) release. Cell viability was assessed using fluorescein diacetate/propidium iodide (FDA/PI) live/dead staining and further characterisation was undertaken by immunohistochemical staining. To model the gut-brain axis, the gut-chip was connected to a second chip containing endothelial cells (ea.hy926) modelling the blood-brain-barrier (figure 2). Cell viability on the gut-brain axis model was assessed using FDA/PI live dead cell stain.

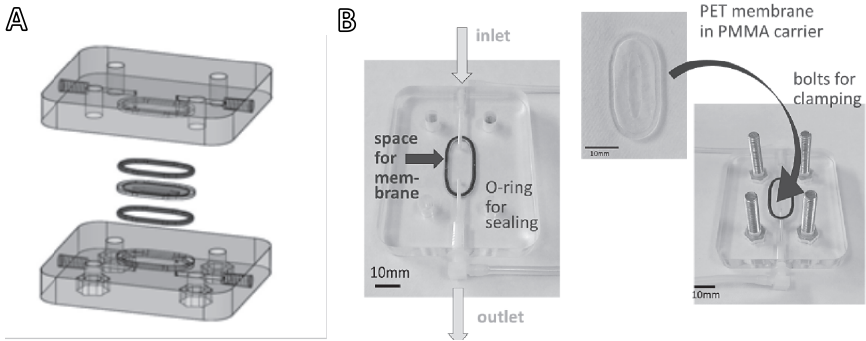
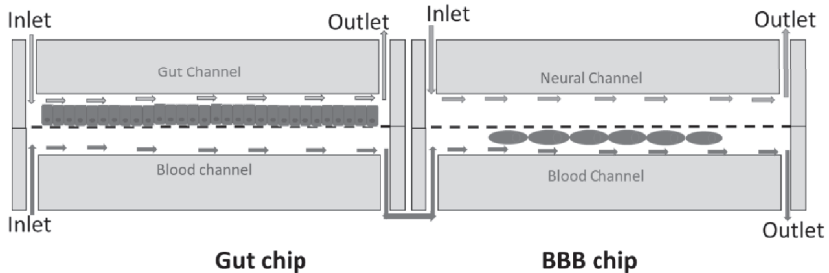


Figure 1 Chip design. (A) Expanded diagram of the microfluidic chip device showing the two outer polycarbonate chambers with inlets and outlets, the O-rings providing for sealing the carrier which contains the PET membrane. (B) Images of dismantled device showing the outer chambers and the placement of the membrane within the chambers. Figure 1 Chip design. (A) Expanded diagram of the microfluidic chip device showing the two outer polycarbonate chambers with inlets and outlets, the O-rings providing for sealing the carrier which contains the PET membrane. (B) Images of dismantled device showing the outer chambers and the placement of the membrane within the chambers.



- Chamber 1: Gut cell line (CAC02)
- Chamber 1: blank membrane
- Chamber 2: Blank membrane
- Chamber 2: Endothelial cell line (ea.hy926)

Figure 2 Schematic of the gut-brain axis on chip. The connection of the gut chip to the BBB chip was maintained via flow of medium from the gut chip to the BBB chip

Results

Comparison of cells grown under static and flow conditions was undertaken using LDH assay and staining techniques (Figure 3). Cell viability was maintained for 72 h on chip, with comparable cell viability to the static cell cultures. The development of tight junction proteins was monitored with the use of ZO-1 antibody stain. It was found that within 48 h of culture on chip, cells expressed the tight junction proteins at the cell boundary indicating that the cells are maintaining adherence to the membrane where they are seeded and maintaining cell barrier properties.

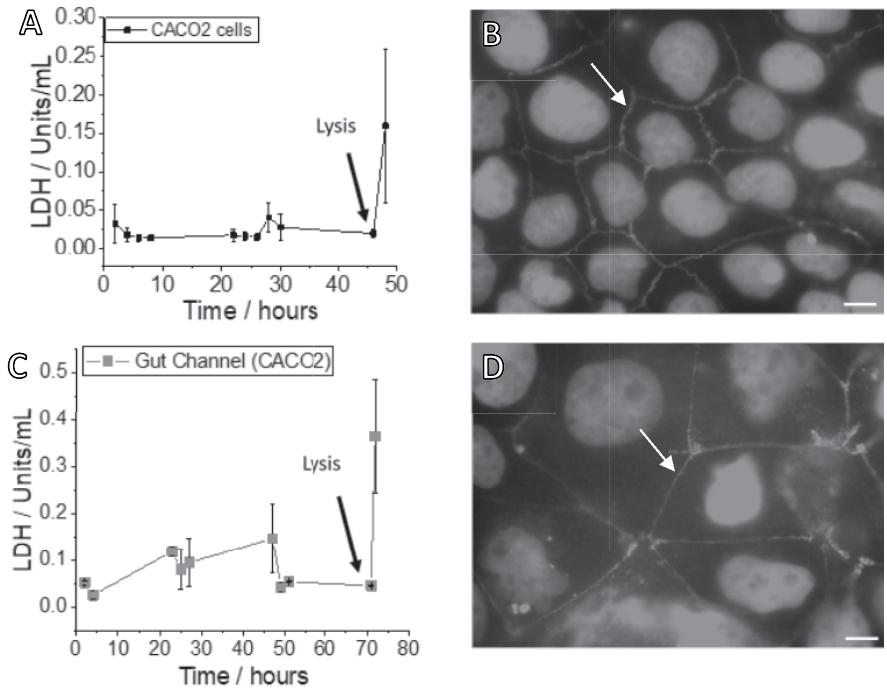


Figure 3 A) LDH release measured from supernatant sampled from cells cultured on a static plate, $n=3$. B) ZO-1 stain for tight junction proteins (indicated by arrowhead) for CACO2 cells grown under static culture conditions for 48 h, imaged at $\times 100$ magnification on a fluorescent microscope. Scale bar indicates $10\mu\text{m}$. C) LDH release measured from effluent collected from gut chip run at a flow rate of $4\mu\text{L}/\text{min}$ $n=3$. D) ZO-1 stain for tight junction proteins (indicated by arrowhead) for CACO2 cells cultured on chip for 48 h imaged at $\times 100$ magnification on a fluorescent microscope. Figure 3 A) LDH release measured from supernatant sampled from cells cultured on a static plate, $n=3$. B) ZO-1 stain for tight junction proteins (indicated by arrowhead) for CACO2 cells grown under static culture conditions for 48 h, imaged at $\times 100$ magnification on a fluorescent microscope. Scale bar indicates $10\mu\text{m}$. C) LDH release measured from effluent collected from gut chip run at a flow rate of $4\mu\text{L}/\text{min}$ $n=3$. D) ZO-1 stain for tight junction proteins (indicated by arrowhead) for CACO2 cells cultured on chip for 48 h imaged at $\times 100$ magnification on a fluorescent microscope

Discussion

The gut chip has shown to maintain CACO2 cell viability for at least 72 h while maintaining key epithelial cell barrier characteristics. The use of flow within the microfluidic chip system also allowed for cells to be cultured under more physiologically relevant conditions through the application of shear stress to the cells.

Conclusions

Preliminary work has successfully established a dual channel chip to model the gut, while allowing for reliability and ease of use. Following initial validation of the chip using cell lines, future work will progress to incorporate full thickness gut biopsy tissue slices on the chip in place of cell lines to allow for a more clinically relevant model.

Summary

Modelling of human organs for biomedical research is currently limited. Animal models provide limited human relevance and traditional cell line models provide limited data. The use of microfluidic chip devices aims to overcome the limitations of existing static cell models. To achieve a more physiologically and clinically relevant model of the gut, a dual flow microfluidic device was designed, fabricated and tested. Results demonstrated that the microfluidic device allows for culture of cell lines while maintaining key characteristics of the cells. Future work will progress the gut chip to incorporate full thickness gut biopsy tissue slices instead of cell lines improving clinical relevance. The chip will subsequently be assessed for effects of the gut and gut-brain axis under normal and inflamed conditions.

References

1. Carding, S. *et al.* (2015) Dysbiosis of the gut microbiota in disease. *Microb Ecol Health Dis*, 26, 26191
2. Dawson, A., *et al.* (2016) A microfluidic chip-based model for the study of full thickness human intestinal tissue using dual flow. *Biomicrofluidics*, 10(6), 064101.

Acknowledgments

I would like to acknowledge Dr Allam and the Allam Trust for sponsorship of this work and the collaboration of Prof S. Carding (Quadram Institute, Norwich).

THE ROLE OF VE-CADHERIN EXPRESSION IN TRIPLE NEGATIVE BREAST CANCER CELLS FOR LYMPHATIC AND VASCULAR EXTRAVASATION

Elisabeth T. A. Boudriot

Division of Medical Biology, Department of Psychiatry and Psychotherapy,
Faculty of Medicine Carl Gustav Carus, TU Dresden, Dresden, Germany

Co-authors: T.T.P. Nguyen, M.L. Moskopp, H.J. Schnittler, A. Deussen, G. Breier

Tutor: Prof. Dr. Georg Breier

Introduction and aim

Breast cancer is the prevalent cancer type among women. 10-20% are classified as aggressive triple-negative breast cancer (TNBC). TNBC represents a therapeutic challenge because it does not respond to conventional drugs targeting estrogen, progesterone, or HER2 receptors. A basic understanding of this cancer type's pathology is needed to advance breast cancer diagnosis and therapy. It is the aim of this project to further elucidate the oncogenic role of vascular endothelial cadherin (VE-cadherin) in TNBC metastasis.

VE-cadherin is a primary component of the lymphatic and vascular endothelial barrier. While VE-cadherin expression was thought to be endothelium-restricted, our research group showed that breast cancer cells can also express VE-cadherin [1]. Recent investigations revealed that 60% of invasive human breast cancers are VE-cadherin positive [2]. VE-cadherin was shown to be involved in cancer cell proliferation, migration, and invasion, thus promoting tumor cell progression [1,3,4].

We hypothesize that VE-cadherin positive tumor cells and endothelial cells can interact via VE-cadherin-based cell-cell contacts. Thus, VE-cadherin expression might promote adhesion and transendothelial migration, key events in extravasation [5].

Methods

Tumor-endothelial cell interaction *in vitro* was characterized quantitatively by adhesion assays and qualitatively by live-cell imaging and subsequent immunofluorescence staining for VE-cadherin, epithelial E-cadherin, and mesenchymal N-cadherin. The VE-cadherin expression of human TNBC cell lines BT-20 and SUM149PT was determined on the protein and mRNA level. For SUM149PT sh5 knockdown cells, VE-cadherin expression was reduced by lentivirus-mediated RNA interference. Primary endothelial cells included human umbilical vein endothelial cells (HUVECs), human dermal lymphatic endothelial cells (HDLECs, PromoCell, Heidelberg), and human pulmonary microvascular endothelial cells (HPMECs, PromoCell, Heidelberg).

Tumor cells were stained with CellTracker Orange CMRA Dye (Invitrogen™, Carlsbad) and added to the confluent endothelial monolayer labelled with CellTracker Green CMFDA Dye (Invitrogen™, Carlsbad). Adhesion dynamics was quantified via fluorescence intensity at time points ranging up to 4 hours. Different concentrations of tumor cells were tested for their adhesive potential to different endothelial cells. Adhesion was analyzed as percentage of adherent cells from all cells in suspension.

Phase contrast live-cell imaging was performed at 37 °C, 5%, CO₂, 10x magnification with an Axio Observer Z.1 microscope (Carl Zeiss, Jena) for 24 hours and 10-minute intervals. Subsequently, fixed cells were qualitatively analyzed using a TCS SP5 confocal microscope (Leica Microsystems, Wetzlar). Cadherin expression between tumor and endothelial cells was assessed by 3D reconstruction with ImageJ (NIH, Bethesda).

Statistical significance was evaluated by paired t-test or two-way ANOVA with $p < 0.05$ (*) considered as statistically significant.

Results

BT-20 cells express less VE-cadherin than SUM149PT on the mRNA and protein level. In BT-20 cells, VE-cadherin is located at intercellular junctions, whereas in SUM149PT cells it is distributed diffusely. BT-20 and SUM149PT cells are E-cadherin positive, while only SUM149PT cells express N-cadherin.

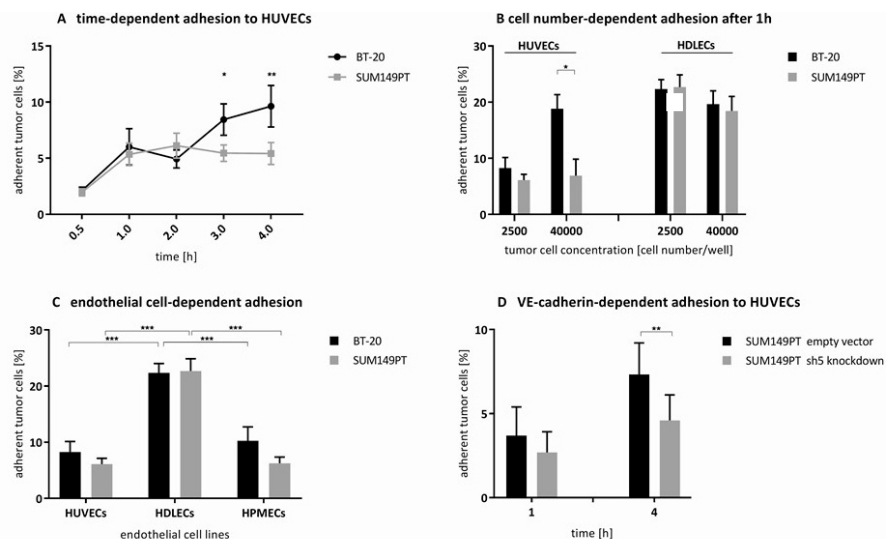


Figure 1. Dependency of tumor cell adhesion on different factors. If not indicated otherwise, adhesion time was 1h and tumor cell concentration was 2500 cells per well. Data displayed as means with SEMs.

Adhesion of tumor cells was tested subject to time, cell number, endothelial cell type, and VE-cadherin expression. Regarding time, BT-20 cells continuously adhere over 4 hours, whereas SUM149PT cells reach maximum adhesion after 1 hour (Fig. 1A, n=5). Regarding cell number, BT-20 cells adhere significantly more than SUM149PT cells to HUVECs (Fig. 1B, n=3). This effect is only present for high cell numbers. For HDLECs, no difference in adhesion between the tumor cell lines is observed. BT-20 and SUM149PT cells adhere significantly more to lymphatic than to macro- or microvascular endothelial cells (Fig. 1C, n=3). VE-cadherin knockdown reduces adhesion to both HDLECs and HUVECs (Fig. 1D, n=5).

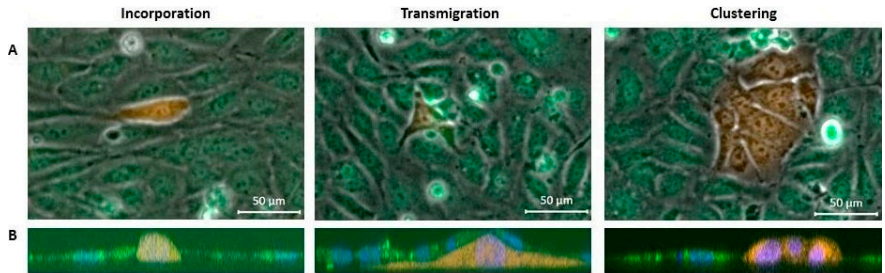


Figure 2. Tumor-endothelial cell interaction visualized by phase contrast live-cell imaging (A) and 3D reconstruction (B). Tumor cells in orange, endothelial cells in green, nuclei in blue.

Live-cell imaging data (Fig. 2) reveals that tumor cells incorporate into and transmigrate under the endothelium, either as single cells or groups to form tumor cell clusters between endothelial cells. In these clusters, E-cadherin is located between tumor cells, whereas N- and VE-cadherin are not detectable. 3D reconstruction data show that transmigrated tumor cells are covered by endothelium with a restored VE-cadherin barrier between the endothelial cells. For incorporated cells, VE-cadherin is not located at tumor-endothelial-cell-contacts (Fig. 3). VE-cadherin at interendothelial cell contacts stays intact.

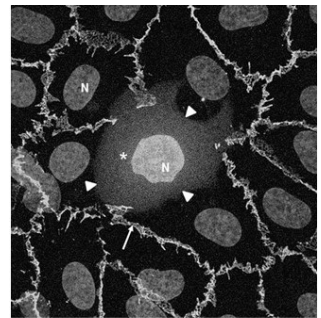


Figure 3. BT-20 tumor cell (*) is incorporated into the endothelium. VE-cadherin (arrow) is expressed at interendothelial junctions. No VE-cadherin (arrowheads) localizes at tumor-endothelial-cell-contacts. Nuclei (N) of endothelial and tumor cells.

Discussion

The time-dependent increase in adhesion is more prominent in BT-20 cells. The data suggest that SUM149PT cells reach a steady state within the first hour. Besides, we observed a cell number and cancer cell line dependency of adhesion to HUVECs but not to HDLECs. Cancer cell line dependency is likely to play a subordinate role (Fig. 1B), as concentrations of circulating tumor cells in the blood are very low [6]. Overall, tumor cells adhere more to lymphatic than to vascular endothelial cells. This accords with clinical observations of frequent lymphatic metastatic dissemination of breast cancer cells [7].

VE-cadherin seems to be involved in adhesion of tumor cells to both lymphatic and blood vascular endothelium. Yet, its role in transendothelial migration remains unclear as VE-cadherin is not localized between endothelial and tumor cells. N-cadherin is detected neither although it had been previously implicated in transendothelial migration [8].

The withdrawal of VE-cadherin from the endothelial borders appears to be an initial key event in transendothelial migration, contributing to endothelial barrier breakdown. This might be a mechanism to ease further tumor cell transmigration for cluster formation. However, it remains to be investigated if incorporation is an essential step of transendothelial migration [9] or if tumor cells can transmigrate differently, e.g. in a diapedesis-like manner. Qualitative analysis showed different tumor cell incorporation and transmigration patterns which are possibly linked to different levels of malignancy.

Conclusions

This study underscores the importance of VE-cadherin as a relevant player in metastasis of TNBC cells. VE-cadherin knockdown reduced the adhesion of TNBC cells. Adhesion preferences of tumor cells for lymphatic over blood vascular endothelium were observed. The underlying mechanisms and pathways remain to be investigated. During incorporation and transmigration, tumor cells lose their VE-cadherin and no VE-cadherin is located at tumor-endothelial-cell-contacts. Thus, VE-cadherin expression promotes adhesion, while its delocalization is key for endothelial barrier breakdown. To investigate the changes in VE-cadherin-location and -expression during transendothelial migration, future research will include live-cell imaging of fluorescent VE-cadherin in tumor cells.

Summary

This study investigates the role of vascular endothelial cadherin (VE-cadherin) in triple-negative breast cancer cells *in vitro*. Tumor cells were tested for their VE-cadherin expression, as well as adhesion, incorporation, and transmigration behavior on vascular and lymphatic endothelial cells. Tumor cells adhered more to lymphatic than to blood vascular endothelium. While VE-cadherin positive cancer cells showed high rates of adhesion, confocal microscopy data suggests that the delocalization or downregulation of VE-cadherin during transendothelial migration is key for the breakdown of the endothelial barrier function.

References:

1. Labelle M, Schnittler HJ, Aust DE, Friedrich K, Baretton G, Vestweber D, Breier G: VE-cadherin promotes Breast Cancer Progression via Transforming Growth Factor- β Signaling. *Cancer Res* 2008; 68, 1388–1397.
2. Rezaei M, Friedrich K, Kemper B, Brendel O, Grosser M, Baretton G, Breier G, Schnittler H: Expression of VE-cadherin in breast cancer cells modulates cell dynamics as a function of tumor differentiation and promotes tumor-endothelial cell interactions. *Histochem Cell Biol* 2018; 149, 15–30.
3. Rezaei M, Friedrich K, Wielockx B, Kuzmanov A, Kettelhake A, Labelle M, Schnittler H, Baretton G, Breier G: Interplay between N-cadherin and VE-cadherin in breast cancer. *Breast Cancer Res* 2012; 14, R154.
4. Breier G, Grosser M, Rezaei M: Endothelial Cadherins in Cancer. *Cell Tissue Res* 2014; 355, 523–527.
5. Reymond N, Borda d'Água B, Ridley AJ: Crossing the endothelial barrier during metastasis. *Nat Rev* 2013; 13, 858–870.
6. Ming Y, Li Y, Xing H, Luo M, Li Z, Chen J, Mo J, Shi S: Circulating Tumor Cells: From Theory to Nanotechnology-Based Detection. *Front Pharmacol* 2017; 8:35.
7. Ran S, Volk L, Hall K, Flister MJ: Lymphangiogenesis and Lymphatic Metastasis in Breast Cancer. *Pathophysiology* 2010; 17; 229–251.
8. Sandig M, Voura EB, Kalnins VI, Siu CH: Role of Cadherins in the Transendothelial Migration of Melanoma Cells in Culture. *Cell Motil Cytoskeleton* 1997; 38, 351–364.
9. Hamilla S, Stroka K, Aranda-Espinoza H: VE-Cadherin-Independent Cancer Cell Incorporation into the Vascular Endothelium Precedes Transmigration. *PLoS ONE* 2014; 9(10), e109748.

BRAIN MAPPING WITH RESTING-STATE FMRI: A NOVEL APPROACH TO PRESURGICAL PLANNING

Paulo Branco

Faculty of Medicine, University of Porto
Faculty of Psychology and Educational Sciences, University of Porto

Co-authors: D. Seixas, S.L. Castro

Tutor: São Luís Castro

Introduction and aims

Language mapping with functional magnetic resonance imaging (fMRI) is a promising tool for presurgical planning as it can map eloquent brain regions noninvasively (Sunaert 2006). Despite its promising status, studies comparing fMRI with the gold-standard technique - direct electrical stimulation - show poor agreement between techniques (Giussani et al. 2010). One key limitation that could explain this poor agreement is that conventional fMRI methods require task execution and active subject collaboration, which cannot be warranted in clinical settings (Price et al. 2006).

Resting-state fMRI (rsfMRI) is an imaging technique that has the potential to overcome these limitations, as it can map function without requiring task execution (Tie et al. 2013). This is achieved by taking advantage of the fact that the brain is functionally connected, even during rest, and that these connectivity patterns are spatially distributed in a manner that resembles major cognitive functions (Smith et al. 2009). Thus, using data-driven techniques, it is possible to characterize and extract the language (and other) network(s) without task execution.

Although group-studies have showed that rsfMRI is a powerful tool for brain mapping, it is currently unknown whether rsfMRI can map language efficiently in single-subjects, and particularly, in patients with brain pathology. The present work examined whether rsfMRI is suitable to map language in single-subjects. To do so, three studies were conducted to shed light on important open questions: is the technique *feasible* in patients with brain lesions? Is it *reliable* over time? Does it map eloquent brain regions that could lead to long-term deficits (e.g., *validity*)?

Methods

Three studies were designed to address the aforementioned open-questions. In the first study, we examined the *feasibility* of rsfMRI for language mapping in tumour and epilepsy patients. To do so, sixteen patients undergoing presurgical planning (brain tumours, intractable epilepsy) were scanned during task-execution (verb-to-noun generation protocol, 8m) and during rest (7m, eyes closed). Language maps were extracted using a general linear model approach for the task-based data, and an independent component analyses (ICA) approach for the resting-state data. To assess whether resting-state fMRI was able to map language regions efficiently, the maps extracted with rsfMRI were spatially compared to the task-based data, using an overlay index, the Dice coefficient. Further, to test the spatial specificity of both techniques, they were independently compared to language regions-of-interest taken from published language templates (Fedorenko et al. 2010). Finally, to assess variability

between subjects, a probability overlay map was calculated, showing areas of high and low convergence across subjects.

In the second study, we examined the *temporal reliability* of the language and sensorimotor resting-state networks. This is key as the efficiency of the procedure is directly tied to its ability to consistently map the same regions - even without a task. To do so, we examined ultra-high resolution data (7 Tesla, Gorgolewski et al. 2015) in eighteen subjects that were scanned during rest (15m, eyes closed), twice in the same day (short-term reliability), and again after one week (long-term reliability). Language and sensorimotor networks were extracted using ICA, and were spatially compared across sessions using the Dice coefficient, and the Intraclass coefficient. To further assess the robustness of rsfMRI, we examined whether data-quality metrics (motion, signal-to-noise ratio) and subject-specific data (pulse, blood pressure, hydration, sleep habits) contributed to the reliability of the technique.

In the third study, we assessed the *validity* of the resting-state language network, that is, whether there is evidence for the direct participation of the language rsfMRI network in language processes. This is crucial as no previous study has examined what language processes were being mapped with resting-state fMRI. To do so, sixteen subjects were scanned during rest (7m, eyes closed), and then performed a multi-level, task-based protocol. During this protocol, subjects read symbols (control condition), pseudowords, words, pseudosentences, and sentences (linguistic conditions); these were experimentally controlled to reflect an increase in language demands, by systematically increasing linguistic content. If regions within the language network indeed play a crucial role for language processing, then higher linguistic demands should elicit higher brain responses within the language network (Bedny et al. 2011). The language rsfMRI network was extracted using ICA, and its response profile were assessed by quantifying the signal percent increases while the subject performs each of the five conditions. To further assess the specificity of the language network, we also examined brain responses to other well-established rsfMRI networks, the default mode network, the dorsal attention network, and the frontoparietal network.

Results

Considering the *feasibility* of the technique, rsfMRI was able to map the language network efficiently for all subjects, and mapping results were similar to conventional task-based fMRI maps (Figure 1). Also, the resting-state language network was more consistent across subjects than task-based maps, and showed better specificity. These results support the idea that rsfMRI may be an alternative to task-based fMRI as it maps the same brain areas.

Considering the *reliability* of the technique, we found high reliability indices with spatial precision at the millimetre level (Figure 2), both in short- and long-term reliability. The reliability indices were also higher than those previously reported in test-retest studies using task-based fMRI. Taken together, this suggests that although the subject was not performing any task, network-level data were stable over time and appropriate for reliable brain mapping.

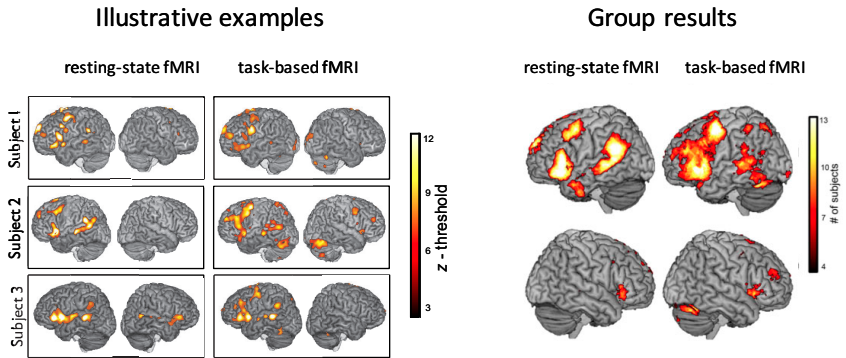


Figure 1. Left panel. Resting-state fMRI and task-based maps for three patients. Right panel. Probabilistic overlay showing regions of high probability of activation for each technique.

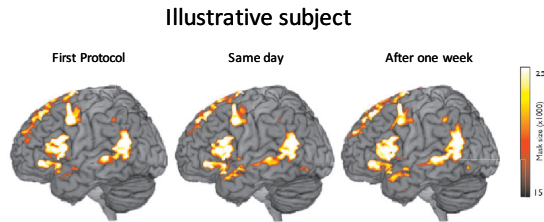
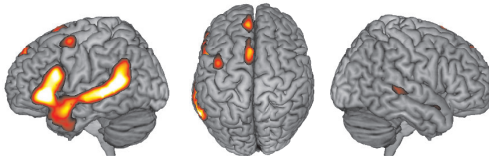


Figure 2. Language networks extracted with rsfMRI for an illustrative subject with average reliability indices.

Finally, considering the *validity* of the procedure, the language network was highly sensitive to language information but did not respond to the nonlinguistic baseline (Figure 3). Moreover, linguistically, rich conditions elicited larger BOLD responses within the whole language network – and this pattern was generalizable across the majority of regions within the resting-state language network. This suggests that the language network was adept at mapping regions that are critical for language processing and thus was able to target eloquent brain regions.

Language rsfMRI network



BOLD response for each condition

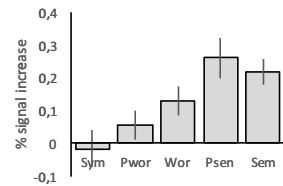


Figure 3. Left panel. Group-level language network mapped with rsfMRI. Right panel. Brain activity within the language network during each task condition. Sym = symbols; Pwor = pseudowords; Wor = Words; Psen = Pseudosentences, Sem = Sentences. Vertical bars denote 95% confidence intervals.

Conclusion

Taken together, the results from the three studies suggest that rsfMRI is a powerful, non-invasive technique for mapping language in the brain, overcoming some of the limitations of current task-based fMRI methods. This shows high promise for future clinical applications of rsfMRI in presurgical planning contexts.

Summary

This work examined the feasibility, reliability and validity of resting-state fMRI for language mapping in presurgical planning. Results from both healthy subjects and patients, and spanning over 60 subjects, showed that language mapping can be efficiently performed with resting-state. More specifically, resting-state is able to map the same regions as task-based fMRI, is reliable over time, and regions mapped with this technique play pivotal linguistic roles. Together, these results have important implications for presurgical planning, providing clinicians with valuable data that can help prevent long-term damage after neurosurgery.

References

1. Price C, Crinion J, Friston K.: Design and analysis of fMRI studies with neurologically impaired patients. *Journal of Magnetic Resonance Imaging* 2006; 23(6), 816-826.
2. Giussani C, Roux F, Ojemann J, Sganzerla E, Pirillo D, Papagno C.: Is Preoperative Functional Magnetic Resonance Imaging Reliable for Language Areas Mapping in Brain Tumor Surgery? Review of Language Functional Magnetic Resonance Imaging and Direct Cortical Stimulation Correlation Studies. *Neurosurgery* 2010; 66(1), 113-120.
3. Tie Y, Rigolo L, Norton I, et al. Defining language networks from resting-state fMRI for surgical planning—a feasibility study. *Human Brain Mapping* 2013, 35(3), 1018-1030.
4. Smith S, Fox P, Miller K, et al.: Correspondence of the brain's functional architecture during activation and rest. *Proceedings Of The National Academy Of Sciences* 2009; 106(31), 13040-13045.
5. Fedorenko E, Hsieh P, Nieto-Castañón A, Whitfield-Gabrieli S, Kanwisher N.: New Method for fMRI Investigations of Language: Defining ROIs Functionally in Individual Subjects. *Journal Of Neurophysiology* 2010; 104(2), 1177-1194.
6. Gorgolewski K, Mendes N, Wilfling D, et al.: A high resolution 7-Tesla resting-state fMRI test-retest dataset with cognitive and physiological measures. *Scientific Data* 2015; 2, 140054.
7. Bedny M, Pascual-Leone A, Dodell-Feder D, Fedorenko E, Saxe R.: Language processing in the occipital cortex of congenitally blind adults. *Proceedings of the National Academy of Sciences* 2011; 108, 4429-4434.
8. Sunaert S.: Presurgical planning for tumor resectioning. *Journal of Magnetic Resonance Imaging* 2006; 23, 887-905.

FLUOXETINE MONOTHERAPY AND AUGMENTATION TREATMENT IN ADOLESCENT DEPRESSION – OUR CLINICAL EXPERIENCE

Dana Cesneková

Clinic of Psychiatry, Department of Physiology, Biomedical Center Martin, Comenius
University in Bratislava, Jessenius Faculty of Medicine in Martin, Slovakia

Co-authors: I. Ondrejka, I. Tonhajzerová, G. Nosáľová

Tutor: Igor Ondrejka

Introduction

Major depressive disorder (MDD) is a serious disorder occurring in childhood and adolescence. The prevalence of depressive disorder is approximately 5-8% in adolescent age, being twice as prevalent in adolescent girls and 0.5-2.5% in prepubertal children (APA, 2015). Genetic predisposition, neuroendocrine, neurochemical biological and psychological factors, including negative life events with poor family background play a major role in developing of depression in pediatric population. Adolescent depression is associated with negative school, social and health outcomes, including depression in adulthood, increased risk of suicidal behaviour or substance abuse (Yorbik et al., 2004). According the severity of depressive symptoms pharmacotherapy, psychotherapy or their combination are indicated as the treatment. Recently, there have been significant increases in research of psychopharmacologic treatments for depression in childhood and adolescence, with randomized controlled trials, but some of them with negative results. Selective serotonin reuptake inhibitors (SSRIs) are the first-line treatment for depression in childhood and adolescence (Ondrejka, 2016). According to the U.S. Food and Drug Administration (FDA) fluoxetine is the only drug approved in pediatric population from 8 years of age indicated for MDD with three positive randomized control trials (FDA, 2015). Fluoxetine monotherapy is considered as a gold standard in acute phase of treatment in children and adolescents with MDD, but according to some studies is not effective enough after an acute phase of treatment (Kennard et al., 2006), especially in adolescent age. In recent years, research is focused on combined/adjuvant therapeutic strategies in treatment of adolescent depression, for example using of olanzapine as an antipsychotic drug with antidepressant effect (Detke, 2015).

Aims

The aim of our study is to evaluate the dynamics of depressive symptoms using fluoxetine monotherapy and combined/adjuvant therapeutic strategy (fluoxetine/olanzapine combination) during acute 6-weeks treatment of adolescent depression as well as related potential adverse effects.

Methods

Forty adolescent inpatients admitted in child department of Clinic of Psychiatry, University Hospital in Martin were randomized into 2 therapeutic lines (fluoxetine monotherapy – FXT and olanzapine/fluoxetine combined therapy – OFC). Fluoxetine dosage was 20 mg/day

and olanzapine dosage 2.5-5 mg/day. Inclusion criteria consist of fulfill diagnostic criteria for non-psychotic MDD according Diagnostic and Statistical Manual of Mental Disorder - DSM-5 (APA, 2015), CDRS-R total score 40, adolescent age (12-18 years), informed consent by parents/guardians. Participants were assessed by clinician using CDRS-R (Children’s Depression Rating Scale-Revised) and CGI-I (Clinical Global Impression Scale – Improvement) describing depressive symptoms, severity of symptoms and clinical impression in general. Following randomization, evaluation visits were weekly during 6 weeks and at baseline in CDRS-R scale (0, 1-6), as well as in CGI scale at each visit, except of baseline (1-6). Adverse effects during the treatment were observed. Data were evaluated by statistical analysis (Pairwise Two-Sided Multiple Comparison Analysis, Dwass, Steel and Critchlow-Fligner Method).

Ethical approval Jessenius Faculty of Medicine in Martin: All procedures performed in studies are in accordance with the ethical standards according to Helsinki Declaration.

Results

Mean age of patients was 16.2±1 years. Both lines FXT and OFC were associated with significant reduction of depressive symptoms in CDRS-R total score after 6-weeks, but the improvement was higher in OFC (33.8±11.3, $p < 0.0001$, at baseline 59.1±7.9) vs. FXT (35.8±12.7, $p = 0.0002$, at baseline 58.1±11.5). OFC has shown significantly greater reduction of depressive symptoms after the 2nd week of treatment in OFC line (39.8±10.1, $p < 0.0001$) (Figure 1), as well as a greater clinical improvement in CGI-I total score in comparison with FXT after 6-weeks (FXT 3.3±1.0 vs. OFC 3.1±1.6, $p=0.03$). Clinical improvement was significantly greater after the 3rd week of treatment in OFC (3.4±0.5, $p < 0.0001$) (Figure 2).

The most common side effects were tremor and headache in fluoxetine monotherapy and headache, increased appetite, weight gain and fatigue in combined therapy.

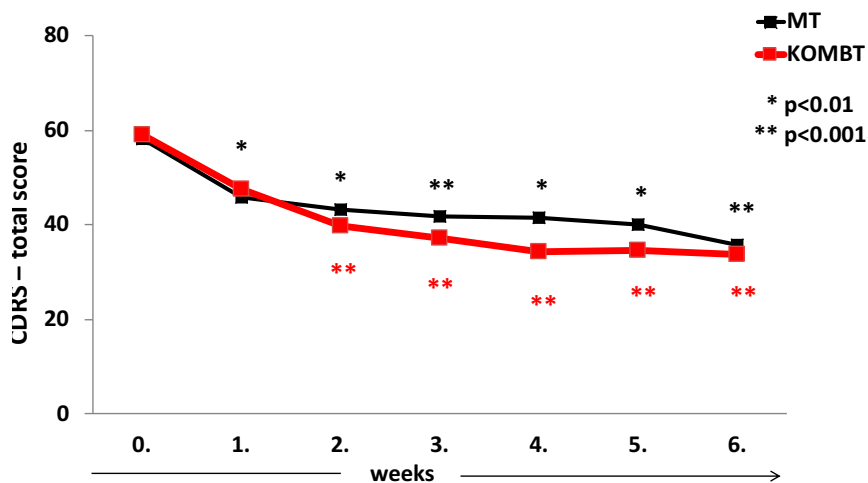


Figure 1. Dynamics of depressive symptoms in CDRS-R scale during 6-weeks' treatment in FXT and OFC line.

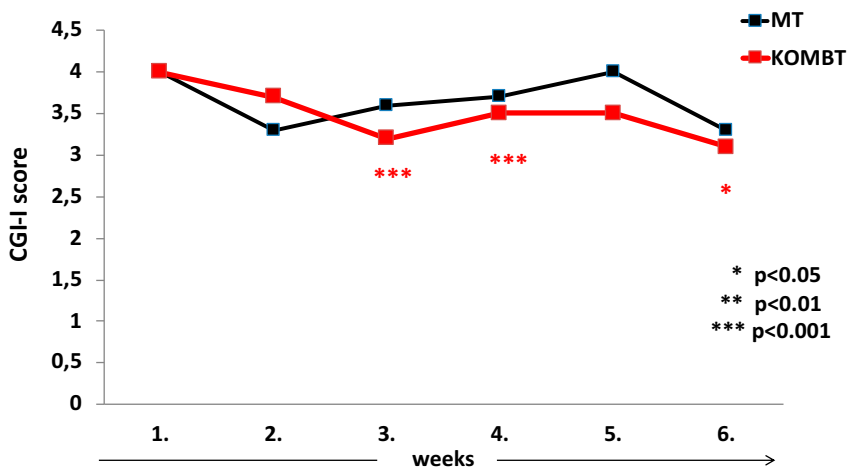


Figure 2 Dynamics of clinical improvement during 6-weeks' treatment according to CGI-I scale in FXT and OFC line.

Discussion

SSRIs antidepressants in pedopsychiatry are indicated in the range spectrum of psychiatric disorders. Clinical trials have shown that fluoxetine in dosage 20-40 mg/day is effective and safe in the acute phase of treatment in MDD, predominantly in younger children (Emslie et al., 2002). However, in adolescents the residual symptoms are common and relaps of depressive symptoms is occurring in more than one-third patients (Kennard et al., 2006). That means only a partially effectiveness of fluoxetine monotherapy after acute phase of treatment. According to the study of Mayes et al. (2007), there is a remission rate 41.5% in children and 32.6% in adolescents after the acute phase of fluoxetine treatment without adjuvant therapy. More effective therapeutic strategies are needed for faster remission rate of disorder. In recent years, the combined or augmented therapeutic strategies are preferred. Olanzapine is an atypical antipsychotic and multi-receptor antagonist effective in psychotic disorders, as well as in reduction of depressive symptoms in bipolar depression (Detke, 2015). Our effort is to confirm its effectiveness as adjuvant therapy in treatment of non-psychotic and unipolar depression in adolescents, that can lead to a higher level of therapeutic effectiveness in acute phase of treatment, as well as after the acute treatment, better response to the treatment, shorter time to remission and relapse prevention in patients with MDD. Our study showed significantly earlier onset of action in OFC in comparison with fluoxetine monotherapy. In addition earlier onset of action (after first week of treatment in pediatric population) play an important role to prevent suicidal behaviour and better stabilization in the treatment of depression with long-term effect. In our opinion, despite the known adverse effects of olanzapine medication, benefits are up to risks.

Conclusion

In our study, both therapeutic strategies showed statistically significant effectiveness in the acute 6-weeks' treatment of MDD, but OFC is more statistically significant in comparison with FXT evaluated by CDRS-R scale, as well as with higher clinical improvement in CGI-I total score. The side effects, such as headache, increased appetite, weight gain and fatigue were at a low intensity.

Summary

Adolescent depression is a serious disease with high level of suicidal risk. Fluoxetine monotherapy is more effective in acute phase of treatment in children than in adolescents. In adolescent age, there is a higher level of depression relapse and residual symptoms are common. Both, monotherapy and combined treatment by olanzapine augmentation are effective, well-tolerated and safe. Our results suggest higher effect and earlier onset of action of adjuvant therapy by low dosage of olanzapine. Adjuvant therapy (by olanzapine augmentation) is predicted to be more useful in the treatment of adolescent depression. More effective therapeutic strategies in treatment of MDD are needed to better stabilization of disorder, prevention of suicidal risk. Further research in this issue is needed.

References:

1. American psychiatric association. Diagnostic and statistical manual of mental disorders. DSM-5. 5th ed. Arlington, VA: American Psychiatric Association; 2013. ISBN 978-0-89042-554-1.
2. DeFilippis M, Wagner KD. Management of treatment-resistant depression in children and adolescents. *Paediatr Drugs*. 2014 Oct;16(5):353-61.
3. Detke HC, Delbello MP, Landry J, Usher RW. Olanzapine/Fluoxetine combination in children and adolescents with bipolar I depression: a randomized, double-blind, placebo-controlled trial. *J Am Acad Child Adolesc Psychiatry* 2015;54(3):217–224.
4. Emslie GJ, Heiligenstein JH, Wagner KD et al. Fluoxetine for acute treatment of depression in children and adolescents: a placebo-controlled, randomized clinical trial. *J Am Acad Child Adolesc Psychiatry* 2002; 41 (10): 1205-1215.
5. Kennard B, Silva S, Vitiello B et al. TADS Team. Remission and residual symptoms after short-term treatment in the Treatment of Adolescents with Depression Study (TADS). *J Am Acad Child Adolesc Psychiatry*. 2006 Dec;45(12):1404-11.
6. Mayes TL, Tao R, Rintelmann JW et al. Do children and adolescents have differential response rates in placebo-controlled trials of fluoxetine? *CNS Spectr*. 2007 Feb;12(2):147-54.
7. Ondrejka I. Liečba psychofarmakami v detskom a adolescentnom veku. In: *Psychofarmakológia*. Vyd. Wolters Kluwer, 2016. S. 467-502. ISBN: 978-80-8168-543-9.
8. Yorbik O, Birmaher B, Axelson D et al. Clinical characteristics of depressive symptoms in children and adolescents with major depressive disorder. *J Clin Psychiatry*. 2004 Dec;65(12):1654-9.

LEGIONELLA SPP. IN THE HOSPITAL'S WATER SYSTEM – INFECTION RISK AND PREVENTION

Miriam Fulová

Institute of Epidemiology, Comenius University in Bratislava, Slovak Republic

Co-authors: M. Kotrbancová, J. Boledovičová, K. Trnková

Tutor: Margita Špaleková

Introduction and aims

Legionella spp. are Gram-negative facultative pathogenic bacteria ubiquitous in aquatic habitats and water distribution systems (1). Legionellae in water environment are adapted for survival and replication within numerous protozoa, as a free-living or biofilm-associated bacterium (2) in 20-45 °C optimal temperature. Bacteria of the genus *Legionella* (mostly *Legionella pneumophilla*) could cause an atypical pneumonia - Legionnaires' disease (LD) by inhalation of legionellae containing aerosols. Systems that produce aerosols were linked to LD cases and outbreaks (e.g. air-conditioning cooling towers, plumbing systems, whirlpool spas) (1). *Legionella* colonization of water systems can lead to hospital-acquired LD especially in immunocompromised patients (3, 4). Early laboratory diagnosis and treatment of LD is crucial because the disease can be even life-threatening, associated with case-fatality rate (CFR) up to 30% (5). The key to prevention of legionellosis is proper maintenance of water systems (water safety plan) including disinfection, technical and operational measures, environmental and clinical surveillance (1,6,9).

The aim of our study was to investigate colonization of *Legionella* in the water system of children's hospital and its impact for acquiring LD among high-risk patients at the oncologic clinic with monitoring effects of control measures.

Methods

Water samples (300 ml) from patients' rooms/bathrooms without/with antibacterial filters were processed and cultivated according to STN ISO 11731. Samples were filtered through membrane filters (0.22µm) and bacteria were released in 20 ml sterile water by shaking for 5 minutes. Samples (0.1-0.5 ml) were inoculated on GVPC medium (BCYE α - Buffered Charcoal Yeast Extract α ketoglutaric acid with glycine, vankomycin, polymyxin B, cycloheximid) directly or treated by KCL-HCL (pH 2.2) 1: 1 / 5 min or by heat (50 °C / 30 min.) and incubated 10 days at 35-37 °C. The morphologically suspected legionella colonies (stereomicroscope) were seeded on BCYE α and blood agar (BA). *Legionella* colonies not growing on BA were identified using immune polyclonal rabbit sera in immunofluorescence and agglutination tests. Selected colonies of legionella and other bacteria were identified also in MALDI-TOF. Water samples were also cultivated for amoeba. The water temperature was measured at distal outputs. Data of ClO₂ levels (ppm) in water were taken from the hospital records. Biological samples from lower respiratory tract were plated on BMPA (BCYE α + vankomycin, polymyxin B, cycloheximid, nystatin) agar without / with treatment by dithiotreitol, acid buffer and cultivated at 35-37 °C 10 days. Sera were tested in microagglutination test with 21 legionella

antigens (*L. pneumophila* serogroup 1- subtypes Philadelphia and Knoxville, *L. pneumophila* serogroups 2-15, *L. micdadei*, *L. dumoffii*, *L. longbeachae*, *L. bozemani*, *L. gormanii*). A commercial ELISA test (BINAX Legionella Urinary Antigen Enzyme Immunoassay kit) was used to prove *Legionella pneumophila* antigen in the patient's urine. Selected biological samples were examined by PCR amplification.

Results

From total 70 water samples tested in the years 2015-2017 (Table 1) - taken before the water disinfection with chlorine dioxide (ClO₂), or at its low level <0.3 ppm - 49 (70%) were legionella positive (5x10¹ - 5x10³ CFU/100ml) and 94% (32/34) amoeba positive (saprophytic and thermotolerant) samples. At a higher level of ClO₂ (> 0.3 ppm), legionella concentrations were reduced to 200 CFU/100ml (95% decrease).

Year	LEGIONELLA			AMOEBAE posit./samples		ClO ₂ (ppm)	hot water temperature °C (mean)
	posit./ samples	% posit. samples	CFU/ 100ml	Saprophytic (36°C)	TTA (44°C)		
2015	19/30	63	< 5.10 ³	20/20	20/20	-	-
2016	14/15	93	< 3.10 ²	-	-	< 0.3	44.1
2017	16/25	64	< 3.10 ³	12/14	12/14	< 0.3	42.7
			< 2.10 ²			> 0.3	
2015 - 2017	without filter 49/70	70	< 5.10 ³	32/34	32/34	< 0.3/ > 0.3	44
2017	with filter 0/19	0	0	0/19	0/19	> 0.3	45
			0			> 0.3	43.9

Table 1: Results of water samples cultivation according to control measures and water temperature CFU – colony forming unit, TTA – thermotolerant amoebae, ClO₂ – chlorine dioxide, filter – antimicrobial filter

After identification of 226 selected bacterial colonies in MALDI-TOF 47% were *Legionella pneumophila* sp. and 26% others (e.g. *Pseudomonas spp.*, *Stenotrophomonas spp.*). The recommended hot water thermal regimen (> 55 °C) was not maintained. Out of 19 water samples tested after the 1st and 2nd month of filter installation in 2017, no legionellae and amoebae were found (Table 1). Before ClO₂ disinfection, we diagnosed five LD cases of the total 26 patients. After adequate ClO₂ disinfection and implementation of filters one LD case out of 32 patients was confirmed. LD in all 6 patients were confirmed by detection of legionella antigen in urine (Table 2).

Patient	Age (years)	Ab in sera (S)	Ag in urine (U)	Cultivation (BAL)	PCR
1	4	negat	posit	negat	ND
2	18	negat	posit	negat	posit – S, U
3	16	negat	posit	ND	posit – S, U
4	2	negat	posit	ND	negat – S, U
5	17	posit	posit	posit	posit – S, BAL; negat - U
6	12	negat	posit	negat	ND

Table 2. Biological samples examination results

Discussion

Legionella colonization of water systems in health-care facilities is relatively common (6). National study in USA revealed legionellae in 70% out of 20 hospitals (6), similar contamination was also detected in Slovakia during 1985 – 2011 (3).

Presented study found in the paediatric oncology colonization of *L. pneumophila* serogroups 5, 8, 10, 3, 1 in 70% and amoebae in 94%. Subsequently reduced legionella, other bacteria and amoebae contamination rates confirmed association with proper disinfection (7) with ClO₂ (> 0.3 ppm) but insufficient water heating (mean 44 °C). The study also confirmed effectivity of antibacterial filters, which completely eliminate all contaminants and should prevent water-borne infections.

Legionellosis is rare in children (8). Greenberg et al. reported 76 LD cases, half in children younger than 2 years. More than 50% acquired LD in hospital and 78% had malignancy with higher CFR than total 33%. Only 24 LD cases aged 0–19 years (0.4% of all) were reported in Europe in 2015 (9). In our study six LD in children aged 2–19 years were detected. Acquiring LD is result of many factors, as patient's immunity, legionellae virulence, mode and duration of water exposure (6). Patients with hospital – acquired LD are in higher risk of fatal outcome (OR = 4.3, p<0.01) than other cases (8), thus early diagnosis and treatment can be life-saving (10) together with water controls.

Conclusions

This research showed that ClO₂ and antimicrobial filters are effective in prevention of legionellae and other water – borne pathogens causing nosocomial infections. Monitoring bacterial colonization, validation and ongoing verification of control measures are important to prevent legionella water recolonization.

Summary

Legionellae are widely found in natural and artificial aquatic environments, where can grow intracellularly in protozoa and with other bacteria in biofilms. At least 61 different *Legionella* species have been described and strains of 26 species by inhalation or aspiration of water aerosols could infect humans, mainly immunosuppressed. *Legionella spp.*, the cause of Legionnaires' disease (LD), are recognized around the world as an important cause of community-acquired pneumonia and hospital-acquired pneumonia. Monitoring for legionellae is important for public health reasons to identify environmental sources which can pose a risk of severe pneumonia with fatal outcome, in nosocomial legionellosis in 20-40%.

The aim of presented study was investigation of legionella colonization of water system in children hospital focused also on examination of oncologic patients for legionellosis and validation of control measures (disinfection by chlorine dioxide – ClO₂, antibacterial filters, water temperature).

Legionella monitoring was performed in 2015-2017. Collected water samples from distal sites of water supply in oncologic clinic were concentrated by membrane filtration (ISO11731:2017), diluted or directly plated on selective GVPC medium, also pre-treated with heat (50 °C/30 min.) and with acid (KCl-HCl pH-2.2). Morphologically suspected legionella colonies during 10 days incubation were stereoscopic evaluated and cultured on BCYE α and blood agar. Legionella isolates growing only on BCYE α were typed with polyclonal rabbit sera in agglutination or immunofluorescence tests, some legionella and other colonies were identified in MALDI – TOF. Water samples were also cultivated for detection of amoebae (saprophytic, thermotolerant).

Out of total 70 water samples were 49 (70%) legionella positive (5×10^1 - 5×10^3 CFU/100ml) and almost all (32/34) were also contaminated by amoebae in 94% mostly before introduction of disinfection by chlorine dioxide, or at low levels of ClO_2 (< 0.3 ppm). High levels of disinfection (>0.3 ppm) resulted in reduced contamination of 95% in less than 200 CFU/100ml concentration. Identification by serotyping and in MALDI-TOF revealed colonization of legionellae of *Legionella pneumophila* sp. of various serogroups 5, 8, 10, 3, 1. Maintaining of hot water temperature regimen (> 55 °C) was not followed all the time therefore validation of control measures and ongoing verification of them were recommended. Very effective was installation of 11 membrane filters in showers and taps for legionella, amoebae and other bacteria elimination from water during 1-2 months, all 19 water samples were negative. Environmental control with measures (including filters) was effective, only one case of LD was detected by examination of 32 patients, while in non-proper disinfection era 5 cases out of 26 investigated patients. All six LD cases were confirmed by detection of legionella antigen in urine.

References

1. Cunha BA, Burillo A, Bouza E.: Legionnaires' disease. Lancet 2016; 387, 376–85.
2. Declerck P, Behets J, van Hoef V et al.: Detection of Legionella spp. And some of their amoeba hosts in floating biofilms from anthropogenic and natural aquatic environments. Water Res 2007; 41, 3159–3167.
3. Špaleková M.: Výskyt a problematika legionelových infekcií v nemocničnom prostredí. Antibiotiká a rezistencia 2011; 1, 24 – 28.
4. Borella P, Bargellini A, Marchegiano P et al.: Hospital-acquired Legionella infections: an update on the procedures for controlling environmental contamination, Ann Ig 2016; 28, 98 – 108.
5. Mercante JW, Winchell JM.: Current and emerging Legionella diagnostics for laboratory and outbreak investigations. Clin Microbiol Rev 2015; 28, 80–118.
6. Stout JE, Muder RR, Mietzer S et al.: Role of environmental surveillance in determining the risk of hospital-acquired legionellosis: a national study with clinical correlations. Infect. Control. Hosp. Epidemiol. 2007; 7, 818 – 824.
7. Trnková K, Kotrbancová M, Špaleková M et al.: MALDI-TOF MS analysis as a useful tool for an identification of Legionella pneumophila a facultatively pathogenic bacterium interacting with free-living amoebae: A case study from water supply system of hospitals in Bratislava (Slovakia). Experimental Parasitology 2018; 184, 97 – 102.
8. Greenberg D, Chiou CC, Famigillieti R et al.: Problem pathogens: paediatric legionellosis – implications for improved diagnosis. Lancet infect Dis 2006; 6, 529 – 535.
9. European Centre for Disease Prevention and Control.: Legionnaires' disease in Europe, 2015. Surveillance report. Stockholm: ECDC; 2017.
10. Kotrbancová M, Špaleková M, Fulová M et al.: Legionelózy a ich diagnostika. Epidemiol. Mikrobiol. Imunol. 2017; 3,133 – 139.

DEOXYRIBONUCLEASE ACTIVITY IN ANIMAL MODEL OF SEPSIS

Eubica Janovičová

Institute of Molecular Biomedicine, Medical Faculty,
Comenius University, Bratislava, Slovakia

Co-authors: L. Lauková, N. Pribulová, P. Celec

Tutor: Peter Celec

Introduction

Extracellular DNA (ecDNA) is DNA released from cells during cell death. Despite the fact, that ecDNA originates from the organism itself, it has proinflammatory properties. Deoxyribonucleases (DNases) are enzymes which cleave DNA. These enzymes are secreted outside of cells, where they can cleave ecDNA (Kishi et al., 2001). EcDNA concentration in plasma is associated with diseases such as kidney and liver damage (Marques et al., 2015) and sepsis (O'Brien et al., 2017). It was shown, in an animal model of sepsis, that injection of exogenous DNase I improves the outcome of sepsis (Laukova et al., 2017). Sepsis is characterized by systemic inflammation. This is accompanied by cell death of not only pathogens which had caused inflammation but also the death of host cells. During this process, ecDNA concentration increases which suggest that it has a role in the pathology of sepsis. The timing of sepsis treatment with DNase appears to also play an important role (Mai et al., 2015). High inter-individual variability of endogenous DNase activity in plasma was observed in mice. Some individuals have higher DNase activity than others. Similarly, survival of mice in animal model of sepsis, where sepsis was induced using ip injection of *E. coli* is also variable. Some mice die during the first few hours after induction and some survive sepsis. Therefore, our aim was to assess the survival of mice in animal model of sepsis and observe endogenous DNase activity of these mice.

Methods

Blood was collected from 50 healthy male CD-1 mice via retroorbital puncture. This blood was centrifuged at 1600g for 10 min at 4°C. Pathogenic *E. coli* were grown overnight in LB media. Bacteria were centrifuged at 5000g for 5 min. Then they were resuspended in saline. Mice were intraperitoneally injected with pathogenic *E. coli* (4×10^8 bacterial cells per mouse). The septic score was observed 3 hours after injection with bacteria. Survival was observed every hour for the next 24 hours and then again, after 48 hours. DNase activity was measured using SRED assay (Nadano et al., 1993). Plasma samples and calibration were pipetted on the gel containing DNA and fluorescent dye. Photos of gel were made using iBOX and measured using ImageJ software. Results were analyzed using GraphPad Prism 6 software. The accepted level of significance was $\alpha < 0.05$.

Results

Endogenous DNase activity was measured using the gel-based method. Variable DNase activity was observed in the SRED assay (Figure 1). Some mice had higher DNase activity in plasma

compared to others. There was no correlation between body weight and endogenous DNase activity ($r=-0.16$; $p=0.28$). Dataset was divided into two groups, mice with high DNase activity and low DNase activity. No difference was found between the survival curve for mice assigned to high DNase activity group and low DNase activity group (Figure 2; Log-rank test; $p=0.99$).

Figure 1. Endogenous DNase activity in mice before injection of *E. coli*. Circles on the left side represent plasma samples from 50 mice. Plasmatic DNase activity in these mice is not the same due to variability. Calibration curve of DNase I was used to calculate DNase activity (the right side of the gel).

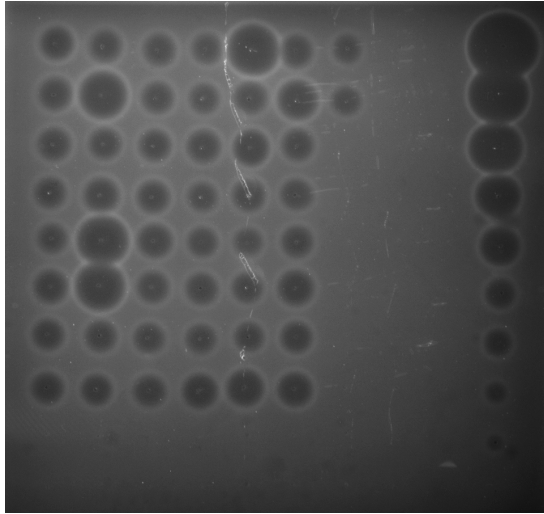
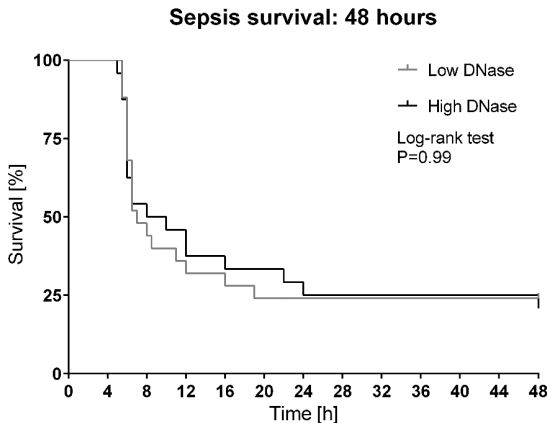


Figure 2. Survival of mice was observed during 48 hours after injection with pathogenic *E. coli*. Two Kaplan-Meier curves were created for mice which were assigned to groups with high DNase activity and low DNase activity according to median DNase activity. There was no difference between two survival curves (Log-rank test; $p=0.99$).



Discussion

Endogenous DNase activity played no role in *E. coli* induced sepsis in CD-1 male mice. No difference was observed between high DNase activity and low DNase activity group in the survival of mice. However, endogenous DNase activity was shown before to fluctuate over time. EcDNA was previously shown to increase during sepsis together with DNase activity (Laukova et al., 2017). Little is known about the role of endogenous DNase activity in diseases. Exogenous DNase activity improved the state of not only sepsis but also stroke (De Meyer et al., 2012), ischemia-reperfusion injury (Albadawi et al., 2016) and hepatorenal injury (Vokalova et al., 2017) in animal models of diseases. There could be several aspects of DNase treatment and DNase activity which need to be considered. First, high endogenous DNase activity in some mice may not be as high as DNase which is exogenous injected DNase. This limitation could be tested by increasing the expression of DNase enzymes. Secondly, purified DNase which is used as a treatment is usually originating from the bovine pancreas which may have a different substrate specificity. Thirdly, DNase activity may be inhibited in blood by the presence of inhibitors or absence of bivalent ions which are needed for its activity. Treatment with DNase could increase DNase activity much more than is normal under physiological conditions. Finally, another issue might be the timing. It has already been shown that too early DNase administration is not beneficial, likely due to the blockage of neutrophil effects on bacteria (Mai et al., 2015). While endogenous DNase activity could be high early in the sepsis model, this might induce more harm than benefit. Last but not least, the temporal variability of DNase is very high and the changes quickly. It is possible that the DNase activity changes from blood sampling time to time when ecDNA is too high and DNase is needed. This should be studied in our further ongoing experiments.

References

1. Albadawi, H., Oklu, R., Raacke Malley, R.E., *et al.*: Effect of DNase I treatment and neutrophil depletion on acute limb ischemia-reperfusion injury in mice. *Journal of vascular surgery* 2016; *64*, 484-493.
2. De Meyer, S.F., Suidan, G.L., Fuchs, T.A., *et al.*: Extracellular chromatin is an important mediator of ischemic stroke in mice. *Arteriosclerosis, thrombosis, and vascular biology* 2012; *32*, 1884-1891.
3. Kishi, K., Yasuda, T., and Takeshita, H.: DNase I: structure, function, and use in medicine and forensic science. *Legal medicine* 2001; *3*, 69-83.
4. Laukova, L., Konecna, B., Babickova, J., *et al.*: Exogenous deoxyribonuclease has a protective effect in a mouse model of sepsis. *Biomedicine & pharmacotherapy = Biomedicine & pharmacotherapie* 2017; *93*, 8-16.
5. Mai, S.H., Khan, M., Dwivedi, D.J., *et al.*: Delayed but not Early Treatment with DNase Reduces Organ Damage and Improves Outcome in a Murine Model of Sepsis. *Shock* 2015; *44*, 166-172.
6. Marques, P.E., Oliveira, A.G., Pereira, R.V., *et al.*: Hepatic DNA deposition drives drug-induced liver injury and inflammation in mice. *Hepatology* 2015; *61*, 348-360.
7. Nadano, D., Yasuda, T., and Kishi, K.: Measurement of deoxyribonuclease I activity in human tissues and body fluids by a single radial enzyme-diffusion method. *Clinical chemistry* 1993; *39*, 448-452.

8. O'Brien, X.M., Biron, B.M., and Reichner, J.S.: Consequences of extracellular trap formation in sepsis. *Current opinion in hematology* 2017; 24, 66-71.
9. Vokalova, L., Laukova, L., Conka, J., *et al.*: Deoxyribonuclease partially ameliorates thioacetamide-induced hepatorenal injury. *American journal of physiology Gastrointestinal and liver physiology* 2017; 312, G457-G463.

SERUM VASCULAR ENDOTHELIAL GROWTH FACTOR IN THE COURSE OF MICROANGIOPATHY IN OBSTRUCTIVE SLEEP APNEA COMORBID TYPE 2 DIABETES PATIENTS

Tamar Kakhniashvili

David Tvildiani Medical University;
Diabetes, Endocrine and Cardio-pulmonary Disease Center „Diacor” Tbilisi, Georgia

Co-authors: N. Tabagari-Bregvadze; E. Sherozia; L. Nikoleishvili

Tutor: Ramaz Kurashvili

Introduction and aims

Type 2 diabetes mellitus (T2DM) is the most common and widespread from all types of diabetes. The disease is associated with high prevalence of macro and microangiopathy. [1, 2, 3] In T2DM pathogenesis hyperglycemia induced oxidative stress causes vascular damage, leading to raise capillary vascular endothelial growth factor (VEGF) concentration, which causes neovascularization primarily in retina and kidney capillary, leading to irreversible changes: proliferative diabetic retinopathy and nephropathy. [4] Recent data suggests that co-existence of T2DM and obstructive sleep apnea (OSA) is very frequent and that OSA worsens diabetes microvascular complications. [5, 6, 7] It is confirmed that VEGF concentration is elevated not only in capillary but also in serum and plasma in T2DM patients, as well as in patients with OSA. [8, 9] We hypothesized that elevated serum VEGF could play a role in the course of microangiopathy in T2DM patients with OSA comorbidity. Our aim was to compare microangiopathy prevalence between the patients with T2DM and T2DM + OSA and compare serum VEGF concentration among them.

Methods

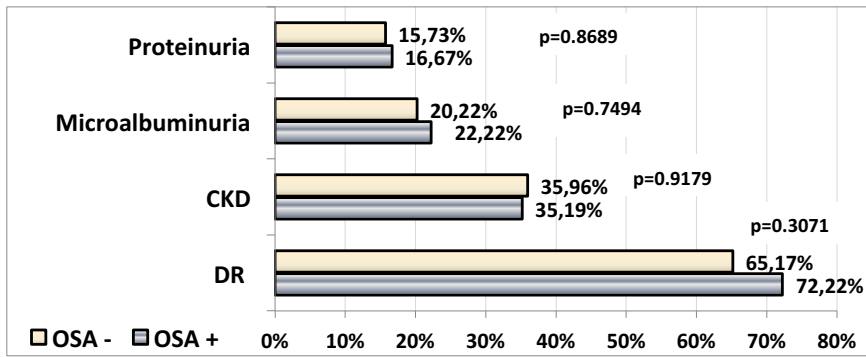
In the prospective, cohort study were included T2DM adult patients, referred to the Diabetes, Endocrine and Cardiopulmonary Disease Center „Diacor”, Tbilisi, Georgia. All of them had signed written informed concept form. Subjects with any other types of diabetes mellitus; pregnancy; alcohol/drug abuse; 3 months before study enrollment acute coronary, cerebrovascular or peripheral vascular disease; active hepatitis or HIV infection; acute inflammation; psychological disease; patients on hemodialysis, polysomnographically confirmed central OSA; cancer and any life threatening conditions; significance thrombocytopenia/ thrombocytosis, leukopenia/leukocytosis, who used systemic anti-VEGF drugs (Aflibercept, Bevacizumab, Ranibizumab) were excluded from the study. The following data were collected: medical anamnesis; demographic and anthropometric data; Epworth sleepiness score data; laboratory (complete blood count, biochemistry, immunology, complete urine test, including microalbuminuria) and instrumental investigation data (fundoscopy, laboratory polysomnography). Venous blood samples were taken at least 10 hours fasting in the morning in clinic „Diacor”. Morning urine was collected and analyzed for creatinine, protein and albumin excretion using standardized methods; VEGF was measured in serum by enzyme-linked immune-sorbent assay technology (Human ELIZA - Kit Catalog No: MBS355343, sensitivity < 1pg/m).

All the laboratory–instrumental investigations assessments are defined according to the European Association for the Study of Diabetes, American Diabetes Association and American Academy of Sleep Medicine guidelines.

Results

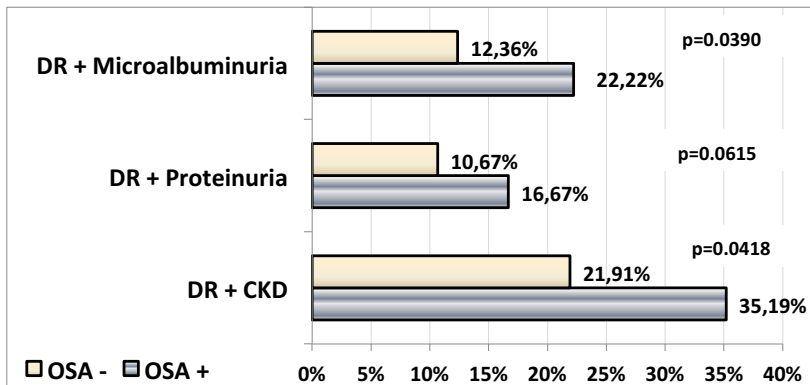
From 263 recruited patients, 31 were excluded and 232 analyzed. 54 (23.27%) patients were diagnosed with OSA and placed in OSA+ group and 178 (76.73%) T2DM patients without OSA comorbidity were placed in OSA- group. For microangiopathy distribution among this 2 groups see the figure 1 and figure 2.

Figure 1: Microangiopathy prevalence in OSA+ and OSA- groups.



Definition of abbreviations: OSA=obstructive sleep apnea; DR=diabetic retinopathy, CKD=chronic kidney disease

Figure 2. Co-existence of Diabetic Retinopathy (DR), chronic kidney disease (CKD), proteinuria and microalbuminuria



Definition of abbreviations: OSA=obstructive sleep apnea; DR=diabetic retinopathy, CKD=chronic kidney disease

For the serum VEGF level according to the microangiopathy among OSA+ and OSA- groups see the table 1.

Table 1: Serum VEGF level according to the microangiopathy

Variables	VEGF OSA-		VEGF OSA+		p value
	(n=178)	46.05 ± 37.61	(n=54)	65.76 ± 36.64	0.0008
Proteinuria	(n=28)	40.43±21.14	(n=9)	49.92 ± 9.03	p=0.2024 (NS)
Microalbuminuria	(n=36)	34.32 ± 15.95	(n=12)	50.70 ± 15.04	p=0.0031
CKD	(n=64)	65.41 ± 46.29	(n=19)	75.72 ± 46.94	p=0.4402 (NS)
DR	(n=116)	51.90 ± 37.43	(n=39)	70.05 ± 39.24	p=0.0097
DR and microalbuminuria	(n=22)	40.02 ± 11.98	(n=12)	57.30 ± 13.12	p=0.0049
DR and Proteinuria	(n=19)	44.72 ± 21.76	(n=9)	65.53 ± 10.90	p=0.0122
DR and CKD	(n=39)	48.28 ± 33.50	(n=19)	66.17 ± 21.34	p=0.0382

Definition of abbreviations: VEGF=vascular endothelial growth factor; OSA=obstructive sleep apnea; DR=diabetic retinopathy, CKD=chronic kidney disease

Discussion

The study shows that the coexistence of diabetic retinopathy and CKD as well as coexistence of diabetic retinopathy and microalbuminuria are significantly frequent in OSA comorbid T2DM patients referred to the clinic „Diacor”. We also found that the prevalence of diabetic retinopathy is higher in OSA+ patients, than in OSA- patients, but not significantly. In OSA comorbid T2DM patients serum VEGF level was significantly higher, than in patients without OSA comorbidity. VEGF level was significantly higher in patients with microalbuminuria; diabetic retinopathy, as well as co-existence of diabetic retinopathy and microalbuminuria; diabetic retinopathy and proteinuria; diabetic retinopathy and CKD in OSA+, than is OSA- groups. Previous studies have shown an association between diabetic retinopathy and OSA and links between CKD and OSA [5, 6]. Differently from these studies, our research evaluated the association between OSA and both-diabetic retinopathy and CKD together and we also studied possible participated marker in the course of microangiopathy in this population. The research has limitations. We recruited the patients from one particular clinic and we are not able to generalize the results for all Georgian population.

Conclusion

According to the results we can suggest that it is important to screen all type 2 diabetes patients in Georgia for OSA, as the disease is quite frequent and is associated with high prevalence of microangiopathy. The fact that blood VEGF level is higher with OSA comorbidity and comparing microangiopathy and serum VEGF level in OSA+ and OSA- groups showed that the level of this marker is higher in OSA+ patients with microangiopathy, than in subjects with microangiopathy, but without OSA, indicates that blood VEGF might be an important participating marker taking place in microangiopathy pathogenesis in OSA comorbid T2DM patients.

Summary

Type 2 diabetes is associated with high prevalence of microangiopathy. Obstructive sleep apnea is a frequent comorbidity in patients with type 2 diabetes. Microangiopathy prevalence is higher in OSA comorbid T2DM patients, than in patients without OSA. Serum VEGF level is higher in OSA comorbidity, than without it and in OSA+ patients with microangiopathy VEGF level is higher, than in patients with microangiopathy but, without OSA comorbidity. Our data suggests, that blood VEGF is a participating marker taking place in microangiopathy pathogenesis in OSA comorbid T2DM patients.

References

1. International diabetes Federation (IDF) Diabetes Atlas. Eighth Edition 2017
2. Eva M. Kohner et al. Diabetic Retinopathy at Diagnosis of Non-Insulin-Dependent Diabetes Mellitus and Associated Risk Factors. United Kingdom Prospective Diabetes Study. ARCH OPTHALMOL / VOL 116, MAR 1998
3. Adler AI, Stevens RJ, Manley SE et al. Development and progression of nephropathy in type 2 diabetes: the United Kingdom Prospective Diabetes Study (UKPDS 64). 2003 Jan;63(1):225-32
4. Dr.Hasanain Ahmed. Kufa Med. The relevance of serum level of VEGF in type 2 diabetic retinopathy. Journal 2012.VOL.15.No.3. 106.
5. Obstructive sleep apnea, retinopathy linked in diabetes. American Thoracic Society's 105th International Conference. San Diego on May 19, 2009
6. Roberto Pisoni, MD Medical University of South Carolina. Sleep apnea may contribute to kidney disease progression. Pennsylvania Convention Center in Philadelphia, PA.American Society of Nephrology (ASN), ScienceDaily. 2014 November.
7. Sleep apnoea and type 2 diabetes. 2015 International Diabetes Federation
8. Joseph W Sassani MD. VEGF Level Correlated With Glycemic Control in Diabetic Retinopathy. Acta Ophthalmologica. Journal Scan / Research · March 25, 2013
9. Ma Jing , Xu Yongjian , Zhang Zhenxiang, Liu Huiguo , Xiong Weining , Xu Shuyun.Serum level of vascular endothelial growth factor in patients with obstructive sleep apnea hypopnea syndrome. Journal of Huazhong University of Science and Technology. April 2007, Volume 27, Issue 2, pp 157-160

EXAMINATION OF SST4 RECEPTOR AGONISTS IN MOUSE MODELS OF NEUROPATHIC PAIN, ANXIETY AND DEPRESSION-LIKE BEHAVIOUR

Boglárka Kántás

Department of Pharmacology and Pharmacotherapy,
University of Pécs Faculty of Medicine, Hungary

Tutor: Zsuzsanna Helyes, Éva Borbély, Ágnes Hunyady

Introduction

Nerve damage of different etiological factors can cause chronic neuropathic pain which often coupled with anxiety and depression, deteriorating quality of life.¹ Adjuvant analgesics are used in clinical practise for treatment however they are often ineffective or have severe side-effects limiting their long-term use. Thereby, development of new analgesic drugs with novel mechanism of action are necessary. Somatostatin has been proven to have analgesic, anti-inflammatory and antidepressant effects mediated by the somatostatin 4 receptor (sst4) without influencing endocrine functions.^{2,3,4,5}

Aims

We examined the in vivo actions of our two patented small molecule non-peptide sst4 agonists (VCC158015, VCC885587 synthesized by Vichem Ltd.) showing strong sst4 receptor activation in previous in vitro studies.

Methods

Tramatic sensory mononeuropathy was induced in male NMRI mice by partial ligation of sciatic nerve.⁶ The mechanonociceptive threshold of the hind paw was measured by dynamic plantar esthesiometry preoperatively and on the 7th postoperative day. Depression-like behavior was examined by tail suspension (TST)⁷ and forced swim (FST)⁸ tests, which represent different neuronal activation mechanisms of depression. Anxiety behavior was tested by elevated plus maze (EPM)⁹ and spontaneous locomotor activity by open field tests (OFT). Agonists or vehicle was administered orally one hour before all examinations.

Results

Both agonists significantly and dose-dependently decreased the operation-induced mechanical hyperalgesia (in 20, 100, 500 µg/kg doses). One of the agonists (VCC885587) in the highest dose influenced the spontaneous locomotor activity in OFT while the other had no effect. Both agonists (100 µg/kg) decreased significantly the depression-like behavior in the TST, however they were ineffective in the FST. Neither agonist showed anxiolytic effect in the EPM.

Discussion

Our orally administered sst4 agonists significantly and dose-dependently decreased neuropathic mechanical hyperalgesia and effectively reduced depression-like behaviour in TST. In previous study has been proven that in TST and FST represent partially different neuronal activation pathways. In sst4 gene deleted animals immobility time measured in FST was significantly higher compared the wild types but there was no difference in TST. In contrast, parenteral treatment with J2156 reduced depression-like behaviour in TST but not in FST These data are in accordance with the present results showing that exogenous activation of sst4 receptors result in antidepressant-like effects only in TST.¹⁰ Anxiolytic effect of any drug in EPM is variable with different mouse strains, therefore increasing the number of animals and repeating the test with other strain is necessary. Decreasing of spontaneous locomotor activity in the highest dose of VCC885587 may refer to sedative sideeffect although it is significantly higher dose than needed to anaglesic effect.

Conclusion

Examined sst4 agonists showed analgesic and antidepressant effects in our tests however their anxiolytic effect did not proved.

Summary

To sum up, orally administered sst4 agonists effectively reduced neuropathic mechanical hyperalgesia and depression-like behavior, therefore they provide novel perspectives for the development of new type of combined analgesic and antidepressant agent.

References:

1. Bair MJ, Robinson RL, Katon W, Kroenke K. Depression and pain comorbidity: a literature review. *Arch Intern Med.* 2003; 163(20):2433-45.
2. Szolcsányi J, Helyes Zs, Oroszi G, Nemeth J, Pintér E. Release of somatostatin and its role in the mediation of the anti-inflammatory effect induced by antidromic stimulation of sensory fibres of rat sciatic nerve. *Br J Pharmacol.* 1998; 123(5): 936–942.
3. Pintér E, Helyes Zs, Szolcsányi J. Inhibitory effect of somatostatin on inflammation and nociception. *Pharmacol. Ther.* 2006; 112: 440-456.
4. Sándor K, Elekes K, Szabó Á, Pintér E, Engström M, Wurster S, Szolcsányi J, Helyes Zs. Analgesic effects of the somatostatin sst4 receptor selective agonist J-2156 in acute and chronic pain models. *Eur J Pharmacol.* 2006; 539(1-2):71-5.
5. Helyes Zs, Pintér E, Szolcsányi J. TT-232. Somatostatin sst1/sst4 Agonist. Treatment of Neuropathic Pain. Treatment of Inflammation. *Drugs Future* 2005; 30(6): 558
6. Seltzer Z, Dubner R, Shir Y. A novel behavioural model of neuropathic pain disorders produced in rats by partial sciatic nerve injury. *Pain* 1990; 43, 205–218.
7. Steru L, Chermant R, Thierry B, Simon P. The tail suspension test: a new method for screening antidepressant in mice. *Psychopharmacology (Berl).* 1985; 85(3):367-70.
8. Porsolt RD, Le PM, Jalfre M. Depression: a new animal model sensitive to antidepressant treatments. *Nature* 1977; 266: 730-732.
9. Lister RG. The use of a puls-maze to measure anxiety in the mouse. *Psychopharmacology (Berl).* 1987; 92(2): 180-185

10. Scheich B, Gaszner B, Kormos V, László K, Ádori C, Borbély É, Hajna Z, Tékus V, Bölskei K, Ábrahám I, Pintér E, Szolcsányi J, Helyes Zs. Somatostatin receptor subtype 4 activation is involved in anxiety and depression-like behavior in mouse models. *Neuropharmacology*. 2016; 101:204-15.

MORTALITY RISK FACTORS AMONG INSTITUTIONALIZED GERIATRIC POPULATION

Anna Kańtoch

Department of Internal Medicine and Gerontology, Faculty of Medicine, Jagiellonian University Medical College, Kraków, Poland

Co-authors: Barbara Gryglewska, Jadwiga Wójkowska-Mach,
Piotr Heczko, Tomasz Grodzicki

Tutor: Barbara Gryglewska MD, PhD

Introduction

Residents of long-term care facilities (LTCF) are regarded as very specific population: often disabled, frail, with multimorbidity, polypharmacy, malnutrition and dementia. It was estimated that the prevalence of hypertension among nursing home residents oscillated around 16-71% and over 70% of them were treated with antihypertensive drugs (Welsh et al., 2014). They are often excluded from randomized trials so there is still the gap in the literature concerning the impact of antihypertensive treatment on mortality in this specific population (Messerli et al., 2008). An expert opinion of the European Society of Hypertension-European Union Geriatric Medicine Society (ESH-EUGMS) Working Group suggested that treating hypertension in very old, frail subjects should be individualized (Benetos et al., 2016).

Aim

The main aim of the study was to evaluate potential mortality risk factors among long-term care residents during one year of follow-up.

Material and Methods

The presented survey was a substudy of the continuous surveillance of infections in LTCF (Wójkowska-Mach et al., 2013).

The study was performed among 172 elderly residents of three long-term care facilities in Poland. The study population was divided into two groups: people who were alive [Group 1] and people who died [Group 2] during one year follow-up period. Medical documentation, blood pressure (BP) measurements, Body Mass Index (BMI) and selected tests including Abbreviated Mental Test Score (AMTS), physical dependence score, Mini Nutritional Assessment (MNA) and Barthel Index were performed in all study participants at the beginning of the study.

Statistical analysis

Results obtained in two analyzed groups were compared using U Mann-Whitney or Chi square tests. Univariate and multivariate logistic regression models were used for investigating the risk factors for mortality.

Results

The analyzed sample consisted of 172 long-term care residents. Group 1 (N=148) and group 2 (N=24) revealed similar age, number of diagnosed diseases, number of used treatment, BMI and BP values. However, group 2 showed significantly lower score in ADL (0 [0; 2.5] vs. 3 [1; 6]), Barthel Index (5 [0; 37.5] vs. 40 [15; 95]), MNA (8 [6;10] vs. 12 [9; 13]), AMTS (4 [2; 7] vs. 8 [6; 9]) and greater physical dependence score (4 [3; 5] vs. 3[1; 3]) than group 1. The statistical analysis showed that the potential risk factors that increased the mortality among residents were: diagnosed diabetes (8.1 OR [95% CI; 3.00 – 21.86], $p < 0.001$), dementia (3.0 OR [95% CI; 1.25 – 7.27], $p = 0.014$) and physical dependence (2.13 OR [95% CI 1.47 – 3.07], $p < 0.001$). The protection factor was diagnosis of hypertension (0.28 OR [0.10 – 0.74], $p = 0.010$).

Discussion

The performed study showed that residents of long-term care facilities with poorer nutritional and functional status, cognitive impairment, urinary incontinence and those who lived in the nursing home were more at risk for mortality outcome. Moreover, those residents who died during the follow-up period were more physically dependent, had a greater number of chronic diseases and took more drugs. The hypertension was found to be the protective factor for mortality while diabetes was the major risk factor leading to death. Our findings are consistent with the results of previous studies, which indicated that the functional dependency had a harmful impact on nursing home mortality (Thomas JM, et al. 2013). However, the impact of blood pressure on mortality in the old population with disabilities is still unclear. In our study, the association between the blood pressure level and mortality rate was not observed. Rådholm et al. revealed that low systolic blood pressure was associated with higher mortality among nursing home residents during follow-up period. The PARTAGE study also showed that there is an interaction between low systolic blood pressure and two or more antihypertensive drugs leading to higher mortality (Benetos et al., 2015).

Conclusion

Lower functional, nutritional, cognitive status, greater dependence and diagnosis of diabetes or dementia were negatively influenced on mortality outcomes. However, occurrence of hypertension may have positive impact on probability of survival among institutionalized individuals.

Summary

Presence of hypertension appeared to be the protective factor for mortality among institutionalized geriatric population.

References

1. Welsh T, Gladman J, Gordon AL.: The treatment of hypertension in care home residents: A systematic review of observational studies. *J Am Med Dir Assoc* 2014;15:8–16.
2. Messerli FH, Sulicka J, Gryglewska B.: Treatment of hypertension in the elderly. *N Engl J Med* 2008. 359:972-3.
3. Benetos A, Bulpitt CJ, Petrovic M et al.: An expert opinion from the european society of hypertension-european union geriatric medicine society working group on the management of hypertension in very old, frail subjects. *Hypertension* 2016; 67(5):820-5.

4. Wójkowska-Mach J, Gryglewska B, Czekaj J et al.: Infection control: Point prevalence study versus incidence study in Polish long-term care facilities in 2009-2010 in the Małopolska Region. *Infection* 2013. 41, 1–8.
5. Thomas JM, Cooney LM, Fried TR.: Systematic Review: Health-related Characteristics of Elderly Hospitalized Patients and Nursing Home Residents Associated with Short-term Mortality. *J Am Geriatr Soc* 2013. 61(6), 902–911.
6. Rådholm K, Festin K, Falk M, et al.: Blood pressure and all-cause mortality: a prospective study of nursing home residents. *Age Ageing* 2016. 45(6):826-832.
7. Benetos A, Labat C, Rossignol P, et al.: Treatment with multiple blood pressure medications, achieved blood pressure, and mortality in older nursing home residents: The PARTAGE study. *JAMA Intern. Med* 2015. 175, 989–995.

DYSFUNCTION OF HPV16-SPECIFIC CD8+ T CELLS INFILTRATING OROPHARYNGEAL CANCER IN RELATION TO THE EXPRESSION OF TIM-3 AND PD-1

Vladimír Koucký

Department of Otorhinolaryngology and Head and Neck Surgery, 1st Faculty of Medicine, Charles University in Prague and Motol University Hospital, Czech Republic
Sotio a.s., Prague, Czech Republic

Co-authors: K. Hladíková, S. Partlová, M. Zábrodský, J. Bouček, R. Špišek, A. Fialová

Tutors: Anna Fialová, Jan Bouček

Introduction

Human papillomavirus type 16 (HPV 16) has been identified as one of the most important etiological agents of oropharyngeal squamous cell carcinoma (OPC) [1]. Following the standard treatment, patients with HPV-associated tumors have a better clinical outcome than patients with tobacco-related carcinomas. Moreover, HPV E6 and E7 oncoproteins represent optimal specific targets for immunotherapy, as they are constitutively expressed and presented by cancer cells [2]. Preclinical studies have reported that anti-HPV E7 vaccines elicited E7-specific CD8+ T cells in tumor-bearing mouse models. Moreover, the presence of HPV-specific T cells was associated with partial regression of E7-expressing TC-1 tumors in immunized mice [3, 4]. In view of these facts the induction of a robust HPV-specific immune response may represent a promising therapeutic strategy. Targeted monotherapies as PD-1:PDL1 blockade shows only modest response rates (13–18%) in head and neck cancer (HNSCC), including HPV associated OPC [5, 6]. Nevertheless, preclinical data have shown that targeting PD-1 pathway simultaneously with either an alternative checkpoint molecule, such as T cell immunoglobulin and mucin domain 3 (Tim-3), or HPV16 E6/E7 oncoproteins, emerges as a promising approach for improvement of current immunotherapy [7]. The aim of this study was to analyze the frequency, phenotype and function of HPV16 E6/E7-specific tumor-infiltrating T cells (TILs) in oropharyngeal tumors and to test the effect of anti-PD1 mAb (nivolumab), soluble Tim-3 (sTim-3) and homeostatic in vitro expansion on these characteristics.

Methods

Blood samples and primary oropharyngeal squamous cell carcinoma specimens were obtained from 51 patients immediately after the surgery. The tumor tissues were processed into single cell suspensions using mechanic and chemical dissociation. Peripheral blood mononuclear cells (PBMCs) were isolated from the peripheral blood by centrifugation on a Ficoll-Paque density gradient. Freshly isolated TILs were expanded for two weeks in a medium containing IL-2. HPV16-specific T cells were detected after co-incubation with autologous monocytes that were isolated using a CD14+ magnetic separation, loaded with HPV16 E6/E7 peptide pools and added to expanded TILs at a ratio 1:10. After a 6h incubation, the cells were stained with antibodies

for the intracellular detection of cytokines. For extracellular and intracellular cell staining standard protocols and purchased fluorochrome-conjugated monoclonal antibodies were used. Labeled cells were analyzed on a BD FACSCanto II and evaluated with FlowJo software. For in vitro blocking studies anti-PD-1 mAb (nivolumab) and soluble Tim-3 were added to the TIL cultures 42h prior to specific stimulation with HPV16 E6/E7 peptide-loaded autologous monocytes. For determination of HPV status of samples real-time PCR and p16 immunohistochemistry were used. Statistical analyses were performed using Statistica® 10.0 software. The results were considered to be statistically significant when $p < 0.05$.

Results

We have detected HPV-specific IFN γ -producing CD8+ T cells in 73.1% of HPV-associated OPC samples, but not in TILs derived from HPV-negative tumor tissues. TNF α -producing CD8+ T cells were detected in 40% of HPV-associated tumors. Specific HPV16 E6/E7 pepmix stimulation induced IFN γ production preferentially in PD-1-Tim-3- and PD-1+Tim-3-CD8+ T cells ($29.7 \pm 13.6\%$ and $55.1 \pm 11.0\%$ from all IFN γ producing cells, respectively). TNF α production was also induced in Tim-3-CD8+ cells.

To confirm the effect of the PD-1/PD-L1 pathway blockade on IFN γ production and Tim-3 expression in CD8+ T cells, we analyzed the phenotype of expanded TILs after 48h incubation with nivolumab with/without the addition of recombinant sTim-3. We observed a slight effect of nivolumab alone on IFN γ production in HPV16 E6/E7 pepmix stimulated CD8+ T cells, however, IFN γ production significantly increased in the presence of nivolumab in combination with sTim-3.

We did not observe any effect of PD-1 blockade on Tim-3 upregulation on expanded TILs. To assess whether the absent effect might be associated with the homeostatic expansion, we analyzed freshly isolated tumor-derived cell suspensions under the same conditions. In the fresh samples, we observed a significant increase in Tim-3 expression on CD8+ T cells in nivolumab-treated cell cultures without any added stimuli, but there was only a minor increase in specifically stimulated cell cultures. Importantly, homeostatic expansion significantly affects the levels of checkpoint molecules PD-1 and Tim-3 on CD8+ and CD4+ T cells as we observed a shift from the prevailing PD-1+Tim-3-CD8+ population to the functionally impaired Tim-3+CD8+ population.

Discussion

It has been suggested that the improved overall survival of HPV-positive OPC patients was related to the immune response [8]. In this study, we characterized a phenotype and functionality of HPV-specific TILs derived from oropharyngeal cancer. Upon specific stimulation, IFN γ was mainly produced by PD-1+Tim-3- and PD-1-Tim-3- CD8+ T cells, thus affirming Tim-3 rather than PD-1 as a marker of advanced dysfunction. Indeed, we observed the highest proportion of IFN γ -producing cells exactly in the PD-1+Tim-3-CD8+ T cell subset. Whether this phenotype is in OPC associated preferentially with HPV-specific CD8+ T cells, or is also relevant in tumor-associated antigen (TAA)-specific CD8+ TILs, remains to be addressed. Also, we observed only a minor effect of nivolumab alone on the IFN γ production by TILs, however, proportions of IFN γ -producing CD8+ T cells substantially increased in the cultures treated with nivolumab in combination with sTim-3. Our data are in accordance with the previously reported synergistic effect of Tim-3 and PD-1 blockade in CT26 tumorbearing mice [9] and in a mouse model of orthotopic HPV16-positive HNSCC [10]. Moreover Tim-3 expression was substantially

increased in fresh CD8+ TILs following the PD-1 blockade, but this effect was markedly lower in cells stimulated with HPV16 E6/E7 peptides than in unstimulated cells. These data suggest that the specific stimulation of anti-HPV16 CD8+ T cells might suppress the upregulation of Tim-3 expression in response to the PD-1 blockade and thus has the capacity to overcome the Tim-3 mediated escape from anti-PD1 therapy.

Conclusion

We have shown that 73.1% of OPC patients with HPV-associated tumors had HPV16-specific TILs able to produce IFN γ upon specific stimulation. Moreover, we propose that Tim-3 rather than PD-1 is a marker of dysfunction in tumor infiltrating T cells and our data suggest that treatments combining anti-PD-1 blockade with therapeutic HPV vaccination and/or the additional blockade of inhibitory pathways, such as Tim-3, might increase specific antitumor immune response in HPV-associated OPC.

Summary

Human papillomavirus (HPV) type 16 infection is one of the most important etiological agents of oropharyngeal squamous cell carcinoma. Patients with HPV-associated carcinomas of the head and neck were reported to have a better prognosis than patients with HPV-negative tumors, no matter the chosen treatment modality. It has been suggested that the improved outcome of HPV-positive patients was related to the immune response. Because HPV16 E6 and E7 oncoproteins are highly immunogenic and constitutively expressed, HPV-specific T cell immunity may play the key role in improving the prognosis of these patients. We detected HPV16-specific tumor-infiltrating T cells in 73.1% of HPV-associated oropharyngeal tumors. HPV16 specific CD8+ TILs were able to produce IFN γ upon specific stimulation and predominantly expressed PD-1 but not Tim-3. Specific IFN γ production was further enhanced after a blockade of both PD-1 and Tim-3 pathways but not after a PD-1 blockade alone. Additionally, the specific stimulation of anti-HPV16 CD8+ T cells suppressed Tim-3 upregulation after the PD-1 blockade. Our data provide the rationale for combination cancer immunotherapy approaches, including a dual blockade of PD-1 and Tim-3 and, potentially, the use of HPV16-directed therapeutic vaccines.

References

1. Torre, L.A., et al., *Global cancer statistics, 2012*. CA Cancer J Clin, 2015. **65**(2): p. 87-108.
2. Best, S.R., K.J. Niparko, and S.I. Pai, *Biology of human papillomavirus infection and immune therapy for HPV-related head and neck cancers*. Otolaryngol Clin North Am, 2012. **45**(4): p. 807-22.
3. Badoual, C., et al., *PD-1-expressing tumor-infiltrating T cells are a favorable prognostic biomarker in HPV-associated head and neck cancer*. Cancer Res, 2013. **73**(1): p. 128-38.
4. Best, S.R., et al., *Administration of HPV DNA vaccine via electroporation elicits the strongest CD8+ T cell immune responses compared to intramuscular injection and intradermal gene gun delivery*. Vaccine, 2009. **27**(40): p. 5450-9.
5. Bauml, J., et al., *Pembrolizumab for Platinum- and Cetuximab-Refractory Head and Neck Cancer: Results From a Single-Arm, Phase II Study*. J Clin Oncol, 2017. **35**(14): p. 1542-1549.

6. Ferris, R.L., et al., *Nivolumab for Recurrent Squamous-Cell Carcinoma of the Head and Neck*. N Engl J Med, 2016. **375**(19): p. 1856-1867.
7. Koyama, S., et al., *Adaptive resistance to therapeutic PD-1 blockade is associated with upregulation of alternative immune checkpoints*. Nat Commun, 2016. **7**: p. 10501.
8. Spanos, W.C., et al., *Immune response during therapy with cisplatin or radiation for human papillomavirus-related head and neck cancer*. Arch Otolaryngol Head Neck Surg, 2009. **135**(11): p. 1137-46.
9. Sakuishi, K., et al., *Targeting Tim-3 and PD-1 pathways to reverse T cell exhaustion and restore anti-tumor immunity*. J Exp Med, 2010. **207**(10): p. 2187-94.
10. Shayan, G., et al., *Adaptive resistance to anti-PD1 therapy by Tim-3 upregulation is mediated by the PI3K-Akt pathway in head and neck cancer*. Oncoimmunology, 2017. **6**(1): p. e1261779.

AGE DEPENDENT NEURONAL ACTIVATION OF STRESS CENTERS IN ACUTE AND CHRONIC STRESS MODELS IN THE RAT

Kovács László Ákos

Department of Anatomy, University of Pécs, Medical School, Hungary

Co-authors: Josef Andreas Schiessl, Anna Elisabeth Nafz, Valér Csernus, Balázs Gaszner

Tutor: Balázs Gaszner

Introduction

Stress is the nonspecific response of the body to threatening demand dedicated to maintain the homeostasis by coordinating adaptive response. The hypothalamus-pituitary-adrenal (HPA) axis is the chief regulator of stress response. The key of the HPA axis is the paraventricular nucleus of the hypothalamus (PVN), releasing corticotropin-releasing factor (CRF) inducing adrenocorticotropin (ACTH) excretion from the anterior pituitary to control glucocorticoid secretion in the adrenal cortex. Cortisol (in humans) and corticosterone (CORT) (in rodents) are dedicated to maintain or restore homeostasis. The maladaptation stress response can be associated with the development of stress-related mood disorders. Numerous stress-related limbic and brainstem centers send afferents converging to the PVN, such as the subdivisions of extended amygdala, the centrally projecting Edinger-Westphal nucleus (cpEW) and dorsal raphe nucleus (DR). Moreover PVN, central amygdala (CeA) and bed nucleus of stria terminalis (BNST) harbour the CRF of the brain

The functional-morphological assessment of acute neuronal activity is widely performed by semi-quantitation of immediate early gene (IEG) expression such as c-fos. Activation of the PVN is shown by c-Fos immunocytochemistry indicating rapid activation of a gene transcription and synaptic activation. This expression peaks 2 hours after stress exposure than declines to baseline. Another member of Jun/Fos proto-oncogene family is fos-b. The long-term activation of neurons is frequently assessed by FosB labeling. The delta splice variant presence of FosB refers to a neuronal activation characterized by chronic dynamics on weeks scale.

The HPA axis reactivity might be altered by age, but little is known about the background of this age-dependency. Sporadic data suggest that stress sensitivity as assessed by semi-quantitation of the neuronal activity marker c-Fos may be influenced by age.

Aims

Here we aimed to perform a throughout lifespan c-Fos mapping in the extended amygdala nuclei: [CeA, basolateral (BLA), medial (MeA) nuclei, BNSTov, ventral (vBNST), dorsomedial (dmBNST), dorsolateral (dlBNST), fusiform (fuBNST)], DR, cpEW and PVN. The second aim of this study was to test if CRF expressing areas show age dependency in their IEG expression in acute and chronic stress.

Methods

200 male rats were separated to eight different age groups: 1-month-old, 1.5-month-old, 2-month-old, 3-month-old, 6-month-old, 12-month-old, 18-month-old and 24-month-old). Rats in all age groups were exposed to 60-mins acute restraint stress (ARS) vs. controls. To test the chronic stress-sensitivity, except for 1- and 1.5-month-old rats, a third animal group was exposed to chronic mild variable stress (CMVS) contained a daytime short- (tilted cage, dark room, shaking, restraint) and a night time long (social isolation, group holding, wet bedding) stress for 2 weeks. Finally, after blood sampling animals were perfused. Adrenals, thymus glands and brains were collected. Blood corticosterone was determined by radioimmunoassay. Series of 30 μm coronal brain section were cut to perform a) c-Fos immuno-labeling with diamino-benzidine in the above listed areas. In the second b) experiment another series of sections was used to perform fluorescent triple labeling for c-Fos, FosB and CRF in the PVN, CeA and BNSTov. After manual cell counting using ImageJ program, results were evaluated by analysis of variance followed by Tukey's post hoc test.

Results

ARS increased CORT in an age dependent manner. Relative adrenal gland weights increased in CMVS groups, while the relative thymus weights were decreased in younger CMVS groups. In the acute model, ARS increased c-Fos expression in all nuclei peaking in 2-month-old group and gradually declined till senescence. Comparison of ARS groups this 2nd month peak expression was significantly high in nine areas (MeA, CeA, BNSTov, dBNST, dmBNST, fuBNST, cpEW and DR- see the BNST in fig. 1) compared to controls. The c-Fos cells characterization showed that CRF-cFos positive cells were not changed by age or ARS in CeA and BSTov. In contrast the number of PVN CRF-cFos neurons were increased by ARS and its magnitude smaller declined with age as shown by their strong statistical interaction (see fig. 2). CMVS elevated the number of FosB neurons in PVN which was not age dependent. Conversely in CeA and BNSTov the FosB expression was not changed by any factor. Multiple labelling showed that the PVN-FosB signal increased in in CRF cells upon CMVS (see fig. 3).

Discussion: In line with earlier findings increase blood CORT titer and c-Fos expression rise indicate the efficacy of ARS. Adrenal gland and thymus weights' data suggest the CMVS was also efficient in our model. The relatively high c-Fos rise in young rats decreased with age, in contrast, the CORT response remained stable. This indicates that the c-Fos expression in the PVN is not a reliable marker of HPA axis activity in the course of aging. On the other hand, other not examined factors and/or brain regions may have contributed to the stability of the HPA axis reactivity. Triple labelling supported that this c-Fos pattern is characteristic for the CRF-positive cells in the PVN, but not in the CeA or BNSTov. In contrast to the CeA and BNSTov, PVN showed increased FosB expression in CRF neurons upon CMVS. Unlike that of c-Fos, the FosB reactivity did not alter with age. This suggests that the FosB expression might be responsible for the stabilization of the HPA axis response in old age, when c-Fos reactivity declines. It has to be considered that the value of our results is limited. We could not provide information about the functional identity of labelled cells. Therefore higher c-Fos expression might refer either increase excitation or inhibition.

Conclusion

To the best of our knowledge this is the first study to provide a systematic comparison of IEGs expression in 11 stress centers of the rat brain in eight age groups. This is the first work to provide throughout lifespan comparison of stress reactivity of the main CRF systems in acute and chronic stress model in the rat. The chronic stress-induced FosB expression remained stable in PVN-CRF cells suggesting their constant sensitivity till senescence that might compensate the decreasing c-Fos sensitivity.

Summary

The major methodical message of this study is that outcomes of similar experimental studies are highly brain region and age sensitive. The model might be useful to see how age can modify the adaptive/maladaptive responses, but further investigations/characterizations and functional behavioral studies are necessary to understand it. All this age dependent tendencies might be associated with both increased and decreased sensitivity in patients suffering from mood disorders (i.e.: major depressive disorder).

Reference

1. Sawchenko, P.E., Li, H.Y., Ericsson, A. (2000). Circuits and mechanisms governing hypothalamic responses to stress: a tale of two paradigms. *Prog Brain Res* 122:61–78.
2. Kellogg, C.K., Awatramani, G.B., Piekut, D.T. (1998). Adolescent development alters stressor-induced Fos immunoreactivity in rat brain. *Neuroscience* 83: 681–9.
3. Kovács, K.J. (2008). Measurement of Immediate-Early Gene Activation- c-fos and beyond. *J. Neuroendocrinol* 20. 665–72.
4. Gaszner, B., Kormos, V., Kozicz, T., Hashimoto, H., Reglődi, D., Helyes, Z. (2012). The Behavioral phenotype of pituitary adenylate cyclase activating polypeptide-deficient mice in anxiety and depression tests is accompanied by blunted c-Fos expression in the bed nucleus of the stria terminalis central projecting Edinger-Westphal nucleus ventral lateral septum and dorsal raphe nucleus. *Neuroscience* 202:283–99.
5. Otake, K. (2005). Cholecystokinin and substance P immunoreactive projections to the paraventricular thalamic nucleus in the rat. *Neurosci Res* 51:383–94.
6. Wilson, M.A., Grillo, C.A., Fadel, J.R., Reagan, L.P. (2015): Stress as a one-armed bandit: Differential effects of stress paradigms on the morphology, neurochemistry and behavior in the rodent amygdala. *Neurobiol Stress* 1:195-208.
7. Kormos, V., Gáspár, L., Kovács, L., Farkas, J., Gaszner, T., Csernus, V. et al. (2016). Reduced response to chronic mild stress in PACAP mutant mice is associated with blunted FosB expression in limbic forebrain and brainstem centers. *Neuroscience* 330:335-58.
8. Romeo, R.D. (2010): Pubertal maturation and programming of hypothalamic–pituitary–adrenal reactivity. *Front Neuroendocrinol* 31:232-40.
9. Bale, T.L., Epperson, C.N. (2015). Sex differences and stress across the lifespan. *Nat neurosci* 18:1413-20.
10. Kovács LÁ, JA, Nafz AE, Csernus V, Gaszner B (2018): Both Basal and Acute Restraint Stress-Induced c-Fos Expression Is Influenced by Age in the Extended Amygdala and Brainstem Stress Centers in Male Rats *Front Aging Neurosci.* 2018; 10: 248.

Results graphs

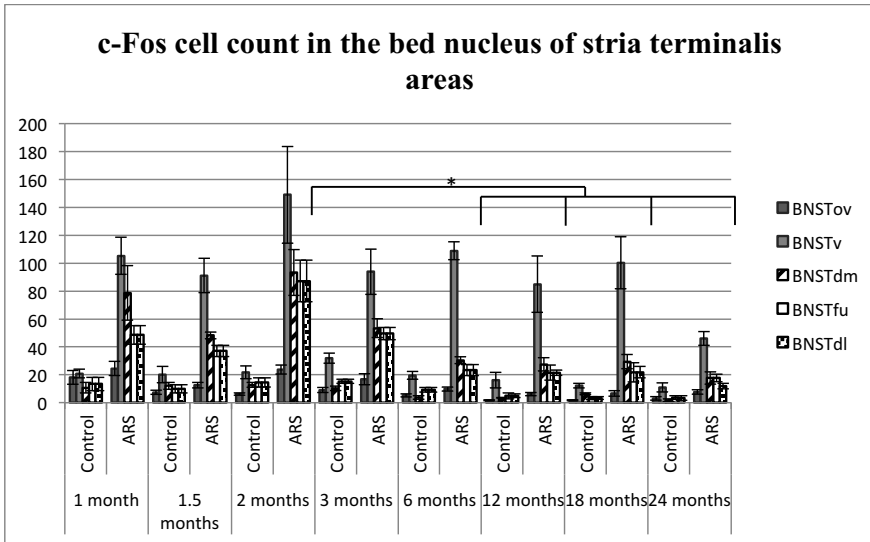


Figure 1.: The c-Fos cell count in the Bed nucleus of stria terminalis areas.

Two-way analysis of variance: in BNSTov: ARS ($F=51.24$ $p<10^{-6}$), age ($F=13.61$ $p<10^{-6}$); in dlBNST ARS ($F=47.43$ $p<10^{-6}$) age ($F=15.11$ $p<10^{-6}$); in vBNST ARS ($F=177.1$ $p<10^{-6}$) age ($F=3,38$ $p<0.005$), in fuBNST ($F=128.96$ $p<10^{-6}$) age ($F=11.68$ $p<10^{-6}$) ARS and age interaction ($F=2.44$ $p<0.05$). Tukey's post hoc value $p<0.05$

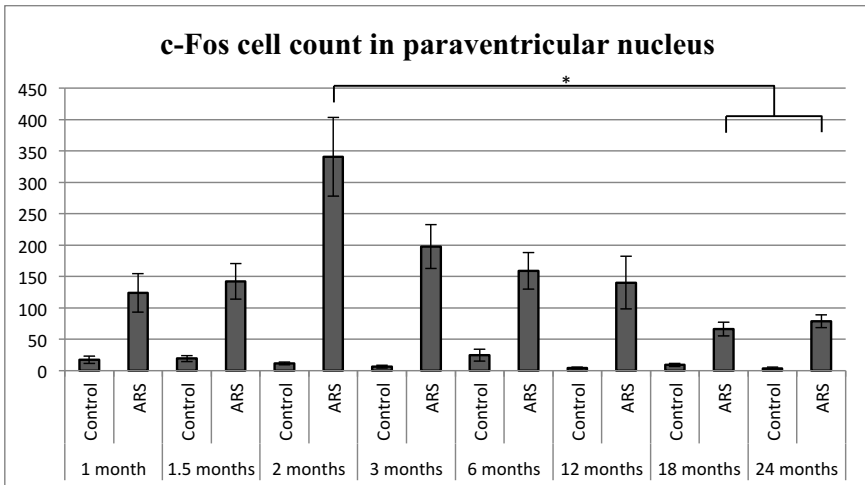


Figure 2.: The c-Fos cell count in the paraventricular nucleus

Two-way analysis of variance: ARS ($F= 278.18$ $p<10^{-6}$), age ($F= 4.99$ $p<0.0005$); ARS and age interaction ($F=2.55$ $p<0.05$). Tukey's post hoc value $p<0.05$

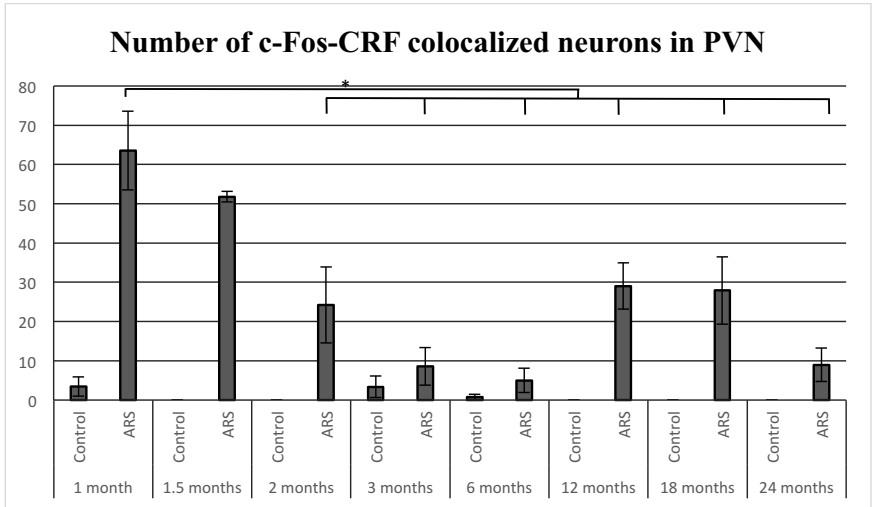


Figure 3.: The c-Fos, CRF double labelled cells' count in the paraventricular nucleus
 Two-way analysis of variance: ARS ($F= 7.71$ $p<10^{-5}$), age ($F= 74.39$ $p<10^{-6}$); ARS and age interaction ($F=7.68$ $p<10^{-5}$). Tukey's post hoc value $p<0.05$

COMPLEMENTARY AND ALTERNATIVE MEDICINE PRACTICE AND HEALTHCARE INTEGRATION IN GEORGIA

Ilia Nadareishvili

David Tvildiani Medical University

Tutors: Giorgi Pkhakadze, Karsten Lunze (Boston University)

Complementary and Alternative Medicine (CAM) is used by a steadily growing number of people across the world, [1] as an important, albeit often overlooked part of global health. The Georgian population has used different forms of CAM for many centuries.

The World Health Organization (WHO) sets out the course for Traditional and Complementary Medicine for the next decade in the Traditional Medicine Strategy 2014-2023, which mandates all the member states to introduce, improve and develop CAM research projects, as the base for policy development in member states and internationally. [1] CAM regulatory models are of high variability among countries. [2, 3] Such structures as the Council of Europe (Georgia is member since 1999) or European Parliament have a few resolutions related to CAM practice. Weaknesses in regulatory frameworks poses risks to patients, [2, 4] creates uncertainty in conventional medical practice as well as in CAM, while preventing the progress in cooperation ensuring effective utilization of CAM benefits. [5]

The aim of the study was to identify active and previous CAM practice regulations in Georgia, their strengths and weaknesses, identify key actors and analyze their related perspectives and needs.

Methods

We used mixed method approach combining qualitative, quantitative research methodology. We identified leading CAM actors through the National Public Registry looking for non-governmental organizations, private commercial companies and other possible bodies specializing in CAM practice, research and other activities.

In depth contextual interviews were conducted over the course of 1 year involving 20 long term CAM users, 15 CAM leading practitioners, Medical Education experts and conventional medicine professional organization leaders. Quantitative survey involved 300 CAM users who filled down a detailed questionnaire at 20 locations across Georgia.

We approached regulatory agency at the Ministry of Labour, Social Security and Health of Georgia for information on current or planned CAM regulations. We also searched through online archives of the Georgian Parliament and other repositories for any mention of CAM in the documents stored in their databases.

Results

CAM use main reasons in Georgia are low satisfaction and prevalent mistrust towards conventional medicine, negative attitudes and misconceptions regarding medications, perception of more attention and care from CAM practitioners compared to conventional physicians and general satisfaction with CAM experience. Patients express high interest in CAM integration into the healthcare and enhancement of physician-practitioner relationships.

We identified a vast variety of CAM practices and products available in Georgian market including through conventional medicine facilities and pharmacy networks. We identified professional unions in some CAM modalities, most of them not working effectively or involved in CAM regulation, quality assurance or integration process.

None of the CAM modalities is currently regulated as medical specialty by the state. There is no specific CAM practitioner certification mechanism, though many of practitioners have a physician certificate. Additionally there are no current plans to develop or install any CAM practice regulations. According to the representative of regulatory agency on medical activities, medical ethics and malpractice responsibility cannot be applied to those not certified as physicians.

CAM products can be registered voluntarily through simplified procedures, with some additional regulations on product marketing. The products are often prescribed by conventional medicine physicians, who though have no specific education or training regarding the used CAM approaches, which raised concerns in medical and academic communities.

Self-regulation wasn't identified, while professional organizations lack resources (both professional and material), authority (no mutual recognition or cooperation) and declare no motivation or reasons to establish and implement self-regulation or develop/deliver CAM education in any format due to low interest from practitioners to get formal education and very low interest seen from the governmental structures in response to proposed initiatives. Practitioners agree that a CAM practitioner should hold an MD degree. Some CAM professional organization leaders have false knowledge and understating on the current regulatory environment, or tend to blame the government for the existing problem.

Attitude to CAM ranged from highly positive to negative among the interviewed conventional medicine physician and professional organization leaders, while frequent patient forwarding in both directions was confirmed. Management by an independent, self-governing board with cooperation with the Ministry of Health was suggested. Necessity for educational programmes is emphasized with MD degree as a base for further CAM education and practice. "Eventually patients' health depends depend on their luck, either they come to a qualified specialist or risk to be harmed" an association president concludes.

Discussion

Professional organizations while currently inactive could play a more active role, as in a few EU countries. [2] Governmental structures lack resources, both human and material in order to pay more attention on the issue and initiate a step by step policy development, based on a parallel research process, as advised for the European countries. [6] Suggestions that self-regulation can be a way out (supported in some way by all our respondents); that it is currently not clear who has the capacity and "expertise" to implement the self-regulations and take leadership, that there is no clear research strategy or will to implement systematic research and that Georgian practitioners in each discipline could work on setting own standards and competences resemble foreign studies'

findings. [7, 8] There is no vision or prospects for “statutory regulations” while this approach seems to gain momentum internationally. [9] The tendency to agree on MD degree as a base for any further CAM career is coherent to the existing regulations in a number of European countries, as evident by the CAMbrella report. [2]

In light of stable if not increasing CAM use in by patients and high rate of non-disclosure to their physicians [10] the problem’s urgency only increases.

Conclusion

Regulations on CAM practice are currently effectively non-existent and Georgia as a whole is currently not in line with the WHO and EU directives and recommendations. Practitioners, physicians, educators and other stakeholders agree on need for some regulations, e.g. self-regulation, while government has no plans to develop such. Establishment of a national working group to develop classification, core regulatory documents is recommended, while awareness on CAM should be raised among all the stakeholders.

Summary

The aim of this study was to analyze CAM regulations in Georgia, identify key actors and analyze their perspectives and needs. Use of CAM to stay persistent while patients need healthcare integration. No current regulatory frameworks on practice, while product registration and marketing ones are acting. Practitioners, physicians, educators and other stakeholders agree on need for some regulations, e.g. self-regulation, while government has no plans to develop such. Establishment of a national working group to develop classification, core regulatory documents is recommended, while awareness on CAM should be raised among all the stakeholders.

Acknowledgment

Research project financial support was provided by Shota Rustaveli National Science Foundaiton (SRNSF) (www.rustaveli.org.ge), grant # PhDF2016_29

References

1. WHO, WHO traditional medicine strategy: 2014-2023, 2013
2. Wiesener et al, CAMbrella WP2 Report “Legal status and regulation of CAM in Europe”, 2012
3. Ajazuddin, & Saraf, S. Legal regulations of complementary and alternative medicines in different countries. *Pharmacognosy Reviews*, 2012, 6(12), 154–160.
4. Ventola, Current Issues Regarding Complementary and Alternative Medicine (CAM) in the United States, *Pharmacy and Therapeutics*, 2010 Sep; 35(9): 514–522.
5. Institute of Medicine (US) Committee on the Use of Complementary and Alternative Medicine by the American Public. *Complementary and Alternative Medicine in the United States*. Washington (DC): National Academies Press (US); 2005. 7, Integration of CAM and Conventional Medicine.
6. Fischer et al, High prevalence but limited evidence in complementary and alternative medicine: guidelines for future research, *BMC Complementary and Alternative Medicine*, 2014 14:46
7. Mills SY. Regulation in complementary and alternative medicine. *BMJ : British Medical Journal*. 2001;322(7279):158-160.

8. Sandy Welsh, Merrijoy Kelner, Beverly Wellman and Heather Boon, Moving forward? Complementary and alternative practitioners seeking self-regulation, *Sociology of Health & Illness* Vol. 26 No. 2 2004 ISSN 0141-9889, pp. 216-241
9. Nadine Ijaz and Heather Boon. *The Journal of Alternative and Complementary Medicine*. Apr 2018 0346
10. I. Nadareishvili, K. Lunze, N. Tabagari, A. Beraia, G. Pkhakadze, Complementary and Alternative Medicine Use in Georgia, *GeoMedNews*, 2017, Nov;(272):157-164.

EXOGENOUS SURFACTANT AND PULMONARY HOMEOSTASIS IN AN ANIMAL MODEL OF LPS-INDUCED ACUTE LUNG INJURY

Zuzana Nová

Biomedical Center Martin, Department of Physiology and Department of Medical Biology,
Jessenius Faculty of Medicine, Comenius University, Martin, Slovakia

Co-authors: M. Kolomaznik, D. Mokra, I. Zila, J. Kopincova, E. Vidomanova,
H. Skovierova, E. Halasova

Tutor: Andrea Calkovska

Introduction

Pulmonary surfactant is a substance produced by the alveolar type II (ATII) cells. It consists of lipids and surfactant specific proteins (SPs) SP-A, SP-B, SP-C and SP-D. It's main function is to reduce surface tension at the air/liquid interface and prevent lung collapse (Echaide et al. 2017). Many factors, e.g. plasma proteins, meconium, proinflammatory substances, proteolytic enzymes or bacteria interfere with alveolar environment and lead to surfactant dysfunction. Lipopolysaccharide (LPS), also named endotoxin, is a constituent of the outer bacterial cell membrane which contributes to the local inflammation and leads to systemic toxicity during Gram-negative infection (Canadas et al. 2011). LPS interferes with all major components of pulmonary surfactant (Kolomaznik et al., 2018) and reduces viability of ATII cells. In animal models, the instillation of LPS to the respiratory system induces acute lung injury (Kolomaznik et al. 2017). Pulmonary inflammation and subsequent changes in SPs expression could be mediated by toll like receptors (TLRs) expressed by ATII cells. LPS activates TLRs and triggers NF- κ B-mediated production of pro-inflammatory cytokines and chemokines such as interleukins IL-1 β and IL-6, tumor necrosis factor α (TNF- α) and type 1 interferons (IFN) (Wu et al. 2011, Wang X et al. 2016). Important factor involved in LPS-induced death of alveolar epithelial cells could be an augmentation of intracellular reactive oxygen species (ROS) (Chuang et al. 2011).

The aim of this study was to evaluate the effect of exogenous surfactant on lung functions and SPs in an animal model of LPS-induced lung injury.

Material and methods

Adult anesthetized rats (Wistar) received intratracheally (i.t.) saline (control) or LPS (*E. coli*, O55:B5) at 500 or 1000 μ g/kg b.w and were ventilated with 40% oxygen. After 1 hour, animals with LPS received no treatment, or Curosurf (Chiesi Farmaceutici, Parma, Italy) at 50 mg of phospholipids/kg. All animals were ventilated for next 4 hrs. At the end of experiment, inflammatory markers and oxidative stress (TBARS) were evaluated in homogenized lung (HL) tissue and bronchoalveolar lavage fluid (BALF). Lung edema was expressed as wet/dry weight ratio. Expression of SPs genes *SFTPA*, *SFTPB*, *SFTPC*, *SFTPD* was analysed by real-time PCR with RPL-13a used as a reference gene.

Results

LPS at 500 µg/kg after 5 hours from i.t. administration induced lung edema ($p < 0.01$), increased levels of IL-1 β ($p < 0.01$), ANGPT2 ($p < 0.05$) in HL and BALF and oxidative stress in HL (TBARS, $p < 0.05$). At least 1.5-fold decrease was present in the expression of all SPs in the lungs after LPS 500 µg/kg ($P < 0.05$ vs. controls), while LPS at 1000 µg/kg further potentiated this effect.

Administration of exogenous surfactant reduced IL-1 β , MCP-1 and ANGPT2 in BALF (all $p < 0.05$), lung edema ($p < 0.05$) and increased the expression of SP-A, B and C.

Discussion

Intratracheal administration of LPS induces inflammation and tissue damage resembling acute lung injury and acute respiratory distress syndrome (Blumenthal et al. 2006). In our study i.t. LPS at 500 µg/kg induced lung edema, inflammation and oxidative damage of lungs demonstrated by increased levels of IL-1 β , ANGPT2 and oxidative stress. It was shown that endotoxin administration causes rapid changes in the composition of the surfactant pool and the resident cell population (Garcia-Verdugo et al. 2008, Wu et al. 2011). LPS also modulates levels of surfactant proteins (SPs) (Kolomaznik et al. 2017) what is consistent with reduced expression of all surfactant proteins in our experiment. There is a growing evidence of surfactant benefit in lung injury treatment (discussed more in Kolomaznik et al. 2017). We tested the effect of a clinically used modified porcine pulmonary surfactant on lung functions and SPs after LPS challenge. Curosurf at low-dose improved lung function and also increased SP-A, SP-B and SP-C expression, which can indicate recovery of local immune processes in the lungs.

Conclusions

In ventilated rats, intratracheal administration of LPS induces changes that resemble bacterial infection with inflammation, oxidative damage and reduced expression of all surfactant proteins. Exogenous surfactant at low-dose restores lung function and increases SP-A, SP-B and SP-C expression, which indicates recovery of local immune processes in the lungs.

Summary

The respiratory system is constantly exposed to toxic substances and pathogens from air or via blood stream, which can damage alveolar epithelium and cause severe respiratory disorders. Lipopolysaccharide (LPS) can reach the airspaces as the major component of the outer membrane of Gram-negative bacteria, and lead to local inflammation and systemic toxicity. LPS affects alveolar type II cells and interacts with surfactant film leading to its inactivation. Endotoxin-induced lung injury can be favorably influenced by intratracheal (i.t.) instillation of exogenous surfactant. We used animal model of acute lung injury caused by i.t. LPS to evaluate effect of endotoxin on lungs. LPS induced lung edema, increased levels of IL-1 β , ANGPT2 and oxidative stress. Also decrease in the expression of all SPs was present in the lungs after LPS administration. Instillation of therapeutic exogenous surfactant Curosurf reduced lung edema, levels of IL-1 β , MCP-1 and ANGPT2 and increased the expression of SP-A, B and C and thus re-established lung homeostasis. The mechanisms of its beneficial effect need to be further clarified.

Supported by VEGA 1/0469/16 and GUK 21/2018.

References

1. Blumenthal S, Borgeat A, Pasch T et al.: Ropivacaine decreases inflammation in experimental endotoxin-induced lung injury. *Anesthesiology* 2006; 104, 961-969.
2. Canadas O, Keough KM and Casals C: Bacterial lipopolysaccharide promotes destabilization of lung surfactant-like films. *Biophys J* 2011; 100, 108-116.
3. Chuang CY, Chen TL, Cherng YG et al.: Lipopolysaccharide induces apoptotic insults to human alveolar epithelial A549 cells through reactive oxygen species-mediated activation of an intrinsic mitochondrion-dependent pathway. *Arch Toxicol* 2011; 85, 209-218.
4. Echaide M, Autilio C, Arroyo et al.: Restoring pulmonary surfactant membranes and films at the respiratory surface. *Biochim Biophys Acta* 2017; 1859, 1725-1739.
5. Garcia-Verdugo I, Ravasio A, De Paco EG et al.: Long-term exposure to LPS enhances the rate of stimulated exocytosis and surfactant secretion in alveolar type II cells and upregulates P2Y2 receptor expression. *Am J Physiol Lung Cell Mol Physiol* 2008; 295, L708-L717.
6. Kolomaznik M, Nova Z and Calkovska A: Pulmonary surfactant and bacterial lipopolysaccharide: the interaction and its functional consequences. *Physiol Res.* 2017; 66 (Supplementum 2), S147-S157.
7. Kolomaznik M, Liskayova G, Kanjakova N et al.: The Perturbation of Pulmonary surfactant by bacterial lipopolysaccharide and its reversal by polymyxin B: function and structure. *Int J Mol Sci.* 2018; 19(7), pii: E1964.
8. Van Helden HP, Kuijpers WC, Langerwerf PE et al.: Efficacy of Curosurf in a rat model of acute respiratory distress syndrome. *Eur Respir J* 1998; 12, 533-539.
9. Wang WN, Zhou JH, Wang P et al.: The localization of SP-B and influences of lipopolysaccharide on it. *Eur Rev Med Pharmacol Sci* 2016; 20, 2338-2345.
10. Wu TT, Chen TL, Loon WS et al.: Lipopolysaccharide stimulates syntheses of toll like receptor 2 and surfactant protein-A in human alveolar epithelial A549 cells through upregulating phosphorylation of MEK1 and ERK1/2 and sequential activation of NF- κ B. *Cytokine* 2011; 55, 40-47.

NATURAL IGM ANTIBODIES PROTECT FROM MICROVESICLE-DRIVEN THROMBOSIS.

Georg Obermayer

Department of Laboratory Medicine, Medical University of Vienna
Vienna, Austria

Co-authors: Taras Afonyushkin, Florian Puhm, Waltraud Schrottmaier,
Michael Schwameis, Alice Assinger, Bernd Jilma, Christoph J. Binder

Tutor: Christoph J. Binder

Background

Natural IgM are germline encoded antibodies that exhibit important housekeeping immune functions (Ehrenstein and Notley 2010). A large part of natural IgM has been found to bind oxidation-specific epitopes (OSE), such as malondialdehyde (MDA)-adducts (Chou et al. 2009). Microvesicles (MVs) are a subtype of extracellular vesicles and important mediators of coagulation (Owens and Mackman 2011). We have recently shown that 50% of circulating MVs are recognized by MDA-specific natural IgM antibodies (Tsiantoulas et al. 2015). While IgM antibodies that bind OSEs have been shown to influence arterial thrombosis as protective factors in atherosclerosis development (Su et al. 2006), we investigated whether they could modulate coagulation more directly.

Aims

To explore whether IgM antibodies in general and natural IgM in particular can directly influence the procoagulatory properties of MVs.

Methods

Flow cytometry was used to assess the IgM positivity of circulating MVs in a small healthy cohort. Thrombin generation (TG) was performed in pooled plasma supplemented with MVs from individual donors. Further clotting tests performed were rotational thromboelastometry (ROTEM), platelet aggregation, fibrin generation (FG) activated partial thromboplastin time (aPTT) and prothrombin time (PT) were used to study the MDA-specific IgM LR04 on coagulation in vitro. A murine pulmonary thrombosis model was used to assess effects of LR04 in vivo.

Results

Pooled human plasma that has been IgM depleted, exhibits an increased thrombin generation potential triggered by MVs. The presence of IgM on circulating MVs of healthy donors inversely correlates with their procoagulant activity. Furthermore, platelet poor plasma from mice lacking sialic acid binding Ig-like lectin G (Siglec-G^{-/-}), which display high amounts of circulating and MV-bound IgM, shows lower spontaneous thrombin generation potential compared to wildtype plasma.

The natural OSE-binding IgM antibody LR04 caused delay of all clotting parameters in ROTEM but had no influence on washed platelet aggregation or aPTT and PT, which are MV-insensitive. In contrast, LR04 significantly delayed MV-induced TG and FG in plasma. A similar delaying effect was observed with other OSE binding antibodies, but not cleaved Fab fragments of LR04. Using flow cytometry, preincubation of MVs with LR04 showed impaired binding of both AnnexinV and Factor Xa to the MV-surface. Importantly, in a pulmonary thrombosis model, co-injection of LR04 significantly increased 30-minute survival of mice when injected with thrombogenic MVs, but not when injected with collagen.

Discussion

Our experiments demonstrate a novel role of IgM antibodies in the direct modulation of coagulation by binding to procoagulatory MVs. This is shown by IgM depletion of plasma leading to increased thrombin generation potential which is also seen in donors MVs which are low for bound IgM. On the other hand, the plasma of Siglec-G^{-/-} mice, which exhibit high free and MV-bound IgM, show lower thrombin generation potential compared to wildtype plasma. Furthermore, OSE-binding IgM antibodies show anticoagulatory properties, both in vitro coagulation assays, as well as in a murine pulmonary thrombosis model, mediated by inhibiting factor Xa binding to MVs. Further studies have to be performed to assess whether OSE-binding IgM antibodies can be used as a risk marker in populations at risk for venous thrombosis, as indicated by one of our previously published studies (Eichinger et al. 2017). Another application for our findings could be the boosting of natural OSE-binding antibodies to reduce thrombosis risk, possibly via immunization strategies previously shown in mice (Binder et al. 2003) to reduce atherosclerotic lesion size.

Conclusion

Our study identifies a previously unknown protective role of MDA-specific natural IgM antibodies in MV-induced coagulation and thrombosis. These effects require the full IgM structure and are exerted on the common pathway of the coagulation cascade. Our findings may open new avenues in the treatment and prevention of thrombosis.

Bibliography

1. Binder, C.J., Hörkkö, S., Dewan, A., Chang, M.-K., Kieu, E.P., Goodyear, C.S., Shaw, P.X., Palinski, W., Witztum, J.L. and Silverman, G.J. 2003. Pneumococcal vaccination decreases atherosclerotic lesion formation: molecular mimicry between *Streptococcus pneumoniae* and oxidized LDL. *Nature Medicine* 9(6), pp. 736–743.
2. Chou, M.-Y., Fogelstrand, L., Hartvigsen, K., Hansen, L.F., Woelkers, D., Shaw, P.X., Choi, J., Perkmann, T., Bäckhed, F., Miller, Y.I., Hörkkö, S., Corr, M., Witztum, J.L. and Binder, C.J. 2009. Oxidation-specific epitopes are dominant targets of innate natural antibodies in mice and humans. *The Journal of Clinical Investigation* 119(5), pp. 1335–1349.
3. Ehrenstein, M.R. and Notley, C.A. 2010. The importance of natural IgM: scavenger, protector and regulator. *Nature Reviews. Immunology* 10(11), pp. 778–786.
4. Eichinger, S., Kyrle, P.A., Kammer, M., Eischer, L., Ozsvar Kozma, M. and Binder, C.J. 2017. Natural antibodies to oxidation-specific epitopes: Innate immune response and venous thromboembolic disease. *Journal of Thrombosis and Haemostasis* 16(1), pp. 31–35.

5. Owens, A.P. and Mackman, N. 2011. Microparticles in hemostasis and thrombosis. *Circulation Research* 108(10), pp. 1284–1297.
6. Su, J., Georgiades, A., Wu, R., Thulin, T., de Faire, U. and Frostegård, J. 2006. Antibodies of IgM subclass to phosphorylcholine and oxidized LDL are protective factors for atherosclerosis in patients with hypertension. *Atherosclerosis* 188(1), pp. 160–166.
7. Tsiantoulas, D., Perkmann, T., Afonyushkin, T., Mangold, A., Prohaska, T.A., Papac-Milicevic, N., Millischer, V., Bartel, C., Hörkkö, S., Boulanger, C.M., Tsimikas, S., Fischer, M.B., Witztum, J.L., Lang, I.M. and Binder, C.J. 2015. Circulating microparticles carry oxidation-specific epitopes and are recognized by natural IgM antibodies. *Journal of Lipid Research* 56(2), pp. 440–448.

RECONSTRUCTION OF PORTAL VEIN BY DIFFERENT TYPES OF ALLOGENOUS VENOUS GRAFTS IN EXPERIMENTAL MODEL OF PANCREATODUODENECTOMY

Richard Pálek

Department of Surgery, Charles University, Faculty of Medicine in Pilsen, Czech Republic

Co-authors: J. Rosendorf, L. Bednář, T. Kříž, O. Brzoň, V. Tégl, K. Bajcurová, P. Mik, A. Jonášová, J. Vimmr

Tutor: Václav Liška, Vladislav Třeška

Introduction, aims

Pancreatic cancer is known as one of the leading causes of cancer mortality in developed countries (1, 2). Nowadays the only potential curative therapy of this disease is radical surgical resection. The standard surgical method for curative resection is pylorus preserving pancreaticoduodenectomy (PPPD) (3).

However the resectability of pancreatic cancer is limited by vessel infiltration. In presence of tumour ingrowth into adjacent arteries the surgical resection is not generally recommended. (4, 5). Infiltration of superior mesenteric vein (SMV) or portal vein (PV) can be solved by vessel resection resulting in comparable morbidity and mortality with standard PPPD (6).

After resection of longer segment of PV the reconstruction is usually performed using autologous venous grafts (e.g. saphenous vein) (7). Unfortunately there are some disadvantages of autologous grafts as prolonged operation time and disproportion of the size.

Allogeneic cadaveric graft of the PV could avoid these disadvantages but PV is usually removed together with the liver for purpose of transplantation. Reconstruction with allogeneic cadaveric grafts was described only in few studies till now. The graft was from iliac or femoral veins (caval system) in all cases (8, 9,10). Anybody according to our knowledge did not study the differences between the properties of grafts from portal system or caval system. Both systems vary by the perfusion pressures following from their functions.

The aim of our study is to verify whether there are any significant differences in characteristic of PV wall or ICV wall which could influence the behaviour of the portal system after interposition of the graft of PV or ICV.

Methods

PPPD with PV reconstruction was performed in 26 Prestice black pied pigs. Animals in PV group received venous graft of PV (n= 13). Animals in ICV group received venous graft of ICV (n= 13). Each of the donor pigs (n= 13) was source of both kind of venous grafts. To avoid incompatibility among donors and acceptors blood cross-matching test was performed.

Venous grafts of PV and ICV were harvested from donor animals under aseptic and antiseptic conditions. Operation of acceptor animals followed the standard protocol of PPPD. Resected PV was reconstructed using PV graft or ICV graft. The diameters of the PV and its main branches were measured prior to the vessel reconstruction and also afterwards together with diameter of both

anastomoses, and length and diameter of the graft. The continuity of the gastrointestinal system was restored afterwards and the laparotomy was closed.

The animals were monitored for the next 4 weeks after operation. Blood sample collections were performed before operation, during the procedure and regularly in postoperative period. Serum markers of liver and kidney functions were followed. All the pigs underwent ultrasound examination before operation, right after operation and then on postoperative days 7, 14, 21 and 28. Doppler ultrasound examination was performed to verify and quantify the blood flow in graft and in PV. The diameters of the PV and its main branches were measured together with the blood flow speed in these locations.

On 28th postoperative day (or during the autopsy in case of death before end of the experiment) the PV was harvested together with the interposed graft and stored in formaldehyde solution for later histological examination.

The samples of PV together with interposed graft as same as the rests of the grafts before implantation were assessed by histological examination. The content of smooth muscle tissue, collagen, elastin and the presence of inflammatory reaction was evaluated.

The data from ultrasound examination and perioperative diameters of the vessels were used to create geometrical models of reconstructed area. These models enabled to design software simulations of blood flow in reconstructed PV. The blood flow speed, wall shear stress and relative residence time were counted to evaluate the risk of thrombosis and the influence of the reconstruction on the blood flow.

Results

The PPPD with PV replacement was performed in 26 piglets. 7 piglets succumbed to the postoperative complications (thrombosis of portal vein – 2, metabolic failure – 2, postoperative bleeding – 1, gastrectasia – 1 and pancreatic pseudocyst – 1). In total we met the portal vein thrombosis in 4 piglets (PV group – 3, ICV group – 1). We did not find any significant differences between serum levels of followed biochemical markers. There were no significant differences of the PV and the graft diameter and no significant differences of the blood flow speed in the PV and in the graft between both groups. Ultrasound examination helped us to diagnose PV thrombosis in one case. According to histological examination the wall of PV graft contains smooth muscle tissue which is not present in case of ICV. After 4 weeks of healing the muscle layer in PV graft lost its stratification and both of the grafts were comparable in histological structure. The software modelling seems to be good method to verify the locations with higher risk of thrombosis. All the thrombi were found near the anastomosis where the relative residence time was higher.

Discussion

According to the biochemical analysis and ultrasound examination the functions of liver and neither the behaviour of the portal system was not involved by the type of interposed graft. Both kind of grafts slightly differentiated in the structure of the wall but they were both comparable after 4 weeks at the end of the experiment. The software modelling showed locations with higher risk of thrombosis where the thrombi were found during autopsy. However the thrombosis occurred only in 4 piglets with comparable results of mathematical thrombosis prediction. It shows that also other factors except of vessel geometry and blood flow speed can cause the thrombosis.

Conclusion

There is no proof of significant differences of characteristic of PV wall or ICV wall which could influence the behaviour of the portal system after interposition of the graft of PV or ICV. The wall of PV graft has more smooth muscle tissue compared to ICV graft but both grafts have comparable structure after 4 weeks after implantation. The usage of ICV graft for reconstruction of PV is feasible and very good alternative.

Summary

Surgical resection is the only potential curative therapy of pancreatic cancer. Resection of infiltrated portal vein (PV) increases operability of the patients. Allogeneous cadaveric venous grafts could be good option for necessary vessel reconstruction. The graft of PV itself is more difficult to get because it's usually removed together with liver for transplantation. Another option is allogeneous graft from inferior caval vein (ICV) or it's main branches. The aim is to compare venous grafts from portal system and caval system before their safe application.

Pancreaticoduodenectomy with PV resection and reconstruction with allogeneous venous graft from PV or ICV was performed in 26 pigs divided in 2 groups according to the type of the graft. The pigs were monitored for 4 weeks after the operation. Markers of renal and liver functions were followed together with regular ultrasound controls. Samples of reconstructed PV together with interposed grafts were histologically examined. Software modelling of reconstructed portal system was used to find areas with higher risk of thrombosis and to compare influence of both kind of grafts on blood flow.

According to the biochemical analysis and ultrasound examination the functions of liver and neither the behaviour of the portal system was not involved by the type of interposed graft. The software modelling showed locations with higher risk of thrombosis where the thrombi were found during autopsy.

There is no proof of significant differences of characteristic of PV wall or ICV wall which could influence the behaviour of the portal system after interposition of the graft of PV or ICV. The usage of ICV graft for reconstruction of PV is feasible and it is a very good alternative.

References

1. Ilic M, Ilic I: Epidemiology of pancreatic cancer. *World J Gastroenterol.* 2016;22(44):9694-9705.
2. Mohammed S, Van Buren G 2nd, Fisher WE: Pancreatic cancer: advances in treatment. *World J Gastroenterol.* 2014 ;20(28):9354-60.
3. Bahra M, Neumann U: Surgical technique for resectable pancreatic cancer. *Recent Results Cancer Res.* 2008;177:29-38.
4. D'Haese JG, Werner J: Resectability of pancreatic cancer: New criteria. *Radiologe.* 2016;56(4):318-24.
5. Bockhorn M, Burdelski C, Bogoevski D et al.: Arterial en bloc resection for pancreatic carcinoma. *Br J Surg.* 2011;98(1):86-92.
6. Ravikumar R, Sabin C, Abu Hilal M et al.: Portal vein resection in borderline resectable pancreatic cancer: a United Kingdom multicenter study. *J Am Coll Surg.* 2014;218(3):401-11.

7. Lai EC: Vascular resection and reconstruction at pancreatico-duodenectomy: technical issues. *Hepatobiliary Pancreat Dis Int.* 2012;11(3):234-42.
8. Meniconi RL1, Ettorre GM, Vennarecci G et al.: Use of cold-stored vein allografts for venous reconstruction during pancreaticoduodenectomy. *J Gastrointest Surg.* 2013;17(7):1233-9.
9. Zhang XM, Fan H, Kou JT et al.: Resection of portal and/or superior mesenteric vein and reconstruction by using allogeneic vein for pT3 pancreatic cancer. *J Gastroenterol Hepatol.* 2016;31(8):1498-503.
10. Kleive D, Berstad AE, Sahakyan MA: Portal vein reconstruction using primary anastomosis or venous interposition allograft in pancreatic surgery. *J Vasc Surg Venous Lymphat Disord.* 2018;6(1):66-74.

All animals were under general anesthesia during all surgical procedures and under analgesedation during any manipulation.

ALTERNATION OF BILE ACID HOMEOSTASIS BY IRON OVERLOAD IN RATS

Alena Prašnická

Department of Pharmacology, Department of Medical Biochemistry, Department of Histology and Embryology, Department of Biological and Medical Sciences, Charles University, Faculty of Medicine in Hradec Kralove, Department of Pharmacology and Toxicology, Charles University, Faculty of Pharmacy in Hradec Kralove, Department of Medical Biochemistry and Laboratory Diagnostics, 1st Faculty of Medicine, Charles University, Prague, Czech Republic

Co-authors: Alena Prašnická, Hana Lastuvková, Jolana Cermanová, Jitka Hájková, Milos Hroch, Jaroslav Mokry, Eva Doleželová, Fatemeh Alaei Faradonbeh, Petr Pavek, Martin Lenicek, Libor Vitek, Petr Nachtigal

Tutor: Stanislav Micuda

Excessive iron accumulation in the liver may affect bile acid metabolism but this effect has not been comprehensively studied. Thus, we evaluated the effect of iron overload on bile acid synthesis, biliary secretion and output through feces in rats. Male Wistar rats fed were administered either with eight doses of saline every second day i.p., or with eight doses of iron (100 mg/kg) in the same timing. Iron-overloaded (IO) rats developed significant iron deposition in the liver. Comparison with control rats showed decrease in bile flow in IO group as a result of decreased biliary excretion of bile acids. The molecular mechanisms responsible for these changes in IO group were decreased protein expression of Cyp7a1, the rate limiting enzyme in the conversion of cholesterol to bile acid, and decreased expressions of Bsep, the transporter responsible for bile acids efflux into bile. IO did not change net BA content in feces reflecting increased conversion of BA into HDCA and reduced intestinal reabsorption. Plasma concentration of BA were therefore not modified in comparison with saline group. IO increased plasma cholesterol concentrations. It corresponded with reduced Cyp7a1 expression but also with increased protein expression of HmgCR, the rate limiting enzyme in liver *de novo* cholesterol synthesis. In summary, this study reports mechanisms modifying metabolism and enterohepatic kinetics of BA during IO. Altered elimination pathways for BA and cholesterol may potentiate liver damage accompanying excessive iron deposition. The study was supported by the Charles University Progres Q40, and the Grant Agency of the Czech Republic project No. 17-068415.

LOW HOX GENE EXPRESSION IN PML-RARA-POSITIVE LEUKEMIA RESULTS FROM SUPPRESSED HISTONE DEMETHYLATION

Kateřina Rejlová

CLIP – Childhood Leukaemia Investigation Prague; Department of Pediatric Hematology and Oncology, Second Faculty of Medicine, Charles University, Prague, Czech Republic

Co-authors: Alena Musilová, Karolína Škvárová Kramarzová, Markéta Žaliovová, Karel Fišer, Meritxell Alberich-Jorda, Jan Trka and Júlia Starková

Tutor: Júlia Starková

Introduction

Homeobox genes (HOX) encode transcription factors that are frequently deregulated in leukemias. Our previous results showed that HOX gene expression differs among genetically characterized subtypes of pediatric acute myeloid leukemia (AML). Specifically, PML-RARa positive AML patients have overall lowest HOX gene expression which positively correlates with expression of histone 3 lysine 27 (H3K27) demethylases - JMJD3 and UTX and negatively with the expression of DNA methyltransferases - DNMT3a and DNMT3b. Interestingly, JMJD3 was already shown to be a direct target of PML-RARA protein (Martens, JH et al, 2010). From these findings we postulated a hypothesis that reduced levels of HOX genes in PML-RARA positive AML are a consequence of suppressed expression of histone demethylases resulting in increased H3K27 methylation and/or of elevated levels of DNMTs leading to *de novo* DNA methylation.

Methods

Gene expression on mRNA level was determined using quantitative PCR (qPCR). Protein levels of studied genes and modified histones were detected using Western blot. Modified histones were also detected directly on HOX genes promoters using chromatin immunoprecipitation with following qPCR or next generation sequencing (NGS). Bisulfite sequencing consisting bisulfite conversion and Sanger sequencing was used for assesment of methylation level on HOX gene promoters. Viability of the cell lines was tested using flow cytometry and cell morphology was determined using light microscopy after staining with May-Grünwald Giemsa-Romanowski solutions.

Results

We treated NB4 (PML-RARa+) cell line by all-trans retinoic acid (ATRA; 1uM), which was described to release the differentiation block caused by the presence of PML-RARa and to degrade the fusion protein. We observed that expression of particular HOX genes (HOXA1, HOXA3, HOXA4, HOXA5, HOXA6, HOXA7, HOXB4, HOXB5, HOXB6) measured by qPCR was significantly increased after ATRA treatment. While level of JMJD3 was significantly increased upon ATRA treatment as well, the expression of UTX did not change. Furthermore, we detected significantly reduced expression of DNMT3b gene. To exclude a non-specific effect of ATRA, independent of PML-RARa, we used ATRA-resistant clones LR2 and MR2 bearing mutations in retinoic acid-binding domain. HOX gene expression together with JMJD3, UTX and DNMT3b

expression did not change upon ATRA treatment. To study the role of JMJD3 in the HOX gene expression regulation, we cultured NB4 cells with a specific inhibitor of histone demethylases, GSK-J4 (1 μ M, 10 μ M), in the presence of ATRA. First, we confirmed the inhibitory effect of GSK-J4 measuring the levels of JMJD3 and UTX. Then we used co-treated cells with ATRA. Co-treatment caused significant decrease in the expression of studied HOX genes (HOXA1, HOXA3, HOXA5, HOXA7, HOXA10, HOXB4, HOXB6) in comparison to ATRA alone which supports the role of JMJD3 in the transcription regulation. Further, we performed chromatin immunoprecipitation (ChIP) to investigate if the changes of HOX gene expression upon ATRA and GSK-J4 treatment would correspond with changes of histone code on HOX gene promoter regions. ATRA treatment caused reduction of repressive histone mark (H3K27me3) on particular HOX gene promoters (HOXA1, HOXA3, HOXA5, HOXA7), by contrast, combinational treatment of ATRA and GSK-J4 reversed this effect. To investigate presence of H3K27me3 in all HOX genes in whole genome we performed ChIP followed by next generation sequencing (ChIP-seq). This method help us to broaden the number of HOX genes regulated by JMJD3 (HOXA4, HOXA10, HOXB2, HOXB3, HOXB5, HOXC4, HOXC10, HOXC13, HOXD1, HOXD4, HOXD9). We also tested hypothesis that DNMT3b, which is decreasing after PML-RARa degradation, regulates expression of HOX genes in PML-RARa⁺ cells. DNA methylation in HOXA5 and HOXA7 promoters did not change after ATRA treatment in both sensitive and resistant clones. Next we were interested if JMJD3 inhibition will interfere with the differentiation effect of ATRA. In NB4 cell line GSK-J4 did not reduce the effect of differentiation caused by ATRA. Interestingly, it led cells to apoptosis. Combination of drugs (ATRA - 1 μ M, GSK-J4 - 1, 2, 5 μ M) increased significantly the percentage of dead cells in comparison to ATRA or GSK treatment alone. Next we measured apoptosis in resistant clones LR2 and MR2. In both cases the highest concentration used of GSK-J4 (5 μ M) in combination with ATRA caused significant increase of dead cells as well.

Discussion

Totally different signature and association of HOX genes, histone demethylases and DNA methyltransferases expression in PML-RARa⁺ AML patients in comparison to PML-RARa⁻ indicates the influence of PML-RARa fusion protein on HOX genes expression. This fact is also supported by AML patients data where FLT3/ITD (internal tandem duplication) is generally connected with high expression of HOX genes except the ones with double positivity including PML-RARa fusion protein (Skvarova Kramarzova et al, 2014; Roche et al, 2004). We showed that in PML-RARa⁺ cells the expression of particular HOX genes is regulated by the presence of PML-RARa protein through the activity of JMJD3. It was already published that PML-RARa⁺ cells are characterized by typical chromatin landscape driven by epigenetic modifiers (Thompson et al, 2003). In addition to HOX genes that are regulated by PML-RARa through JMJD3, we have also shown genes are probably regulated by different mechanisms like in case of HOXB6 (Giampaolo et al, 2002). We also did not observed any changes in DNA methylation although DNMT3b was changed after PML-RARa degradation. It could be explained by previously shown fact that only DNMT3a but not DNMT3b physically interacts with PML-RARa (Cole et al, 2016). Furthermore we detected synergistic apoptotic effect of ATRA and GSK-J4 co-treatment. This result is in concordance with the study, where the GSK-J4 alone have cytotoxic effect only in T-ALL cells and not AML (Ntziachristos et al, 2014).

Conclusions

In this study we have explored the specific regulation of HOX genes in PML-RARa+ cells in which overall lower expression of HOX and histone demethylases genes was observed. In comparison to the PML-RARa- AML patients. We show that releasing PML-RARa-mediated block leads to the increased expression of particular HOX genes and reduced level of H3K27me3 on their promoters which is regulated by JMJD3. Additionally we show possible treatment benefit for ATRA-resistant PML-RARa+ AML patients using combination of ATRA and GSK-J4 inhibitor causing synergistic apoptotic effect.

Summary

We found that PML-RAR+ AML patients have the distinct signature of the histone demethylases and HOX genes with specific association in expression of histone demethylases, DNA methyltransferases and HOX genes in comparison to the other subtypes of AML patients. We showed that releasing of PML-RARa differentiation block using ATRA increased expression of particular HOX genes and also JMJD3 histone demethylase. By contrast the specific inhibition of JMJD3 reversed this effect. We evaluate that this effect, independent on process of differentiation, was driven by the presence or absence of PML-RARa fusion protein. We demonstrate that in case of PML-RARa+ cells changes in chromatin activity based on presence of repressive histone mark (H3K27me3) correspond with changes in HOX gene expression. Using JMJD3 specific inhibitor and ChIP-seq we identified list of HOX genes which are regulated by PML-RARa through histone methylation changes mainly driven by JMJD3. Moreover we detected synergistic apoptotic effect of ATRA and GSK-J4 co-treatment, which may provide a new therapeutic opportunity for patients with APL resistant to current treatment based on ATRA.

References

1. Cole CB, Verdoni AM, Ketkar S, et al. PML-RARA requires DNA methyltransferase 3A to initiate acute promyelocytic leukemia. *J Clin Invest*. 2016;126(1):85–98.
2. Giampaolo A, Felli N, Diverio D, et al. Expression pattern of HOXB6 homeobox gene in myelomonocytic differentiation and acute myeloid leukemia. *Leukemia*. 2002;16(7):1293–1301.
3. Ntziachristos P, Tsigos A, Welstead GG, et al. Contrasting roles of histone 3 lysine 27 demethylases in acute lymphoblastic leukaemia. *Nature*. 2014;514(7523):513–517.
4. Roche J, Zeng C, Baron A, et al. Hox expression in AML identifies a distinct subset of patients with intermediate cytogenetics. *Leukemia*. 2004;18(6):1059–1063.
5. Thompson A, Quinn MF, Grimwade D, et al. Global down-regulation of HOX gene expression in PML-RARalpha + acute promyelocytic leukemia identified by small-array real-time PCR. *Blood*. 2003;101(4):1558–1565.
6. Skvarova Kramarzova KFK, Mejstrikova E, Rejlova K, et al. Homeobox gene expression in acute myeloid leukemia is linked to typical underlying molecular aberrations. *J Hematol Oncol*. 2014;7:94.

DETERMINANTS OF PATIENT SURVIVAL FOLLOWING ACUTE EBOLA VIRUS INFECTION

Natasha Y. Rickett

Department of Infection Biology, Infection and Global Health, University of Liverpool

Co-authors: Xuan Liu, Sam Haldenby

Tutors: Julian A. Hiscox, Miles W. Carroll

Introduction

The 2013-2016 outbreak of *Zaire ebolavirus* (EBOV) in West Africa was unprecedented in scale and has sparked a great deal of interest into the pathogen. EBOV is the most pathogenic species in the family *Filoviridae*. Early symptoms are non-specific and flu-like, but these rapidly dissolve into systemic issues, frequently resulting in death. Fatal infections are associated with uncontrolled inflammation, while survivors have an initial robust antiviral response followed by an effective antigen-specific response (Chertow *et al.*, 2014). However, there are a myriad of other factors influencing patient outcome, including viral load and co-infections (Lauck *et al.*, 2014; Rosenke *et al.*, 2016). The aim of this study is to elucidate some of these factors, which could have major therapeutic implications.

Methods

Diagnostic blood samples were taken from patients upon arrival to the Ebola Treatment Centre in order to test for the presence of *Plasmodium spp.* (via rapid diagnostic test) and Ebola virus (via qRT-PCR). RNA-sequencing was performed on 179 outbreak patient samples in order to assess which genes, if any, are differentially expressed in fatal versus non-fatal infections.

Results

Here we demonstrate that higher viral load and malaria co-infection are correlated with poor patient outcome. The RNA-seq data allowed us to explore various avenues of research. One such path was the comparison of malaria testing methodologies – i.e. co-infection confirmed by RNA-seq or rapid diagnostic test (RDT). The RDT was employed in the field, however, our RNA-seq data suggests this may have led to under-reporting of *Plasmodium spp.* Furthermore, there are a number of genes that are differentially expressed according to patient outcome – e.g. those associated with blood clotting and complement regulation (Fig. 1). These were upregulated in individuals who went on to die to infection when their transcriptomic profiles were compared to individuals who survived (pathways shown in Table 1). These data allowed the employment of a machine learning technique in order to create a genetic profile for an average survivor – able to predict patient outcome with 85% accuracy, suggesting that the response of survivors is different to that of fatalities during EBOV infection (Liu *et al.*, 2017).

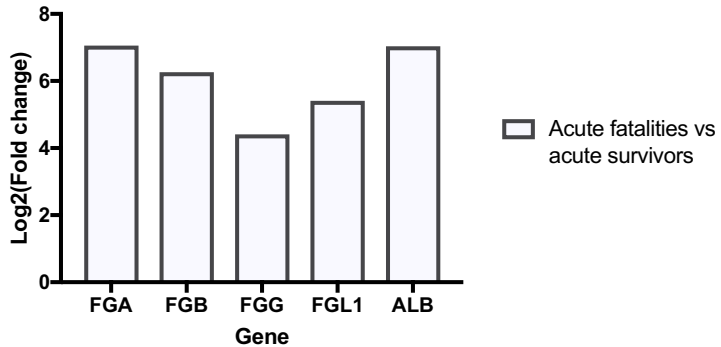


Figure 1: Graph illustrating differentially expressed genes in individuals who went on to die or survive following acute Ebola virus infection.

Table 1: Pathways enriched or downregulated according to patient outcome. Those with z-scores >0 describe the pathways upregulated in fatal cases compared to those who eventually survived infection, with <0 showing the opposite.

Ingenuity Canonical Pathways	-log(p-value)	z-score
Acute Phase Response Signaling	15.60	3.317
LXR/RXR Activation	10.10	2.496
HMGB1 Signaling	2.66	2.236
Leukocyte Extravasation Signaling	2.18	2.236
Colorectal Cancer Metastasis Signaling	1.79	2.236
IL-8 Signaling	1.77	2.236
Production of Nitric Oxide and Reactive Oxygen Species in Macrophages	1.30	2.236
CXCR4 Signaling	1.57	2
Coagulation System	7.02	0.378
Complement System	9.69	0
PTEN Signaling	1.37	-2

Discussion

The identification of these differentially expressed genes could illuminate some of the factors influencing patient outcome. This, along with the formation of a “survivor profile”, could have clinical implications in the future, both in terms of novel therapeutics and allocation of hospital resources.

Conclusions

There are a number of genes that are differentially expressed according to patient outcome. These are associated with pathways such as the acute phase response, IL-8 signalling and blood coagulation. This upregulation in individuals who go on to die from infection could explain some of the immunopathology that sufferers of Ebola infection can incur.

Works cited

1. Chertow, D. S. *et al.* (2014) 'Ebola Virus Disease in West Africa – Clinical Manifestations and Management', *New England Journal of Medicine*, 371(22), pp. 2054–2057. doi: 10.1056/NEJMp1411794.
2. Lauck, M. *et al.* (2014) 'GB virus C co-infections in West African Ebola Patients', *Journal of Virology*, (December). doi: 10.1128/JVI.02752-14.
3. Liu, X. *et al.* (2017) 'Transcriptomic signatures differentiate survival from fatal outcomes in humans infected with Ebola virus', *Genome Biology*. *Genome Biology*, 18(1), p. 4. doi: 10.1186/s13059-016-1137-3.
4. Rosenke, K. *et al.* (2016) 'Plasmodium Parasitemia Associated With Increased Survival in Ebola Virus-Infected Patients.', *Clinical infectious diseases*, p. ciw452. doi: 10.1093/cid/ciw452.

SEX DIFFERENCES IN ADRENERGIC VESSEL TONE – A ROLE OF ESTROGEN

Kristin Riedel

Institute of Physiology, Medical Faculty Carl Gustav Carus, TU Dresden

Co authors: Kopaliani I, Tolkmitt J., Weber S., Schlinkert P., Zatschler B., Müller B.,
Hentsche C., El-Armouche A., Morawietz H., Matschke K., Deussen A.

Tutor: Andreas Deussen

Introduction

Hypertension and related cardiovascular diseases are more prevalent in men than in women. This may be partly explained by sex-differences in sympathetic sensitivity in vessels, because increased sympathetic drive promotes vascular dysfunction (Ref. 1). Women show a weaker vasoconstriction towards noradrenergic stimulation than men (Ref. 2). Previously we revealed that these sex-differences in rats rely on more β -adrenoceptors on vascular endothelium in vessels of females compared to males (Ref. 3). However, the role of sex hormones in regulation of β -adrenoceptor expression and translational relevance for sex-specific vessel constriction and relaxation in humans is unknown.

Aims

We investigated the role of female and male sex-hormones on sex-specific differences in adrenergic vasoconstriction and vasorelaxation in a rat model, along with investigation of similar differences and the role of endothelium in human vessels.

Methods

All experiments were approved by Institutional Ethics Committee and local authorities (permission number: DD24-5131/338/65, permission number: EK 307-12-2015). Five weeks old female and male wistar rats were assigned to 4 study groups (each n=6): sham-operated control, ovariectomized (OVX)/orchietomized (ORCHX), OVX/ORCHX substituted with β -Estradiol, progesterone or testosterone propionate (2 mg/kg orally, twice a week) or vehicle. At age of 12 weeks, aortas were isolated for assessment of vasoconstriction (norepinephrine) and vasorelaxation (β_1/β_2 agonist isoprenaline, β_3 agonist BRL) with and without selective β -blockers and NO-synthase inhibitor (L-NMMA). Same method was used to assess vasoconstriction and vasorelaxation in human mammary arteries, which were obtained from the Heart Center Dresden (patient age: 50 to 70 years). A qRT-PCR was performed for quantification of β -adrenoceptor mRNA levels in rat aorta and mammary arteries, whereas levels of sex hormones were assessed in rat plasma.

Results

Aortas of sham operated females constrict less towards norepinephrine and relax more towards isoprenaline than aortas of sham operated males (Fig. 1). Compared to sham operated females,

OVX profoundly increased vasoconstriction (Fig. 1 A) and reduced vasorelaxation and therefore abolished sex-differences in adrenergic sensitivity. The difference was restored by substitution of estrogen (Fig. 1), but not progesterone in females.

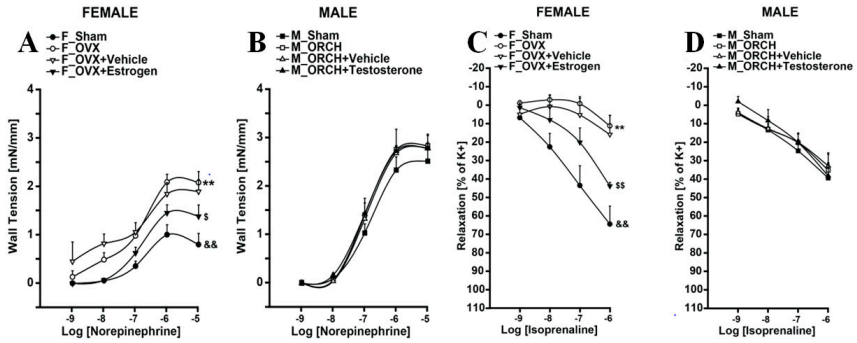


Figure 1. Norepinephrine-induced vasoconstriction of female **A** and male **B** rats. Vasorelaxation induced by isoprenaline in aorta of female **C** and male **D** rats. ** $P < 0.01$ vs sham. \$ $P < 0.05$ vs sham. && $P < 0.01$ vs sham male. Values are mean \pm SE. $n = 6$.

Consistently, mRNA levels of $\beta 1$ - and $\beta 3$ -, but not $\beta 2$ - adrenoceptors were significantly ($P < 0.05$) higher in aortas of sham operated females than in aortas of sham operated males (Fig. 2). Ovariectomy abolished this difference by decreasing $\beta 1$ - and $\beta 3$ - adrenoceptor expression in female rats. Consequently, estrogen substitution in ovariectomized females largely ($P < 0.05$) restored $\beta 1$ - and $\beta 3$ - adrenoceptor expression. Orchiectomy and testosterone treatment did not change aortic vasoconstriction and vasorelaxation nor β -adrenoceptor expression in aortas of male rats. Plasma levels of β -Estradiol were decreased by OVX and restored by oral substitution of estrogen.

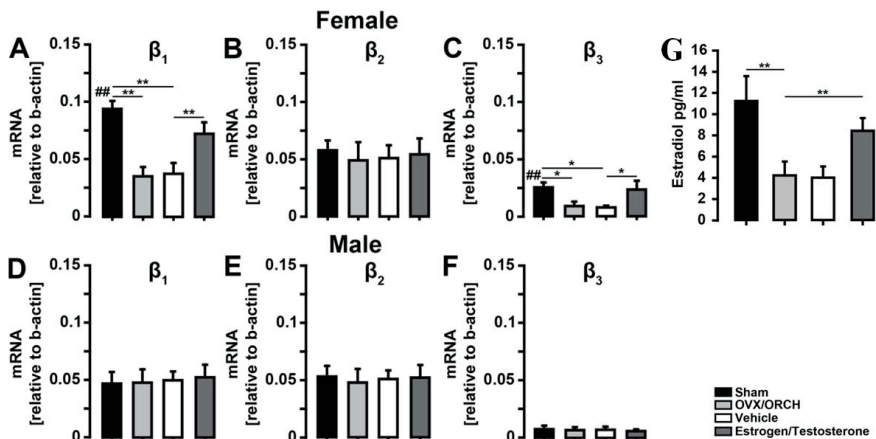


Figure 2. mRNA levels of β -adrenoceptors in aorta of female A-C and male D-F rats. G Plasma levels of β -estradiol in females ** $P < 0.01$, * $P < 0.05$. Values are mean \pm SE. n=6

Mammary arteries of women constricted less ($P < 0.05$) in response of norepinephrine than arteries of men (Fig. 3 A, B). Removal of endothelium eliminated this sex-specific difference by significantly ($P < 0.05$) increasing vasoconstriction in arteries of women, without affecting vasoconstriction in arteries of men (Fig. 3 A, B). Vasorelaxation caused by isoprenaline was greater ($P < 0.05$) in mammary arteries of women compared to arteries of men (Fig. 3 C, D). This sex-specific difference in vasorelaxation was also abolished after removal of the endothelium. Levels of β_1 - and β_3 -adrenoreceptor mRNA were higher in mammary arteries of women compared to arteries of men (Fig. 3 E-G).

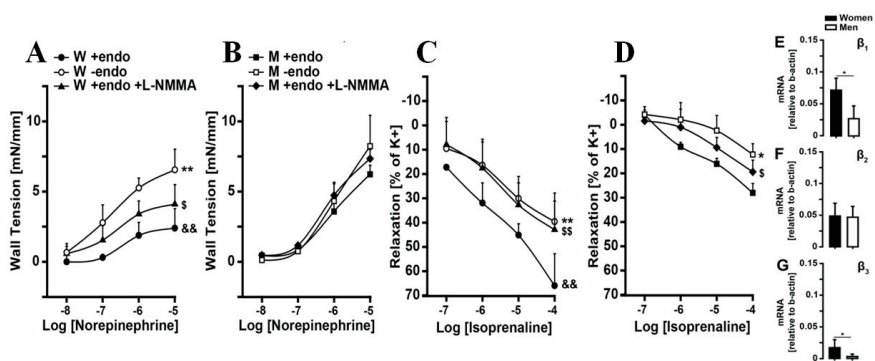


Figure 3. Norepinephrine-induced vasoconstriction and isoprenaline-induced vasorelaxation in human mammary arteries in women A, C and men B, D with or without L-NMMA and endothelium. Expression of vascular β -adrenoreceptors in mammary arteries E-G. ** $P < 0.01$, * $P < 0.05$, \$ $P < 0.05$, \$\$ $P < 0.01$ vs +endo. && $P < 0.01$ vs +endo male. Values are mean \pm SE. n=7 women, n=19 men.

Discussion

We demonstrate that estrogen determines sex-specific differences in adrenergic vasoconstriction and vasorelaxation in a rat model by regulating vascular β 1- and β 3-adrenoceptor expression in females. While OVX abolishes sex-differences in vasoconstriction and vasorelaxation, along with expression of β 1- and β 3-adrenoceptor, estrogen substitution restores these differences. Furthermore, we demonstrate translational relevance of these differences in human vessels and reveal critical role of endothelium in determination of sex-specific vasoconstriction and vasorelaxation. Finally, we also demonstrate that testosterone and progesterone have no influence on vascular β -adrenoceptor expression in rats and therefore on sex-differences in adrenergic vasoconstriction and vasorelaxation.

Conclusion

We reveal that sex-differences in a rat model are estrogen, but not progesterone or testosterone dependent. Estrogen determines these differences via regulation of vascular β 1- and β 3-adrenoceptor expression. We also reveal strong translational relevance of these findings in humans.

Summary

Sex-differences in adrenergic vasoconstriction and vasorelaxation may partly explain differences in prevalence of hypertension between men and women. Because vessels of females have more endothelial β 1- and β 3-adrenoceptors, they constrict less and relax more to adrenergic stimulation. In a rat model, we found that estrogen, but neither testosterone nor progesterone regulates vascular β 1- and β 3-adrenoceptor expression and thereby sex-specific differences in vasoconstriction and vasorelaxation. In human mammary arteries, similar differences exist, which strongly depend on endothelium and nitric oxide. Further studies need to address the molecular mechanisms of estrogen in regulation of the vascular β -adrenoceptor expression.

References

1. Guyenet PG: The sympathetic control of blood pressure. *Nat Rev Neuroscience* 2006; 7, 335-346.
2. Kneale et al.: Gender differences in Adrenergic Sensitivity. *JACC* 2000; Vol 36, No. 4
3. Al-Gburi, S. et al.: Sex-difference in expression and function of beta-adrenoceptors in macrovessels: role of the endothelium. *Basic Research in Cardiology* 2017; Vol. 112, 3, 29

FORTIFICATION OF ANASTOMOSIS ON GASTROINTESTINAL TRACT WITH NANOMATERIALS

Jáchym Rosendorf

Department of Surgery, Medical faculty in Pilsen, Charles University

Co-authors: R. Pálek, L. Červenková, T. Kříž, M. Dolanský, L. Bednář, M. Klíčová, J. Horáková, D. Lukáš, V. Třeška

Tutor: Václav Liška

Introduction

Leakage of an anastomosis in gastrointestinal (GI) surgery is one of the main complications ranging from mild cases which can be treated only conservatively (antibiotic therapy) to more severe ones needing a reoperation^{1,2}. The rate of leakage differs according to the type and location of anastomosis. Rather higher rates with more severe consequences can be found in colorectal surgery especially in distal anastomoses on the rectum³. There are many risk factors contributing known to us, and yet today the problem remains unresolved, raising the morbidity and mortality of patients.

Another kind of complication is an intestinal passage blockage. It can occur practically in any time in the patient's life after the surgery due to either stenosis in the site of the anastomosis constructed or formation of adhesions creating thick fibrous strings in the abdominal cavity. This is also often a reason for patient readmission to a hospital and relaparotomy in some of the cases^{4,5,6}.

There has been several studies investigating on decreasing the risk of the complications above, but no such attempt has been successful yet in solving the both type of complications and being used in the clinical praxis nowadays.

Nanomaterials seem to be interesting structures for a barrier type of application in the site of anastomosis, they haven't been used yet in this kind of experiment according to our knowledge.

Goals

Goal of our study is to investigate on the influence of nanomaterials on the formation of adhesions in the abdominal cavity and on healing of the anastomosis on gastrointestinal tract in an experiment on pig.

Methods

The materials used in our study were fabricated by electrospinning of solutions of Polycaprolactone (PCL) and copolymer of polycaprolactone and polylactic acid (PLCL), the materials have been tested in vitro before. The materials are already in use in human medicine in different application forms. We performed an experiment on a large mammal model. We used 24 pigs both males and females divided into three groups. In full anaesthesia we constructed three hand sutured anastomoses on the small intestine in the very same positions (70, 90 and 110 cm past the Treitz ligament) using monofilament 4/0 atraumatic suture. In the two experimental groups we applied a piece of the nanomaterial to the constructed anastomoses, overlapping the suture circularly. We did not apply the material in the control group.

Three weeks of observation and fixed realimentation according to a scheme followed. We didn't observe any clinical signs of GI obstruction (intolerance of peroral income, vomiting) and signs of developing sepsis, peritonitis. After the observation period we subjected the animals to relaparotomy, searched in the abdominal cavity for any signs of anastomotic leakage or GI blockage, we also noted the severity of peritoneal adhesions in the abdominal cavity, noted changes in diameter of the small intestine. We collected the samples, fixed them in buffered formaldehyde 4 %.

The adhesions were scored according to our new scoring system developed specially for this purpose. The sample of intestine was cut on the mesentery and divided into 4 segments, each segment receiving score rangin from 0-2. Zero points for no adhesions in the segment, one point for segment partially in adhesions, two points for fully adhered segment.

The samples were subjected to histological examination. We searched for morphological changes in the intestinal wall. In immunohistochemical satining for von Willebrand factor we stereologically measured the volume fraction of vessels, counted the level of infiltration of the tissue by immunocompetent cells (neutrophiles, macrophages). We also searched for the continuity of mucosa. All results were statitically processed using STATISTICA software and suitable statistical tests.

Results

All animals survived the whole duration of the experiment. Nor ileus nor sepsis developed in any of the animals. There were also no signs of peritonitis in any of them. All animals tolerated peroral alimentation. One animal in the control group and one animal in the group with PLCL presented with vomiting single time. All animals from the group with PCL tolerated the peroral alimentation fully according to our scheme. There were adhesions of different severity in the site of the anastomoses in most of the cases. No stenosis more than half of the intestines diameter was observed. Some level of dilatation of the proximal intestine appeared in all of the animals. The smallest amount of adhesions appeared in the control group, however the variability inbetween the animals within one group was high, so the differences were not statistically significant.

There were no deviations in the morphology of the intestinal wall. The level of infiltration by neutrophiles and macrophages was with no statistically significant differences inbetween the groups. Both the level of vascularization and the content of collagen appeared to be the same in the area of the anastomosis in all the groups of animals

Discussion

We have designed a suitable way to score adhesions in the site of anastomosis, which can be used further for other experiments. According to the literature, there is no such scoring system nowadays. Our aim to create a barrier kind of protection against anastomotic leakage has promising results, there were noted no negative effects of the material on the surrounding tissues or the whole organism. Nordentoft et al.⁷ experimented with different materials for fortification of the anastomosis, getting similar results.

Conclusions

We have successfully designed an experiment to establish the effect of nanomaterials on anastomotic healing on non complicated anastomosis and we were the first to use this kind of material in this application. The results show that the material has promising properties to be used and tested further

in this kind of application. However the low rate of complications leaves the question whether the material prevents anastomotic leakage open. Bearing this thought we aim to perform a new experiment treating an anastomosis with an iatrogenic defect.

Summary

Anastomotic leakage and formation of adhesions are two types of complications we focused on in our study. Both of them are current problems of visceral surgery. There has been many studies on different materials being used as a barrier protection in the site of the anastomosis, but none of the solutions are in clinical use yet. Nanomaterials seem to be interesting structures for use as a barrier protection from anastomotic leakage, their influence on the healing of an anastomosis and formation of peritoneal adhesions is yet unknown. Therefore, we designed an experiment on pigs to study the material in vivo. We applied the nanomaterial created from polycaprolactone and copolymer of polycaprolactone and polylactic acid to the anastomosis on the small intestine and compared the results with a control group without the use of the material. We were first to use this material in this kind of application. The results showed that the material has promising properties, however further tests are still needed to prove its impact on formation of adhesions and anastomotic leakage.

References

1. Pommergaard HC, Achiam MP, Rosenberg J. Colon anastomotic leakage: improving the mouse model. *Surg Today*. 2014 May;44(5):933-9
2. Cirocco W. Rectal resection following neoadjuvant therapy in a Midwest community hospital setting: The case for standardization over centralization as the means to optimize rectal cancer outcomes in the United States. *Am J Surg*. 2018 Sep 10. pii: S0002-9610(18)30979-6
3. von Breitenbuch P, Piso P, Schlitt HJ. Safety of rectum anastomosis after cytoreductive surgery and hyperthermic intraperitoneal chemotherapy. *J Surg Oncol*. 2018 Sep;118(3):551-556
4. Diamond MP, Freeman ML. Clinical implications of postsurgical adhesions. *Hum Reprod Update*. 2001 Nov-Dec;7(6):567-76
5. Arung W, Meurisse M, Detry O. Pathophysiology and prevention of postoperative peritoneal adhesions. *World Journal of Gastroenterology: WJG*. 2011;17(41):4545-4553
6. Van Goor H Consequences and complications of peritoneal adhesions. *Colorectal Dis*. 2007 Oct; 9 Suppl 2:25-34
7. Nordentoft T. Sealing of gastrointestinal anastomoses with fibrin glue coated collagen patch. *Dan Med J*. 2015 May;62(5)

INFLUENCE OF SPECIFIC PARENTERAL NUTRITION ON SELECTED METABOLIC MARKERS AND THEIR CONSEQUENCES

Pavel Skořepa

Department of Military Internal Medicine and Military Hygiene, Faculty of Military Health Sciences, University of Defence, Hradec Králové, Czech Republic

Co-authors: V. Bláha, L. Sobotka

Tutor: Jan Horáček

Introduction

Glucose and lipids in total parenteral nutrition (TPN) not only provide energy for metabolic needs, but also act as important structural or signal molecules in the intermediate metabolism, and have a role in the outcome of critically ill patients. Omega-3 fatty acids contained in fish oils have shown efficacy in the treatment of chronic and acute inflammatory diseases due to their pleiotropic effects on inflammatory cell signalling pathways. In a variety of experimental and clinical studies, omega-3 fatty acids attenuated hyperinflammatory conditions and induced faster recovery. On the other hand parenteral preparations based on fish oil have not been shown to benefit patients in the ICU, and the use of olive oil, as compared with soybean oil, did not affect either inflammation or outcomes in several trials. Currently, the lack of high-quality evidence precludes any recommendation on the use of specific lipid formulae in critically ill patients. Non-esterified fatty acids (NEFA) or free fatty acids circulate from adipose tissue to its sites of utilization, particularly during fasting and post-absorptive states.

Aims

Clarify the influence of glucose and lipids in parenteral nutrition in critically ill patients on selected metabolic parameters and thereby contribute to the optimization of nutritional support in the severely ill. To compare changes in serum concentration and composition of unesterified essential fatty acids (eg. omega-3 and omega-6) in non-surgical critically ill patients during the first nine days of hospitalization when giving specific types of TPN – glucose-based versus lipid-based.

Methods

Prospective randomized monocentric clinical study on general internal ICU of FN HK in the years 2015-2018. Two groups of patients receiving isocaloric isoprotein full parenteral nutrition differing in glucose (6 vs. 3 g / kg / day) and lipid (0 vs. 1.1 g / kg / day). Samples were taken prior to feeding, followed by 1, 3, 6 and 9 days. Measurement of analytes by spectrophotometer (Farma-Spect Shimadzu) using enzymatic methods according to the relevant analyte (Wako, Japan). Statistical analysis using SPSS

Results

A group of 50 patients were studied. After initiation of TPN, the NEFA concentration decreased in both subgroups (Wilcoxon rank sum test, $p = 0.029$). The decrease in concentration was more

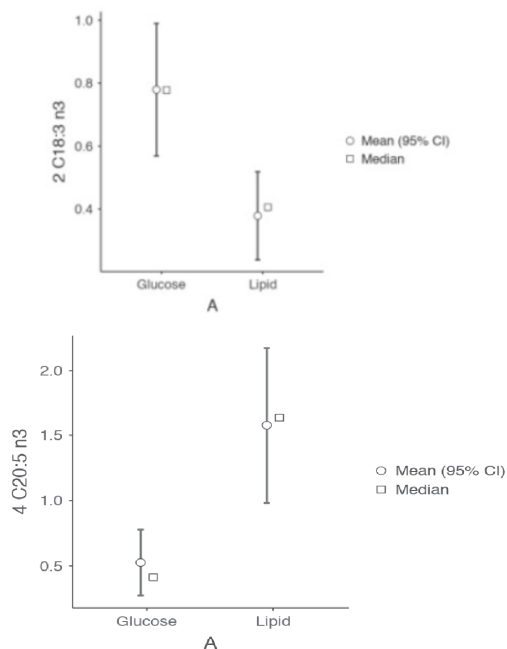
significant in patients who received glucose-only TPN (Mann-Whitney test, $p < 0.001$ and $p = 0.046$). In the area of further lipid analysis, statistically significant ($p < 0.01$) differences in the composition of unesterified essential fatty acids (omega-3 and omega-6) were found. Statistically significant ($p < 0.05$) higher levels of omega-3 α -linoleic (C18:3), omega-6 dihomo-linoleic (C20:3), omega-7 palmitoleic (C16:1) acids, desaturase-9 and AA/EPA ratio; and lower levels in omega-3 eicosapentanoic (C20:5), docosahexaenoic (C22:6), omega-6 linoleic (C18:2) acids and desaturase delta 5 were found in the group of glucose-based TPN. There were no significant differences between the groups in concentration of other NEFAs: C12:0, C14:0, C16:0, C18:0, omega-3 (C22:6), omega-6 (C18:3, C:20:4), and omega-7 (C18:1).

Discussion

The provision of glucose over lipid based TPN resulted in a rapid and significant increase in ALA with difference in the AA/EPA ratio. This study indicates that different types of TPN specifically alter levels of non-esterified fatty acids. Interestingly, although glucose-based parenteral nutrition did not contain any lipids nor omega fatty acid supplements, it led to an increase in the levels of some omega fatty acids during the first days of total parenteral nutrition. This finding gives deeper insight into the metabolism of glucose and lipids in critically ill patients in relation to administered nutrition. Whether these alterations in NEFAs are associated with attenuated inflammatory conditions or improved survival rates needs further investigation.

Summary

With regard to clinical practice, there are significant differences in lipid metabolism in critically ill patients by using different types of parenteral nutrition.



HU PROTEIN PLAYS AN IMPORTANT ROLE IN VIRULENCE OF *FRANCISELLA TULARENSIS*

Pavla Stojková

Department of Molecular Pathology and Biology, Faculty of Military Health Sciences,
University of Defence in Hradec Kralove, Czech Republic

Co-authors: P. Špidlová, J. Lenčo, H. Řehulková, L. Krátká and J. Stulík

Tutor: Petra Špidlová

Introduction

Gram negative bacterium, *Francisella tularensis*, is the causative agent of zoonotic disease called tularemia (McCoy and Chapin, 1912). Due to its low infection dose it is considered to be a biological weapon and it is classified as a category A select agent. *F. tularensis* is one of the most pathogenic human pathogens known and can be spread by aerosol transmission to cause highly fatal pneumonic tularemia (Dennis et al., 2001). *Francisella* virulence is associated with its ability to survive inside of the phagocytic cells and to escape into the cytoplasm, cause apoptosis of host cell and subsequently attack other host immune cells. Its phagosomal escape and intracellular replication are dependent on gene cluster called *Francisella* pathogenicity island (FPI) that encodes type VI secretion system through MglA/SspA/PigR complex regulation. *Francisella* FPI gene mutants are unable to replicate in cytosol and do not trigger inflammasome activation (Celli and Zahrt, 2013; Checroun et al., 2006). This study hypothesizes that the HU protein could be other regulator of FPI proteins or direct regulator of PigR. HU protein is one of group of histone like proteins. *Francisella* HU protein is encoded by *hupB* gene and forms homodimer consisting of HU β subunits. In other bacteria HU protein is associated with virulence (Mangan et al., 2011), oxidative stress response, cell division, DNA protection (Oberto et al., 2009; Preobrajenskaya et al., 1994) and many other important bacterial cell cycles. Also in *F. tularensis* HU protein is a key player in its virulence and cannot be neglected.

Methods

We showed that FPI proteins are affected by histone like HU protein at both transcription and protein level. Using semi-quantitative comparative approach based on iTRAQ peptide labeling we compared proteome of deletion mutant strain in *hupB* gene with fully virulent wild type strain FSC200. After high pH reversed-phase peptide fractionation and LC-MS/MS analysis we evaluated the iTRAQ data using Proteome Discoverer software (Thermo Fisher Scientific). Protein levels of PigR and IglG were verified using targeted quantification of proteins using liquid chromatography-parallel reaction monitoring (LC-PRM). Full versions of proteomic analyses are available in study Stojkova et al. (2018): doi: 10.1080/21505594.2018.1441588.

Next we studied effect of HU protein on FPI proteins and PigR on transcription level. Using semi-quantitative reverse transcription followed by PCR we verified gene expression level for FPI genes and *pigR*. RNA from WT, complemented and mutant strains was isolated using RNeasy Mini Kit

(Qiagen, 74106) according to the manufacturer's instruction. Aliquots of RNA were used for reverse transcription and obtain cDNA was used for PCR. Samples were analyzed by gel electrophoresis and intensities of bands were determined by Bio1D software (CertainTech, Sterling, VA, USA).

Finally we were focused on target regulation sites of HU protein on *Francisella* genome. Chromatin immunoprecipitation followed by MiSeq sequencing was used. *Francisella* strain expressing HU protein fused with human influenza hemagglutinin peptide (HA tag) was used for selective enrichment of the protein-DNA complex of interest. Deletion mutant strain was used as negative control. Bacterial strains were treated by 1% formaldehyde (20 min, RT, 80 rpm) for crosslinking of protein-DNA complexes. 500 mM Tris was used for quenching reactions (20 min, 4°C, 80 rpm). After bacterial cell lysis and DNA shearing the target protein-DNA complexes were isolated by Pierce Anti-HA Agarose Beads (Thermo Fisher Scientific, 26182). Reverse crosslink (65°C, O/N), Proteinase K and RNase A were used for samples treatment. Aqueous solutions of target DNA sequences were obtained using Nucleospin gDNA Clean-up Kit (Machery Nagel, 1703/003). Ligation libraries and MiSeq sequencing based on Illumina platform were performed in collaboration with Institute of Microbiology Czech Academy of Sciences in Prague. Sequencing data were evaluated using online commonly available tools for ChIPseq analysis.

Results

This study well documented influences of HU protein on protein, transcription and gene level in *F. tularensis* subsp. *holarctica* FSC200. Proteomic analysis revealed big changes, the levels of almost a quarter of proteins were significantly changed (198 proteins with significantly decreased synthesis and 244 proteins with significantly increased synthesis) due to deletion of *hupB* gene in comparison with WT (Fig. 1). All FPI proteins but IglG (IglG was not identified at all in iTRAQ experiment) were found among proteins that exhibit decreased synthesis in *hupB* null mutant strain. When we looked at known FPI regulators, namely MglA, SspA and PigR proteins, iTRAQ analysis showed that there is no significant change related to MglA and SspA proteins. Targeted quantification analysis proved the significantly decreased synthesis of IglG protein as well as PigR in FSC200/*hupB* mutant strain (Fig. 2). Besides FPI proteins, many other proteins with decreased synthesis implying the important HU role in metabolic processes; such as for example cell redox homeostasis, LPS biosynthesis and stress response, were identified. Among proteins with increased synthesis, for example, RNA binding protein Hfq, that acts as a global regulator of gene expression in stress tolerance and pathogenesis and was found to be a positive regulator of FPI genes. In order to verify the proteomic data on transcription level we performed reverse transcription-PCR of *pigR* (Fig. 3) and FPI gene transcripts. We showed their significantly decreased expression in mutant strain in contrast to WT. Analysis of data from ChIPseq is currently underway. Nevertheless, the preliminary results indicate the involvement of the HU protein in regulation of PigR expression on gene level and thus HU protein can regulate FPI synthesis.

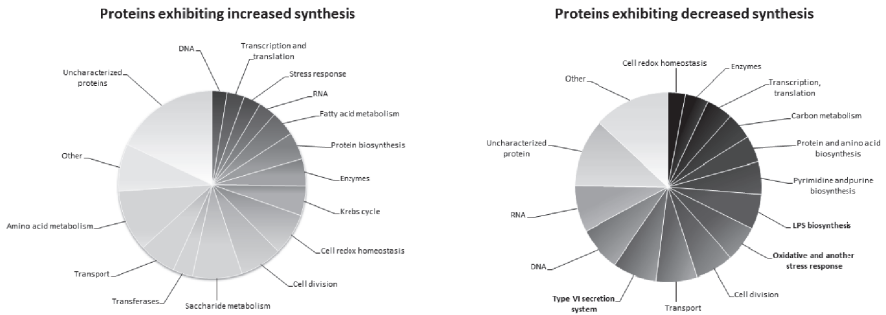


Figure 1: Group of proteins exhibiting increase/decrease synthesis in *hupB* null mutant *F. tularensis*.

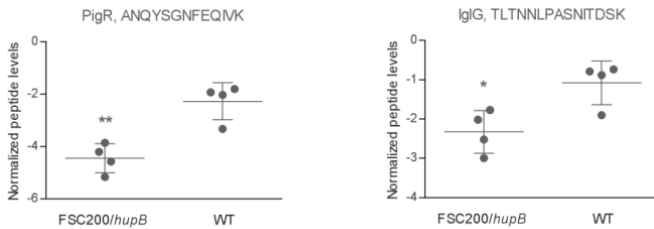


Figure 2: Target proteomic analysis of PigR and IglG. Figure 2: Target proteomic analysis of PigR and IglG.

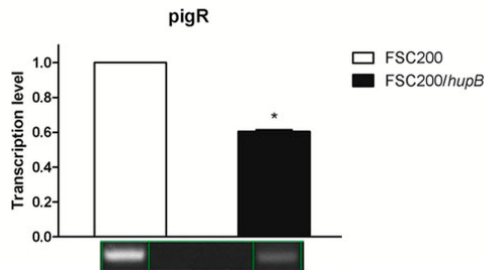


Figure 3: Transcription level of *pigR*. Figure 3: Transcription level of *pigR*.

Discussion

The FPI proteins represent group of virulence factors whose production is dependent on the functional HU protein. FPI proteins, especially, IglABCDEJIH, VgrG, PdpABCE and DotU that are chiefly responsible for escape of bacteria to the cytoplasm and their intracellular survival and are involved in the assembly of type six secretion system of *Francisella*, too. So far, it was believed that the expression of FPI proteins is strictly dependent upon action of three transcription

regulators called MglA, SspA and PigR. The protein levels of MglA and SspA detected in the FSC200/*hupB* mutant and WT did not significantly differ, therefore it can be assumed that reduced synthesis of PigR in *hupB* mutant is responsible for down regulation of FPI and thus defect in intracellular replication of bacteria. We aimed to study the role of HU protein on different levels (protein, transcription and gene) for better understanding of its influence on *Francisella* pathogenesis. Taken together, our findings thus strongly suggest the involvement of HU protein in regulation of *pigR* and thus FPI genes expression and make it an important component of *Francisella* virulence.

Conclusions

The results of this study highlight the importance of HU protein in *Francisella* virulence. The quantitative proteomics revealed that diminished expression of the PigR transcription factor in *hupB* null mutant strain might be responsible for the defect in the FPI proteins production. Our further results corroborate and support the importance of HU protein in PigR and FPI expression. Globally the obtained results further extend the current knowledge of the *Francisella* virulence mechanisms and might contribute to the development of a novel strategy for effective treatment of tularemia disease.

References

1. Celli, J., and Zahrt, T.C. (2013). Mechanisms of *Francisella tularensis* Intracellular Pathogenesis. Cold Spring Harb. Perspect. Med. 3.
2. Checroun, C., Wehrly, T.D., Fischer, E.R., Hayes, S.F., and Celli, J. (2006). Autophagy-mediated reentry of *Francisella tularensis* into the endocytic compartment after cytoplasmic replication. Proc. Natl. Acad. Sci. U. S. A. 103, 14578–14583.
3. Dennis, D.T., Inglesby, T.V., Henderson, D.A., Bartlett, J.G., Ascher, M.S., Eitzen, E., Fine, A.D., Friedlander, A.M., Hauer, J., Layton, M., et al. (2001). Tularemia as a biological weapon: medical and public health management. JAMA 285, 2763–2773.
4. Mangan, M.W., Lucchini, S., O Croinin, T., Fitzgerald, S., Hinton, J.C.D., and Dorman, C.J. (2011). Nucleoid-associated protein HU controls three regulons that coordinate virulence, response to stress and general physiology in *Salmonella enterica* serovar Typhimurium. Microbiology 157, 1075–1087.
5. McCoy, G.W., and Chapin, C.W. (1912). Further Observations on a Plague-Like Disease of Rodents with a Preliminary Note on the Causative Agent, *Bacterium tularensis*. J. Infect. Dis. 10, 61–72.
6. Oberto, J., Nabti, S., Jooste, V., Mignot, H., and Rouviere-Yaniv, J. (2009). The HU regulon is composed of genes responding to anaerobiosis, acid stress, high osmolarity and SOS induction. PloS One 4, e4367.
7. Preobrajenskaya et al. (1994). The protein HU can displace the LexA repressor from its DNA-binding sites. Mol. Microbiol. 13, 459–467.
8. Stojkova, P., Spidlova, P., Lenco, J., Rehulkova, H., Kratka, L., and Stulik, J. (2018). HU protein is involved in intracellular growth and full virulence of *Francisella tularensis*. Virulence 9, 754–770.

BRIEF AND EASY VISUAL PARIETAL ATROPHY SCORE (PAS) ON BRAIN MAGNETIC RESONANCE IMAGING IN EARLY-ONSET ALZHEIMER'S DISEASE

David Šilhán

Department of Neurology, Charles University,
Third Faculty of Medicine, Prague, Czech Republic

Tutor: Aleš Bartoš

Introduction

Brain magnetic resonance imaging (MRI) is an important tool, which can support diagnosis of Alzheimer's disease (AD) in clinical practice. Mediotemporal atrophy of the hippocampus on brain MRI is typical for late-onset AD (patients older than 65 years) [1-3]. Parietal atrophy is more common in less frequent early-onset AD (patients younger than 65 years) [4,5]. Parietal lobe structure can be evaluated on brain MRI using several approaches. However, these methods are often time consuming or require specialized software and are therefore not suitable for routine clinical practice.

Aim

Our main intention was to develop a simple and reliable visual scale for evaluating parietal atrophy on brain MRI, which could support diagnosis of AD in routine clinical practice.

Methods and participants

Our visual scale named Parietal Atrophy Score (PAS) is based on semi-quantitative assessment of three parietal structures on T1-weighted MRI coronal slices in the range of whole parietal lobes. We rated atrophy of sulcus cingularis posterior, precuneus and parietal gyri (Figure 1). Each structure was ranked into three categories: 0 – a normal size without atrophy, 1 – a borderline finding or 2 – a prominent atrophy. These ratings were summarized into one parietal atrophy score for each hemisphere (Figure 2) and then these two into one score for the entire brain.

Using our visual rating scale, we evaluated the parietal regions in 74 elderly subjects with normal Mini-Mental State Examination score (MMSE mean $29 \pm SD$ 1 point) with a wide range of age between 48-87 years to describe findings in normal aging [6].

We also measured intra-observer and inter-observer agreement between different raters using kappa statistics to assess reliability of the PAS scale. All raters evaluated the same brain MRI examinations of 25 selected persons using our visual scale.

Then we used PAS scale to compare parietal atrophy between a group of 32 patients with late-onset AD (MMSE 22 ± 4 points, mean age = 80 years) and 36 age-matched cognitively normal elderly subjects (MMSE 29 ± 1 point, mean age = 80 years). Finally, we compared the structures of the parietal lobes between a group of 26 patients with early-onset AD (MMSE 22 ± 4 points, mean age = 63 years) and 21 age-matched cognitively normal persons (MMSE 29 ± 1 point, mean age = 64 years).

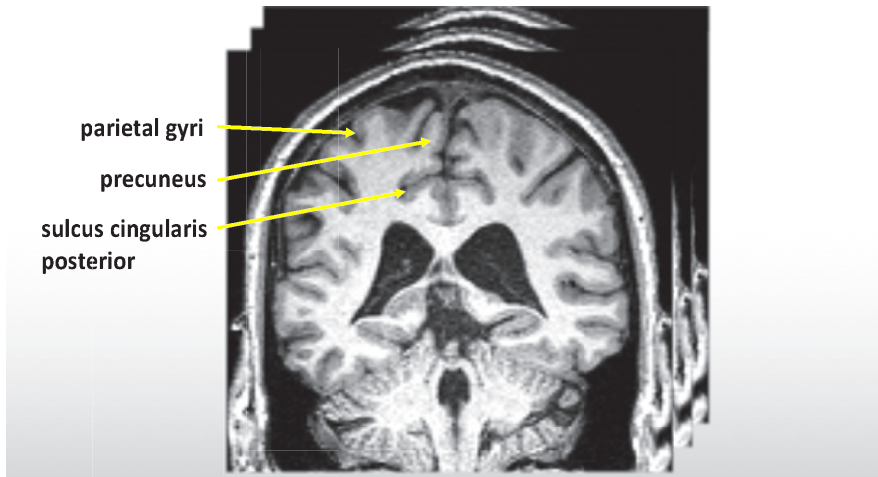


Figure 1 Three structures assessed using Parietal Atrophy Score (PAS) on T1-weighted coronary slices in the range of whole parietal lobes on brain magnetic resonance imaging

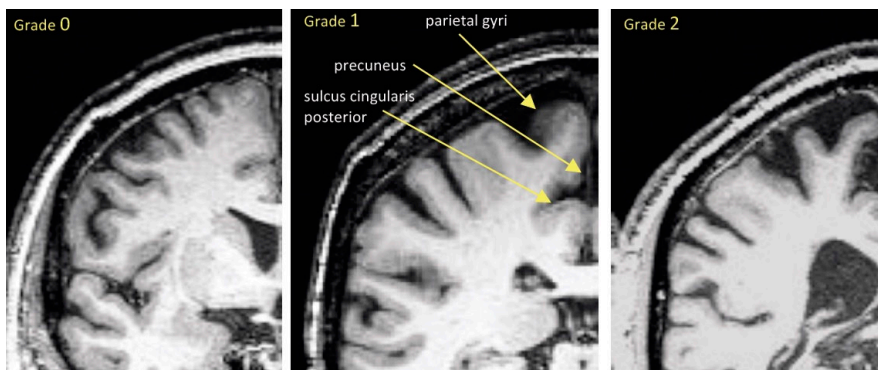


Figure 2 Three grades of parietal atrophy score for right parietal lobe: 0 – a normal size without atrophy, 1 – a borderline finding and 2 – a prominent atrophy

Results

Evaluation of one brain MRI examination using PAS is brief and takes about 1,5 minutes.

We found that natural aging is accompanied with a negligible parietal atrophic changes ($r = 0,2$; $p = 0,05$).

Intra-rater agreement was almost perfect with weighted-kappa value of 0,9. Inter-rater agreement was substantial with weighted-kappa values ranging between 0,60 – 0,75.

The patients with late-onset AD had a significantly more pronounced atrophy of sulcus cingularis posterior only on the left ($p < 0,01$) and parietal gyri on the right ($p < 0,05$) compared to cognitively normal subjects. Other structures were not different ($p > 0,05$).

The patients with early-onset AD had a significantly more pronounced atrophy of almost all the right and left parietal lobe structures compared to cognitively normal individuals ($p < 0,01$, in case of sulcus cingularis posterior on the left $p < 0,0001$). The only exception was the right precuneus which was not different between the groups (Figure 3).

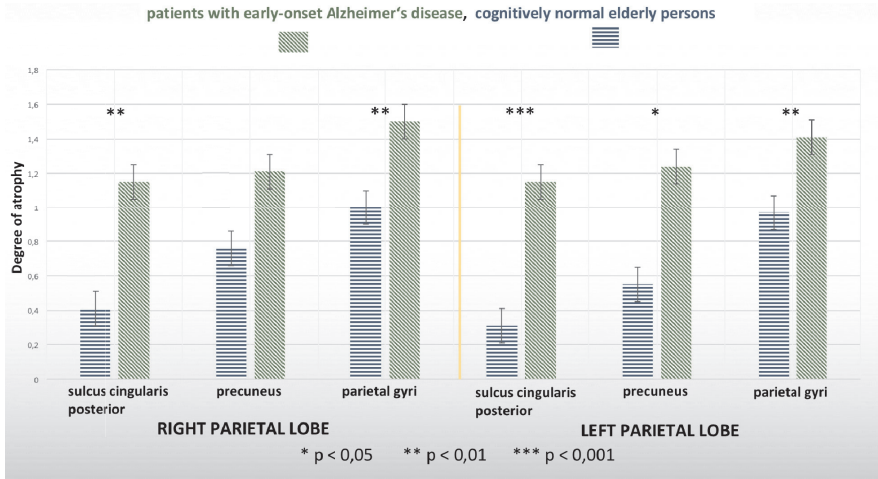


Figure 3 Semi-quantitative degrees of atrophy of individual structures in parietal lobes using Parietal Atrophy Score (PAS) ranging from 0 to 2 in patients with early-onset Alzheimer’s disease and age matched cognitively normal elderly persons

Discussion and conclusion

The new visual scale Parietal Atrophy Score (PAS) is a time-saving and reliable system for assessing parietal atrophy on brain MRI which is almost age-independent in the elderly individuals [6]. This approach does not require specialized software or expertise. Visual evaluation and basic knowledge about brain MRI structures are sufficient. These qualities make the PAS scale a suitable method for routine clinical practice.

Atrophic changes in parietal lobes are not typical for early stages of late-onset AD according to our results and other studies [5]. Mediotemporal atrophy seems to be better biomarker of late-onset AD [5].

The PAS scale can detect more pronounced atrophy of parietal lobes in patients with early-onset AD and therefore can support this diagnosis in clinical practice. Some structures of parietal lobes are more affected by atrophy than the others. Atrophy of the sulcus cingularis posterior can be considered the best biomarker of early-onset AD in the context of parietal atrophy.

We believe that the PAS scale can also contribute to differential diagnosis of early-onset AD and frontotemporal lobar degeneration (FTLD). Both dementias have similar age of onset. However, parietal atrophy is associated with early-onset AD and not with FTLD. We are going to verify it in our next study.

Summary

We developed visual scale named PAS for rating parietal atrophy on brain MRI. This approach is based on assessing of atrophy in three regions of parietal lobes on T1-weighted coronary slices. Evaluated structures are sulcus cingularis posterior, parietal gyri and precuneus. The PAS scale is quick, simple and reliable approach which can detect more pronounced parietal atrophy in patients with early-onset AD and therefore can support this diagnosis in routine clinical practice.

Acknowledgement: to organization ADNI for providing data.

Supported by PROGRES Q35, LO1611 and MH CZ DRO 00023752, 260388/SVV/2018

References

1. Liu Y, Paajanen T, Zhang Y, et al. AddNeuroMed Consortium: Analysis of regional MRI volumes and thicknesses as predictors of conversion from mild cognitive impairment to Alzheimer's disease. *Neurobiol Aging*. 2010, 31:1375–85.
2. Fennema-Notestine C, McEvoy LK, Hagler DJ Jr, et al. The Alzheimer's Disease Neuroimaging Initiative: Structural neuroimaging in the detection and prognosis of pre-clinical and early AD. *Behav Neurol*. 2009, 21:3–12.
3. Jack CR, Shiung MM, Gunter JL, et al. Comparison of Different MRI Brain Atrophy Rate Measures with Clinical Disease Progression in AD. *Neurology* 2004;24; 62(4): 591–600.
4. Galton CJ, Patterson K, Xuereb JH, et al. Atypical and typical presentations of Alzheimer's disease: a clinical, neuropsychological, neuroimaging and pathological study of 13 cases. *Brain*. 2000;123 Pt3:484-98.
5. Frisoni GB, Testa C, Sabattoli F, et al. Structural correlates of early and late onset Alzheimer's disease: voxel based morphometric study. *Journal of Neurology, Neurosurgery and Psychiatry* 2005;76:112-114.
6. Šilhán D, Ibrahim I, Tintěra J, et al. Parietální atrofický skór na magnetické rezonanci mozku u normálně stárnoucích osob. *Cesk Slov Neurol N* 2018; 81(4): 414-419.

ALCOHOL-ABUSE DRUG DISULFIRAM TARGETS CANCER VIA P97 SEGREGASE ADAPTOR NPL4

Zdeněk Škrott

Laboratory of Genome Integrity, Institute of Molecular and Translational Medicine,
Faculty of Medicine, Palacky University Olomouc

Co-authors: M. Mistrík, D. Majera, T. Oždian, J. Bartek

Tutor: Martin Mistrík

Introduction and Aims

Drugs often interact with more molecules than intended and such interaction with these off-targets could manifest not only as adverse side effects, but importantly also as positive side effects, which may be useful to treat certain disease and drug can be repurposed[1]. As drug repositioning accelerates approval process and lower the financial cost, it is highly promising approach with growing importance and interest. Disulfiram, also known as Antabuse, is used for more than sixty years as alcohol deterrent. Its metabolite binds irreversibly to aldehyde dehydrogenase, an enzyme critical for proper metabolism of ethanol, leading to marked accumulation of acetaldehyde. Importantly, it is becoming apparent that disulfiram targets cancer too[2,3]. Many reports agreed on the dependence on copper for disulfiram to exert anti-tumour effect. Its mechanism of action has been explained by several ways including the inhibition of proteasome, which relay on the presence of copper[4]. The objective of this work was to find why copper potentiates disulfiram effect and to find its mechanism of action in cancer cells.

Methods

Cell lines were cultured in appropriate medium (DMEM, RPMI) supplemented with 10% fetal bovine serum and penicillin/streptomycin; and maintained at humidified, 5% CO₂ atmosphere at 37°C. U2OS cells were used to generate stable cell line expressing NPL4-GFP. Cells were transfected by NPLOC4-GFP pCMV6-Entry vector (Origene) using FugeneHD protocol. Cell viability and proliferation was analysed by XTT (according to manufacturer protocol) and CFA assays. Copper-dithiocarbamate complex was analysed by HR-MRM analysis performed on HPLC-ESI-QTOF system consisting of HPLC chromatograph Thermo UltiMate 3000 with AB Sciex TripleTOF 5600+ mass spectrometer. Chromatographic separation was done by PTFE column filled by C18 sorbent. Analysis was performed at room temperature and flow rate 1500 µL/min. Mobile phase consisted of acetone 99.9%, water 0.1% and 0.03% formic acid. Liquid nitrogen-frozen biological samples (30-100 mg) were immediately processed by homogenization in 100% acetone in ratio 1:10 sample vs. acetone. Next, sample was immediately spun at 4°C, 20000G, 2min. Supernatant was decanted into a new 1,5 ml Eppendorf tube and immediately spun for 30 min using small table centrifuge (BioSan FVL-2400N) placed inside -80°C freezer. Supernatant was quickly decanted into glass HPLC vial and analysed. Cellular proteins were analysed by Immunoblotting and immunofluorescence analysis.

Results and discussion

Disulfiram rapidly decompose to diethyldithiocarbamate in human body and as dithiocarbamates are strong metal chelators, we argued that bis-diethyldithiocarbamate-copper complex (CuET) is formed *iv-vivo*, providing the anti-cancer metabolite. We developed a method for CuET analysis, by which we confirmed the CuET metabolite in several tissues including liver, brain, plasma and tumour taken from mice treated by disulfiram or disulfiram/copper combination. The analysis revealed that first, higher CuET formation in disulfiram/copper group versus disulfiram alone, second, preferential CuET accumulation in tumours compared to other tissues; together supporting CuET as the final anti-cancer metabolite of disulfiram *in-vivo*. Importantly, I also detected CuET in plasma taken from alcoholics after single disulfiram dose, confirming CuET as new metabolite of disulfiram in humans.

The anti-cancer activity of disulfiram has been explained by several mechanisms, and the proteasome, which is responsible for protein degradation, was suggested as possible target. However, I found that despite the degradation of specific proteasome substrates (I κ B, Ub-GFP) is clearly suppressed by CuET, the proteasome is not inhibited by CuET. Thus, I hypothesised CuET does not target the proteasome at all, but rather a protein called p97, which acts upstream the proteasome extracts ubiquitinated proteins from complexes, membranes or chromatin. Interestingly, I detected immobilisation of ubiquitinated proteins on various cellular structures, including membranes, chromatin and large complexes consistent with p97 segregase malfunction. Unexpectedly, p97 itself was found immobilised on these structures. p97 does not work alone but associates with various cofactors, among them NPL4 and UFD1 as the most important. I analysed also the behaviour of these cofactors and found prominent immobilisation of NPL4 cofactor. Subsequent experiments showed rapid and total immobilisation and complete loss of solubility and hence the function of this otherwise very mobile cofactor. Importantly, ectopic overexpression of NPL4, significantly protected the cells from CuET induced toxicity or inhibition of protein degradation. In subsequent experiments, I identified putative zinc-finger domain of NPL4 as supposed binding site of CuET and the requirement of putative zinc-finger domain integrity for proper NPL4 conformation and function. Image analysis (Fig. 1) of cells revealed that NPL4 forms clearly visible aggregates in response to CuET. The aggregated NPL4 recruits p97 and subsequently also other proteins involved in aggregation such as ubiquitin, small ubiquitin-like modifier SUMO, TDP-43 protein and heat-shock protein 70. Finally, these bulky aggregates trigger heat-shock response, unfolded-protein response, ubiquitin stress, malfunction of UPS and other p97-dependent processes, and cell death as a final consequence.

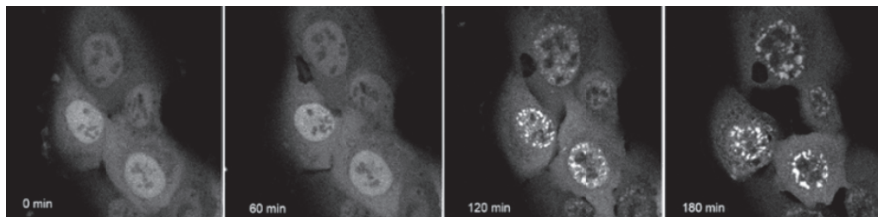


Fig. 1. NPL4 gradually forms aggregates after CuET treatment (1 μ M, U2OS cells expressing NPL4-GFP).

Conclusions

Collectively, my research work, as a part of broader project, helps to explain anti-cancer effect of alcohol-abuse drug disulfiram. It should encourage copper supplementation with disulfiram in upcoming clinical trials. Validation of CuET as the active metabolite and development of method for its detection in human samples should help clinical oncologist to set proper dose, monitor impact of the treatment and explain potential variability of outcomes. Identification of NPL4 protein as a molecular target of CuET is surprising given the NPL4 has never been mentioned as a potential anti-cancer target in scientific literature. This study should promote further research on NPL4 potentially leading to development of better inhibitors and identification of subset of sensitive tumour types to NPL4 inhibition. Finally, with respect to disulfiram safety, very good long-term tolerability and established clinical practice, these results should motivate series of clinical trials to identify specific cancer types responding to disulfiram. Repurposing of disulfiram as anti-cancer drug could be especially important for developing countries. As the financial cost of new drugs is extremely high, they could be inaccessible for countries with weak health-care system. The cost of a few US dollars for one-month therapy makes disulfiram ideal candidate for such countries to combat cancer.

Summary

This work was focused on repurposing drug disulfiram for cancer therapy. Disulfiram, also known as Antabuse, is an old anti-alcohol drug that has been shown to be effective in various preclinical cancer models. However, the unknown active metabolite, the unclear mechanism of action and unidentified molecular target, all obstruct repurposing disulfiram for use as an anti-cancer agent. In this work, we have described a new disulfiram metabolite in humans, disulfiram-copper complex, as the active metabolite toxic to cancer cells and accumulating in tumours. Moreover, we have found that in the cells, disulfiram-copper complex binds to the NPL4 protein, an adaptor of p97 segregase, which is essential for the degradation of proteins involved in several regulatory and stress responses. Binding of the disulfiram-copper complex to NPL4 induces its conformational change and aggregation. NPL4 aggregates subsequently attract p97 and other stress proteins leading to induction of heat-shock and unfolded-protein responses, impairment of protein degradation, ubiquitin stress, and cell death as a consequence. Collectively, these should encourage further clinical tests, help clinicians to monitor the treatment and identify suitable patients who might benefit from disulfiram. Finally, it should promote eventual repurposing of this old, safe and unexpensive drug to combat cancer worldwide.

References

1. Boguski MS, Mandl KD, Sukhatme VP. Repurposing with a difference. *Science* 2009; 324, 1394-1395.
2. Skrott Z, Cvek B. Diethyldithiocarbamate complex with copper: the mechanism of action in cancer cells. *Mini-Reviews Med Chem* 2012; 12, 1184–1192.
3. Skrott Z, Mistrik M, Andersen KK et al. Alcohol-abuse drug disulfiram targets cancer via p97 segregase adaptor NPL4. *Nature* 2017; 552, 194–199.
4. Chen D, Cui QC, Yang H et al. Disulfiram, a Clinically Used Anti-Alcoholism Drug and Copper-Binding Agent, Induces Apoptotic Cell Death in Breast Cancer Cultures and Xenografts via Inhibition of the Proteasome Activity. *Cancer Res* 2006; 66, 10425–10433.

PERIPUBERTAL CANNABIDIOL TREATMENT PREVENTS MOLECULAR AND BEHAVIORAL CHANGES IN NEURODEVELOPMENTAL MODEL OF SCHIZOPHRENIA

Tibor Štark

Department of Pharmacology, Faculty of Medicine,
Masaryk University, Brno, Czech Republic

Co-authors: V. Di Marzo, C. D'Addario, M. Maccarrone, F. Drago,
R. Mechoulam, A. Sulcova

Tutor: V. Micalé

Introduction

Growing evidence indicates involvement of endocannabinoid system (ECS) in pathophysiology of schizophrenia (SCZ)¹. Based on neurodevelopmental hypothesis, the origin of SCZ typical phenotype with onset at adulthood could lie in prenatal period (in the form of stressors interacting with genetic predisposition)². Given that preventive treatment with antipsychotics seems to reduce the risk of transition to psychosis in vulnerable individuals³, we investigated 1) effects of methylazoxymethanol acetate (MAM) prenatal administration on behavioural phenotype and molecular ECS levels at both neonatal and adult age, and 2) effects of peripubertal pharmacological modulation of the ECS to evaluate its potential to counteract schizophrenia-like phenotype in adulthood.

Materials and Methods

Animals and Experimental design

Fifty timed-pregnant Sprague-Dawley rats were obtained from Charles River (Germany) at gestational day (GD) 13. They were housed individually and randomly assigned to two groups for intraperitoneal administration of MAM or vehicle (CNT) on gestational day 17 (GD 17), as previously described⁴. The offspring were weaned from mothers on the postnatal day (PND) 22. They were randomly assigned to treatment groups (n=15/group) and housed two to three per cage with food and water accessible *ad libitum* and constant environmental conditions. Detailed experimental design is depicted in Fig.1. All experiments were conducted in accordance with all relevant laws and regulations of animal care and welfare. The experimental protocol was approved by the Animal Care Committee of the Masaryk University, Faculty of Medicine, Czech Republic and carried out under the European Community guidelines for the use of experimental animals.

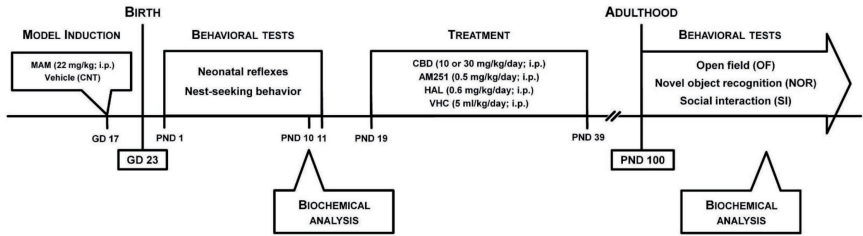


Fig.1: Experimental design

Drugs

For prenatal model induction, methylazoxymethanol acetate (Midwest Research Institute, Kansas City, USA) was dissolved in saline (22 mg/kg)⁴. All compounds for peripubertal treatment (including vehicle treatment – VHC) were administered intraperitoneally (5 ml/kg) from PND 19 to PND 39. The non-psychotropic cannabinoid cannabidiol (CBD), kindly provided by Prof. Raphael Mechoulam (Hebrew University, Jerusalem, Israel), was dissolved in Tween80 and saline (1:49; 10 and 30 mg/kg). The CB1 antagonist/inverse agonist AM251 (Sigma-Aldrich) was dissolved in dimethylsulfoxide, Tween80 and saline (1:1:8; 0.5 mg/kg). The typical antipsychotic haloperidol (HAL; Haloperidol-Richter®, Czech Republic) used as positive control was dissolved in saline (0.6 mg/kg).

Behavioural testing

From PND 1 to 11, new-born pups were submitted to the battery of 6 neonatal reflexes (see Fig.2)⁵: A) *Righting*: pup rapidly returns to its four feet when placed on its back; B) *Cliff Aversion*: pup withdraws from the edge of a flat surface when its snout and forepaws are placed over a cliff (60 cm); C) *Forelimb placing*: pup raises and places its forepaw on a cardboard with which it has been stroked against the dorsal surface of the paw; D) *Forelimb grasping*: pup grasps strongly the barrel of 16-gauge needle or toothpick when the palm of its forepaw is touched; E) *Bar holding*: pup holds itself-only on to a toothpick with its forelimbs for 5 s; F) *Negative geotactic reaction*: pup turns approximately 180° to either side and moves toward the upper end when placed head down on an inclined surface (30°). The percentage of pups manifesting presence of the reflex was scored on each experimental day.

Novel Object Recognition (NOR) test was used to evaluate cognitive-like deficit at adulthood (PND 100+). Rat was placed in plexiglass arena (45×45×30 cm) with two identical objects and let to explore them (5 min). After 3 min inter-trial interval in home cage, tested rat was returned to the same arena for the second trial (5 min) with one familiar object and one novel object (visually different in size, shape and colour). Duration of exploration of familiar (Tf) and novel object (Tn) were evaluated and discrimination index was calculated as $DI = (Tn - Tf)/(Tn + Tf)$ ⁶.

Social Interaction (SI) test was used to identify negative-like symptom at adulthood (PND 100+). Each animal was allowed to freely explore an unfamiliar congener in the open-field metal box (60×60×60 cm; 10 min). Social behaviour was defined as sniffing, following, grooming, mounting, and nosing. Frequency and duration of social interactions were measured as main parameters.

Assessment of endocannabinoid system elements

After the behavioral testing, animals were sacrificed and endogenous levels and expression of ECS elements were evaluated in collected brain samples (whole brains in neonatal samples, different brain regions). Ligands anandamide (AEA), 2-arachidonoyl glycerol (2-AG), oleoylethanolamine (OEA), palmitoylethanolamine (PEA), their enzymes of biosynthesis and degradation, and receptors (CB1, CB2, TRPV1) were assessed using GC-MS, methylation analysis, qPCR and Western blot⁷.

Statistical analysis

Data were analysed using Fisher's exact test (neonatal reflexes), unpaired t-test (neonatal ECS) or 2-way ANOVA (factors: model and treatment; adult data) followed by Fisher's test of LSD. All data are presented as means±SEM. Statistical significance was accepted at $p < 0.05$.

Results

At birth, the full development of all tested neonatal reflexes was delayed in prenatally MAM-exposed rats ($p < 0.05$; $p < 0.01$; $p < 0.001$; Fig.2A-F). On molecular level, we observed increased level of 2-AG ($p < 0.05$) in the whole neonatal brains accompanied by increased mRNA expression of DAGL β , the enzyme of 2-AG biosynthesis ($p < 0.05$; Fig.2G, K). There were no changes in the AEA levels despite altered mRNA expression of its enzymes of degradation (FAAH) and synthesis (ABHD4) (Fig.2H, K).

At adulthood, prenatally MAM-exposed rats spent less time interacting with their congener ($p < 0.001$), while early chronic treatment with cannabidiol (30 mg/kg) and AM251 (0.6 mg/kg) was able to reverse this social deficit ($p < 0.001$, $p < 0.01$; Fig.3A). Number of interactions did not differ among the groups maintaining motor activity intact (Fig.3B).

Cognitive performance was also impaired in MAM model, as described by decreased discrimination index ($p < 0.01$). Again, cannabidiol (30 mg/kg), but neither AM251 nor haloperidol, was able to reverse MAM-induced recognition deficit ($p < 0.01$; Fig.3C).

On molecular level, DNA methylation of CB1 receptor gene was decreased ($p < 0.01$) and mRNA and protein expression were increased ($p < 0.01$, $p < 0.001$) in prefrontal cortex of adult rats prenatally exposed to MAM. Early intervention with cannabidiol during peripubertal period was able to reverse these alterations on all levels ($p < 0.05$, $p < 0.001$; Fig.3D-F). Other treatments could not induce consistent turnover of MAM-induced CB1 alterations in adult MAM rats, except for increased DNA methylation by HAL ($p < 0.001$) and decreased mRNA ($P < 0.001$) expression by AM251. It is in accordance with the partial (AM251) or complete (HAL) lack of behavioral recovery.

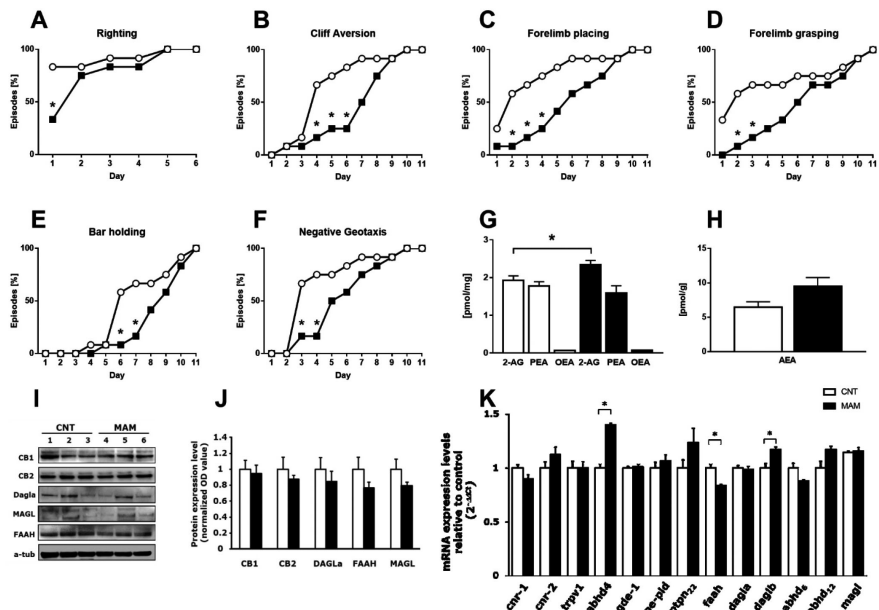


Fig. 2: Evaluation of neonatal reflexes of MAM-exposed and control pups (A-F); concentration of endocannabinoids (G, H), protein (I, J) and mRNA expression (K) of ECS elements in collected brains of neonatal MAM-exposed and control pups.

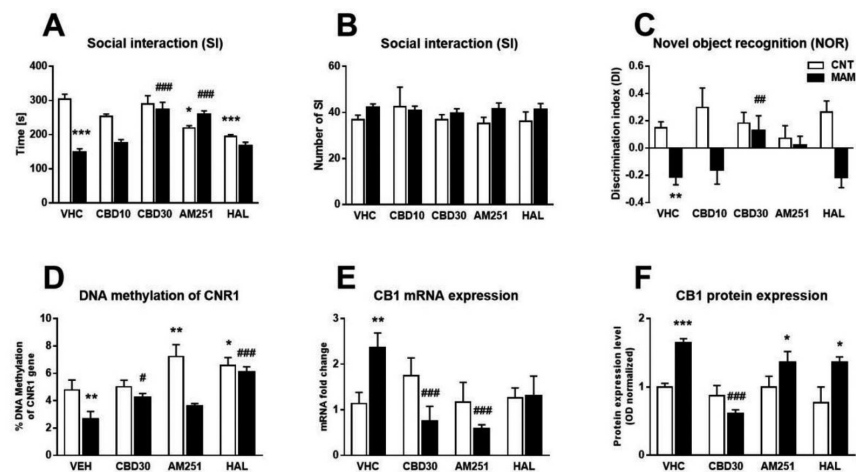


Fig. 3: Behavioral and molecular alterations in adulthood: time spent in social interaction (A); number of social interactions (B); discrimination index of recognition memory (C); exploration times of novel object recognition testing phase (D); DNA methylation of gene promoter (E), mRNA expression (F), and protein expression (G) of CB1 receptor in prefrontal cortex. * $p < 0.05$, ** $p < 0.01$ and *** $p < 0.001$ vs CNT/VHC; # $p < 0.05$, ## $p < 0.01$ and ### $p < 0.001$ vs MAM/VHC.

Discussion

Gestational MAM exposure delayed the maturation of neonatal reflexes, which could, together with elevated level of 2-AG, represent a predictive factor for CNS dysfunctions in neurodevelopmental disorders like schizophrenia. Moreover, given that 2-AG can suppress glutamate release via CB1 receptors⁸, we hypothesize neonatal induction of 2-AG signalling might reduce glutamatergic neurotransmission (a typical hallmark in schizophrenia) and thus contribute to the development of social and cognitive deficits observed in adulthood.

Our research showed that the negative and cognitive-like symptoms in MAM rats coincide with the decreased DNA methylation of gene promotor and elevated expression and protein levels of CB1 receptor specifically restricted to the prefrontal cortex. The peripubertal age is a pivotal period for the development of prefrontal cortex, dysregulation of which is involved in the pathophysiology of SCZ⁹. Our results further suggest this critical time as suitable for preventive antipsychotic treatment. Early and repeated CBD administration in peripubertal period completely normalized MAM-induced behavioural alterations mimicking cognitive and negative symptoms of schizophrenia. These effects are in line with adult treatment effects in animal studies and they translate to human studies as well¹⁰. CBD-evoked behavioural recovery was accompanied by consistent turnover of cannabinoid CB1 receptor alterations in the prefrontal cortex (increased DNA methylation, paralleled decreased mRNA and protein expression), without having *per se* any effect in control rats.

Conclusion

Our results suggest that the delayed onset of innate neonatal reflexes as an index of impaired brain maturation together with changes in ECS signaling could represent a potential predictive factor for late-arisen abnormalities resembling schizophrenia phenotype. MAM-induced behavioral and molecular alterations which mimic schizophrenia phenotype in adulthood could be reversed by peripubertal pharmacological intervention with cannabidiol. Thus, the potential of early monitoring and modulation of ECS would deserve further attention.

Acknowledgements

This work was financed from the SoMoPro II Programme, co-financed by European Union, the South-Moravian Region and the specific research at the Masaryk University (MUNI/A/1063/2016). This publication reflects only the author's views and the Union is not liable for any use that may be made of the information contained therein.

References

1. Kucerova, J., Tabiova, K., Drago, F. & Micale, V. Therapeutic potential of cannabinoids in schizophrenia. *Recent Patents CNS Drug Discov.* **9**, 13–25 (2014).
2. Jones, C. A., Watson, D. J. G. & Fone, K. C. F. Animal models of schizophrenia. *Br. J. Pharmacol.* **164**, 1162–1194 (2011).
3. McGorry, P. D. Early intervention in psychosis: obvious, effective, overdue. *J. Nerv. Ment. Dis.* **203**, 310–318 (2015).
4. Lodge, D. J. & Grace, A. A. Gestational methylazoxymethanol acetate administration: a developmental disruption model of schizophrenia. *Behav. Brain Res.* **204**, 306–312 (2009).

5. Baharnoori, M., Bhardwaj, S. K. & Srivastava, L. K. Neonatal behavioral changes in rats with gestational exposure to lipopolysaccharide: a prenatal infection model for developmental neuropsychiatric disorders. *Schizophr. Bull.* **38**, 444–456 (2012).
6. Zamberletti, E. *et al.* Gender-dependent behavioral and biochemical effects of adolescent delta-9-tetrahydrocannabinol in adult maternally deprived rats. *Neuroscience* **204**, 245–257 (2012).
7. D’Addario, C. *et al.* A preliminary study of endocannabinoid system regulation in psychosis: Distinct alterations of CNR1 promoter DNA methylation in patients with schizophrenia. *Schizophr. Res.* (2017). doi:10.1016/j.schres.2017.01.022
8. Melis, M. *et al.* Endocannabinoids mediate presynaptic inhibition of glutamatergic transmission in rat ventral tegmental area dopamine neurons through activation of CB1 receptors. *J. Neurosci. Off. J. Soc. Neurosci.* **24**, 53–62 (2004).
9. Volk, D. W. & Lewis, D. A. Impaired prefrontal inhibition in schizophrenia: relevance for cognitive dysfunction. *Physiol. Behav.* **77**, 501–505 (2002).
10. Osborne, A. L., Solowij, N. & Weston-Green, K. A systematic review of the effect of cannabidiol on cognitive function: Relevance to schizophrenia. *Neurosci. Biobehav. Rev.* **72**, 310–324 (2017).

GUT MICROBIOTA COMPOSITION AND SHORT-CHAIN FATTY ACID LEVELS IN HUMAN CANCER CACHEXIA: A PILOT STUDY

J. Übachs

Department of Surgery and Department of Medical Microbiology, NUTRIM School of Nutrition and Translational Research in Metabolism, Department of Gynaecology, GROW school of Oncology and Developmental Biology, Maastricht University, the Netherlands

Co-authors: J. Ziemons, H.H.van Eijk, R.F.P.M. Kruitwagen, T. Van Gorp, J. Penders, S.W.M. Olde Damink, S. S. Rensen

Tutor: not specified

Introduction

Cancer cachexia is a complex syndrome characterized by weight loss, inflammation, and disturbed energy metabolism. Recent animal studies suggest that the gut microbiota could be involved in the pathogenesis of cancer cachexia by modulating key metabolic pathways of the host through short-chain fatty acids (SCFAs) production. We hypothesized that the relative abundance of bacteria known to be associated with deranged metabolism is different in cachectic patients, accompanied by reduced fecal SCFA levels.

Materials and Methods

Stool samples were collected preoperatively from patients suffering from breast cancer (n=18), lung cancer (n=16), or pancreatic cancer (n=20). Cachexia was defined as weight loss >5% in the last six months. Relative abundance of *Akkermansia muciniphila*, Lactobacilli, and butyrate producers was quantified by qPCR. Fecal levels of the SCFAs acetate, propionate, and butyrate were assessed by liquid chromatography-mass spectrometry.

Results

Prevalence of cancer cachexia was 17% (n=3), 19% (n=3) and 70% (n=14) in breast, lung and pancreatic cancer patients, respectively (20 cachectic and 34 non-cachectic patients, in total). The relative abundance of the indicated bacteria was not different between the different cancer types nor between cachectic and non-cachectic individuals. Acetate, propionate, and butyrate levels were consistently lower in cachectic individuals, but the differences were not significant (acetate: 12.5±3.4 vs. 14.3±2.6 µmol/g, p=0.51; propionate: 11.8±2.6 vs. 29.2±10.9 µmol/g, p=0.46; butyrate: 25.7±3.0 vs. 50.0±15.8 µmol/g, p=0.86). Fecal SCFA levels were associated with BMI as well as with abundance of Lactobacilli and *Akkermansia muciniphila*.

Conclusion

The current data suggest that gut microbiota composition and fecal SCFA levels are not affected in human cancer cachexia, although the number of samples was limited. Microbiota analyses by next-generation sequencing and inclusion of more patients are ongoing. This will provide more extensive data and a more reliable data-analysis.

“RADIOMICS” FEATURES IN BODY COMPOSITION IMAGING ASSOCIATED WITH MUSCLE WASTING AND POOR SURVIVAL AFTER PANCREATIC CANCER RESECTION

Gregory van der Kroft

Department of General, Gastrointestinal, Hepatobiliary and Transplant Surgery, Uniklinikum RWTH-Aachen, Department of Surgery Maastricht, Department of Radiation Oncology (MAASTRO), GROW, School of Oncology and Developmental Biology, Maastricht University Medical Center, the Netherlands

Co-authors: Ralph Brecheisen, Leonard Wee, David P.J. van Dijk, Sander S. Rensen, Andre Dekker, Roman Eickhoff, Angalie A. Röth, Florian Ulmer, Ulf P. Neumann, Steven W.M. Olde Damink

Tutor: not specified

Introduction

Skeletal Muscle radiation attenuation (SM-RA) is associated with myosteatosi s and mortality following pancreatic cancer surgery [1]. Computerized radiological image analysis enables investigation of image-derived phenotypes by extracting large numbers of quantitative features (radiomics) [2-4]. We identified radiomics features that correlated strongly with SM-RA and evaluated their association with mortality after surgery for head of pancreas cancer.

Methods

This was a retrospective multicentre study of 330 patients from hospitals in Aachen-Germany (n=202) and Maastricht-the Netherlands (n=128) undergoing elective pancreatic cancer resection between 2010 and 2017 for the treatment of cancer of the pancreatic head. Computed tomography images through the 3rd lumbar vertebrae were manually segmented into muscle, visceral-, and subcutaneous adipose tissue compartments. SM-RA was measured in the muscle compartment; in total, 339 radiomics features were extracted from all three compartments. Radiomics features associated with SM-RA were identified using Pearson correlation coefficients and tested for mortality association in univariate logistic regression. Multivariate logistic regression of SM-RA-correlated radiomics features against mortality was performed using elastic regularization with 5-fold cross-validation and 20 sampling repetitions per fold.

Results

Sixteen radiomics features were strongly correlated to SM-RA ($r>0.75$, $p<0.001$). In univariate analysis, all radiomics features were significantly associated to mortality at 90 days ($p<0.02$) and 2 years ($p<0.03$). Radiomics features slightly improved the Area-Under-receiver-operator Curve (AUC) metric relative to SM-RA alone, both for 90-day mortality (0.71 vs. 0.77, respectively) and 2-year mortality (0.55 vs. 0.64, respectively) prediction.

Conclusion

Six-teen radiomics features were found after univariate analysis to be strongly correlated to SM-RA and were significantly associated with mortality in patients undergoing pancreatic cancer resection. In ROC analysis radiomics features were associated with a slight improvement in 90-day and 2-year mortality prediction. We propose that radiomics features contain more information than SM-RA alone, leading to slightly improved discrimination. The robustness and veracity of radiomics features as predictors of post-resection mortality need to be investigated further in a substantially larger multi-institutional cohort.

References

1. van Dijk, D.P.J., et al., *Myosteatosi predicts survival after surgery for periampullary cancer: a novel method using MRI*. HPB (Oxford), 2018.
2. Aerts, H.J., et al., *Decoding tumour phenotype by noninvasive imaging using a quantitative radiomics approach*. Nat Commun, 2014. **5**: p. 4006.
3. Limkin, E.J., et al., *Promises and challenges for the implementation of computational medical imaging (radiomics) in oncology*. Ann Oncol, 2017. **28**(6): p. 1191-1206.
4. Traverso, A., et al., *Repeatability and Reproducibility of Radiomic Features: A Systematic Review*. Int J Radiat Oncol Biol Phys, 2018.

INHIBITION OF P38 RE-EXPRESSES E-CADHERIN AND PREVENTS VASCULAR INVASION IN MELANOMA

Judith Wenzina

Skin and Endothelium Research Division (SERD), Department of Dermatology,
Medical University of Vienna, Vienna, Austria

Co-authors: S. Holzner, A. Forsthuber, E. Puujalka, P. Petzelbauer

Tutor: Peter Petzelbauer

Introduction and aims

Melanoma, a malignant tumor of melanocytes, is responsible for 75% of skin cancer deaths worldwide. A hallmark of melanoma is that even thin lesions have a high risk for metastasis due to their striking ability of lymphatic and blood vessel invasion. Invasive melanoma is usually associated with epithelial-mesenchymal transition (EMT) [1]. EMT is characterized by a highly mobile cell that has lost E-Cadherin (CDH1) expression and has gained expression of EMT markers such as SNAIL1/SNAIL2, ZEB1/ZEB2, TWIST, Goosecoid, SIX1, FOXC2, and TCF4 [2, 3]. Due to therapeutic advances, the survival rate of melanoma patients has improved [4]. However, there is still a large portion of non-responders. We aim to establish a new treatment concept: Targeting the p38 pathway prevents vascular invasion.

Methods

We are working with 22 patient-derived melanoma cell lines which have been characterized by Agilent Gene Expression Microarrays. We selected E-Cadherin as the single best surface marker gene for an “epithelial” phenotype and the loss of E-Cadherin being a sign for mesenchymal transformation. We confirmed this assumption by correlating the expression of EMT genes with the absence or presence of E-Cadherin.

Moreover, we have developed and validated new assays measuring the ability of melanoma cells for vascular invasion. Gap formation assay: Blood endothelial cells (BECs) were seeded as a monolayer to confluence, melanoma spheroids were added for 2 hours, endothelial cell monolayer disruption and gap formation was quantified by confocal laser scanning microscopy. ECIS® resistance assay: Array plates from ibidi® were equilibrated with medium and 12000 endothelial cells per well were seeded, the electrical cell impedance system (ECIS®) was used to monitor cells continuously. After resistance at 4000Hz reached a stable plateau $>1000\Omega$, 12000 melanoma cells were added.

Results

E-Cadherin expression correlated with high phospho-JNK1/2 and low phospho-p38 levels in our cell lines (Figure 1). Knock down of JNK1/2 downregulated E-Cadherin mRNA levels to almost zero. In contrast, GLI2, a transcriptional repressor for E-cadherin, was upregulated. Furthermore, GLI2 knock down in JNK1/2 knock down cells prevented this effect.

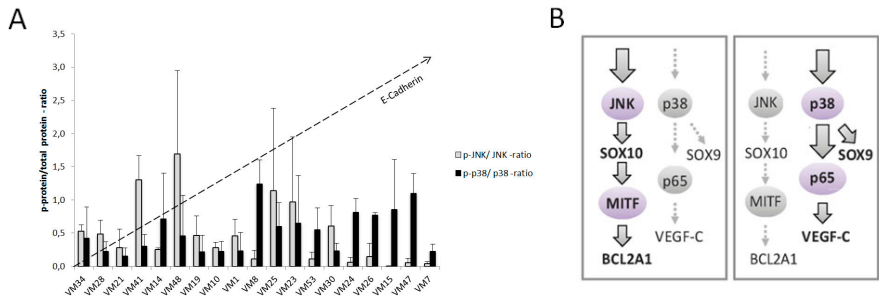


Figure 1. A Phospho/total protein ratios for JNK and p38 in melanoma cell lines, data obtained by western blot quantification, cells are ranked according to levels of E-Cadherin expression; B Regulatory pathways of JNK and p38 in human melanoma [5].

We next tested the invasive potential of JNK1/2 knock down cells compared to control cells. In the gap formation assay JNK1/2 knock down cells produced a significantly larger gap area in the monolayer when compared to control. Moreover, the cells transfected with shRNA for JNK1/2 disrupted the barrier function of the endothelial monolayer more efficiently. Importantly, JNK1/2 knock down leads to an upregulation of p38 signaling. We therefore used a p38 inhibitor or a MK2 (downstream target of p38 α) inhibitor in order to produce the opposite effect – an upregulation of E-Cadherin. Spheroids of cells treated with a p38 or MK2 inhibitor reduced the gap formation in the endothelial monolayer compared to DMSO treated cells and induced downregulation of Hsp27. In contrast, the control cells treated with DMSO were more potent to decrease the transendothelial resistance compared to the cells treated with a MK2 inhibitor. Similar results were obtained for the inhibition of p38. Hence, melanoma cells with an active p38/MK2 signaling induced vascular barrier disruption and endothelial retraction in vitro and were able to seed to lungs after tail vein injection into SCID mice.

Discussion

We show that the inhibition of the p38/MK2 signaling cascade reduces the metastatic potential of melanoma cells. In our previous study, we already showed that the angiogenesis promoting factor VEGF-C is dependent on p38 signaling. Additionally, inhibition of the p38 down-stream target MK2 decreases expression of Hsp27. Hsp27 is known to be upregulated among various cancer types like breast cancer, endometrial cancer and leukemia. Extracellular Hsp27 has a pro-angiogenic effect due to the ability to bind to receptors stimulating the VEGF transcription. Intracellular Hsp27 interacts with microtubule protein actin that is essential for cell movement and therefore also contributes to metastasis. In breast cancer it is associated with invasiveness and the resistance to chemotherapy [6].

A rate limiting step for metastasis is the endothelial transmigration of tumor cells. We simulated this step using three independent assays (gap formation, resistance assay, in vivo). We show that p38 high cells induce changes in endothelial cells concerning cytoskeletal remodeling, cell contact disruption and increased permeability due to growth factors and cytokines secreted by tumor cells. Gap formation can be dependent on soluble or cellular factors. In case of our melanoma spheroids,

the endothelial gap formation is restricted to contact areas directly below tumor spheroids suggesting cellular factors being responsible. Using RGD sequences could revert the gap formation and therefore confirmed this suggestion.

Conclusions

P38 activation leads to an invasive phenotype, hence to high levels of VEGF-C and therefore contributes to lymphangiogenesis. Blocking the p38/MK2 pathway may serve as an adjuvant treatment option to prevent vascular dissemination of melanoma.

Summary

Melanoma cells signaling through p38/MK2 are characterized by a loss of E-cadherin/CDH1 expression, by the expression of proliferative/invasive gene signatures and display vascular invasion. Blocking p38/MK2 redirects signaling to JNK, re-induces CDH1 expression and prevents vascular invasion.

References

1. Paluncic J, Kovacevic Z, Jansson P.J et al.: Roads to melanoma: Key pathways and emerging players in melanoma progression and oncogenic signaling. *Biochim Biophys Acta* 2016; 1863, 770-784.
2. Peinado H, Olmeda D, Cano A: Snail, Zeb and bHLH factors in tumour progression: an alliance against the epithelial phenotype?. *Nat Rev Cancer* 2007; 7, 415-428.
3. Yang J, Weinberg RA: Epithelial-mesenchymal transition: at the crossroads of development and tumor metastasis. *Dev Cell* 2008; 14, 818-829.
4. Singh S, Zafar A, Khan S et al.: Towards therapeutic advances in melanoma management: An overview. *Life Sci* 2017; 174, 50-58.
5. Puujalka E, Heinz M, Hoesel B et al.: Opposing roles of JNK and p38 in lymphangiogenesis in melanoma. *J Invest Dermatol.* 2016; 136, 967-977.
6. Singh MK, Sharma B, Tiwari PK: The small heat shock protein Hsp27: Present understanding and future prospects. *J Therm Biol* 2017; 69, 149-154.

A MECHANISTIC ROLE FOR CXCR2-MEDIATED CELLULAR SENESENCE IN DIABETIC WOUND REPAIR

Holly N. Wilkinson

Centre for Atherothrombosis and Metabolic Disease, Hull York Medical School,
The University of Hull, United Kingdom.

Co-authors: Christopher Clowes, Kayleigh L. Banyard,
Paolo Matteuci and Kimberly Mace.

Tutor: Matthew J. Hardman

Introduction

Non-healing “chronic” wounds, which primarily affect the elderly and diabetic, are a major area of unmet clinical need, causing a huge financial and societal burden (1). One potential contributor to the recalcitrant nature of chronic wounds is cellular senescence, defined as a stable, yet irreversible, loss of cellular proliferation (2). Senescence is a dynamic autonomous stress response, integral to long-term tumour suppression (3). However, senescent cells are widely thought of as a negative outcome of advanced cellular age as they are ineffectively cleared from the ageing body, accumulate, and drive age-related disease. The latter occurs because non-dividing senescent cells remain metabolically active, secreting pro-inflammatory cytokines, growth factors and proteases (termed the senescence-associated secretory phenotype; SASP). The SASP actively alters the tissue microenvironment and drives inflammation (4). Macrophages (Mφs) are a crucial cell type in the inflammatory phase of wound healing. Intriguingly, many SASP components are pro-inflammatory cytokines, also expressed by Mφs (5). Hence, it is unsurprising that transient induction of a senescent phenotype may promote regeneration in both liver and skin, partly through SASP regulation (6 and 7). Despite current knowledge of senescent cell regulation in wound repair, the role of senescence in pathological skin wound healing remains unknown.

Aims

The primary aim of this study was to determine the mechanistic link between cellular senescence and diabetic wound healing. A secondary aim was to explore the therapeutic potential of manipulating cellular senescence to promote healing in a clinically meaningful human *ex vivo* wound model.

Methods

Animal Experiments. Wild-type (WT; C57Bl/6), NDb (Lepr^{+/+}) and Db (Lepr^{-/-}) mice were wounded at 8-10 weeks, while “aged” WT mice were wounded at 80-90 weeks. Wounds were collected at 7 days post-injury (n=5 mice per group). **SA-βGAL Staining.** OCT-embedded skin and wounds were sectioned and stained for SA-βGAL positive (senescent) cells. **RT-qPCR.** RNA was isolated from cells and tissue using phenol-chloroform, reverse transcribed and amplified using Takyon mastermix. **Macrophage Experiments.** Mouse bone marrow mononuclear phagocytes were differentiated into macrophages (Mφs) using L929 cell conditioned media (CM). Mφs were

polarised to M1 (LPS and IFN- γ) and M2 (anti-IFN- γ and IL-4) states and also profiled for senescence via SA- β GAL and RT-qPCR. Antibody arrays (R&D systems) were performed on M ϕ CM. SASP Experiments. CM from NDb and Db M ϕ s was added to human skin fibroblasts *in vitro*, which were screened for senescence markers via RT-qPCR. Human *in vitro* Wounding. Human keratinocytes were scratched in a monolayer and treated for 24 hours before being stained with crystal violet. Human *ex vivo* Wounding. Skin wounds (2mm) were created in the centre of skin 6mm biopsies and cultured *ex vivo* for 3 days, with topical treatments applied daily. Wound healing was assessed via keratin 14 staining. Statistical Analysis. Independent *t* tests, one-way ANOVA and two-way ANOVA was performed with *post-hoc* analysis where appropriate.

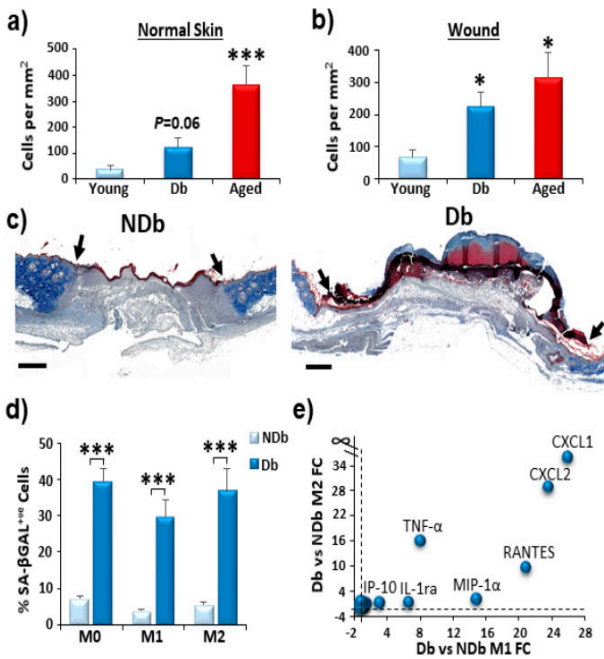


Figure 1. Heightened senescence is observed in diabetic wounds, while diabetic macrophages produce a CXCL1/2-enriched SASP. SA- β GAL staining in normal skin (a) and wounds (b). NDb (non-diabetic) and Db wound histology (Masson's Trichrome staining, c, bar = 500 μ m). SA- β GAL staining in NDb and Db macrophages (M ϕ s; d) and cytokine array showing increased CXCL1 and CXCL2 in Db M ϕ conditioned media (e). ∞ = KC not expressed in the NDb M2 condition. Mean +/- SEM. * = *P*<0.05, *** = *P*<0.001. n=5 per group.

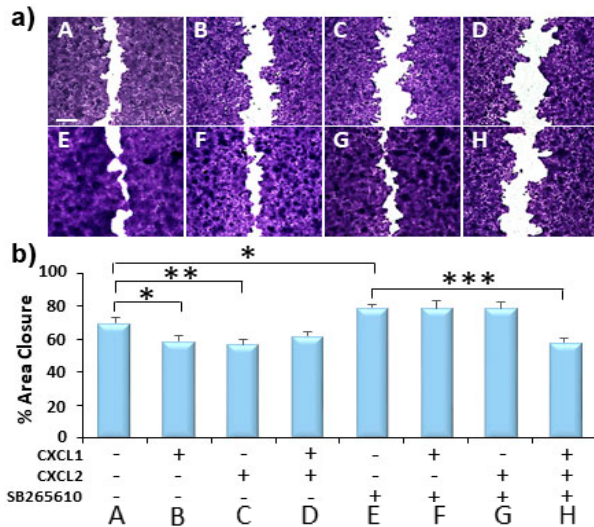


Figure 2. Blockade of CXCR2 signalling promotes human keratinocyte migration *in vitro*. Human epidermal keratinocytes were treated with CXCL1, CXCL2 and SB265610 (a CXCR2 antagonist) alone or in combination. Scratch migration assays were collected after 24 hours. Representative crystal violet-stained images (a, bar = 250 μ m) and quantification (b). Mean \pm SEM. * = $P < 0.05$, ** = $P < 0.01$, *** = $P < 0.001$. Three independent experiments.

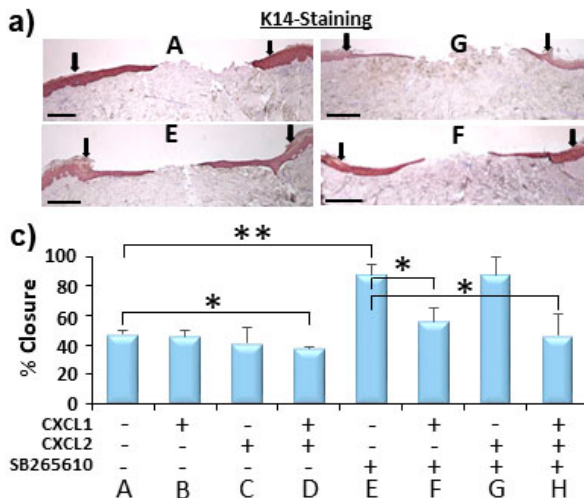


Figure 3. Dampening CXCR2 signalling promotes human *ex vivo* wound healing. Human *ex vivo* wounds were treated with the ligands, CXCL1 or CXCL2, or the compound, SB265610 (a CXCR2 antagonist) alone or in combination. Wounds were collected 3 days post-injury and wound healing assessed via keratin 14 (K14) staining. Representative images (a, bar = 200 μ m, wound edges depicted by arrows) and quantification (b). Mean \pm SEM. * = $P < 0.05$, ** = $P < 0.01$. n = 3 donors.

Results

SA- β GAL staining revealed increased numbers of senescent cells in aged skin ($P<0.001$), and increased senescent cells in aged and diabetic wounds ($P<0.05$, compared to young; **Figure 1a-b**). M ϕ s were next isolated from the bone marrow of NDb (normal healing) and Db (non-healing) mice (**Figure 1c**, arrows depict wound edges). Here, Db M ϕ s were highly senescent in M0 (non-polarised), M1 and M2 states ($P<0.001$, **Figure 1d**) and produced a CXCL1/2-enriched SASP (**Figure 1e**). The cytokines, CXCL1 and CXCL2, share a common receptor, CXCR2 (**8**). The effect of blocking CXCR2 signalling was next determined in human wound repair models. During *in vitro* human keratinocyte scratch closure, CXCR2 blockade (CXCR2 antagonist, SB265610) accelerated migration ($P<0.05$), while treatment with CXCL1 ($P<0.05$) and CXCL2 ($P<0.01$) alone led to a significant delay in epidermal migration (**Figure 2**). Finally, treatment of *ex vivo* human skin wounds with SB265610 significantly increased epidermal wound closure ($P<0.01$), while combined CXCL1/CXCL2 treatment delayed epidermal wound closure ($P<0.05$; **Figure 3**).

Discussion

Our novel findings provide important new insight into the importance of cellular senescence in diabetic wound healing. Particularly, diabetic M ϕ s, which are functionally impaired during wound healing (**9**), exhibit increased senescence and produce a SASP-rich secretome. Importantly, the most highly expressed SASP factors, CXCL1 and CXCL2, signal through a common receptor, CXCR2. CXCR2 signalling is known to promote senescence *in vitro* (**8**), and blockade of CXCR2 in our human wound models accelerated healing. Collectively, these and other data (not shown) strongly suggest CXCR2-mediated senescence to be an important mechanistic player in diabetic pathological wound repair.

Conclusions

These data imply a hitherto unappreciated role for CXCR2 in mediating cellular senescence in pathological wound repair. Our data suggest that excessive CXCL2 may directly contribute to the diabetic wound healing phenotype, with CXCR2 antagonism promoting wound closure. Collectively, our findings provide a basis for the development of new chronic wound therapies targeting cellular senescence to promote wound closure.

Summary

Here we explored the role of senescence in pathological diabetic murine wound healing and demonstrated, for the first time, a significantly increased level of senescence in diabetic murine wounds. We find that diabetic macrophages produce a CXCR2-enriched SASP, while blockade of CXCR2 signalling is able to accelerate *ex vivo* human skin wound healing. Together, these data suggest a new mechanistic, and functionally important, role for CXCR2 in mediating cellular senescence in diabetic wound repair.

References

1. Wilkinson HN, McBain AJ, Stephenson C, Hardman MJ.: Comparing the effectiveness of polymer debriding devices using a porcine wound biofilm model. *Adv Wound Care* 2016; 5(11), 475-485.
2. Harding KG, Moore K, Phillips TJ.: Wound chronicity and fibroblast senescence—implications for treatment. *Int Wound J* 2005; 2, 364-368.
3. Campisi J, di Fagagna FdA.: Cellular senescence: when bad things happen to good cells. *Nat Rev Mol Cell Biol* 2007; 8, 729.
4. Freund A, Orjalo AV, Desprez PY, Campisi J.: Inflammatory networks during cellular senescence: causes and consequences. *Trends Mol Med* 2010; 16, 238-246.
5. Sagiv A, Krizhanovsky V.: Immunosurveillance of senescent cells: the bright side of the senescence program. *Biogerontology* 2013; 14, 17-628.
6. Krizhanovsky V, Yon M, Dickins RA, Hearn S, Simon J, Miething C, et al.: Senescence of activated stellate cells limits liver fibrosis. *Cell* 2008; 134, 657-667.
7. Demaria M, Ohtani N, Youssef, SA, Rodier F, Toussaint W, Mitchell JR, et al. : An essential role for senescent cells in optimal wound healing through secretion of PDGF-AA. *Dev Cell* 2014; 31, 722-733.
8. Acosta JC, O'Loghlen A, Banito A, Gujjarro MV, Augert A, Raguz S, et al.: Chemokine signaling via the CXCR2 receptor reinforces senescence. *Cell* 2008; 133, 1006-1018.
9. Bannon P, Wood S, Restivo T, Campbell L, Hardman MJ, Mace KA.: Diabetes induces stable intrinsic changes to myeloid cells that contribute to chronic inflammation during wound healing in mice. *Dis Mod Mech* 2013; 6, 1434-1447.

INDEX

ANTUNES Isabel	14
BABIĆ PERHOČ Ana	19
BALDWIN Lydia	23
BOUDRIOT Elisabeth	27
BRANCO Paulo	31
CESNEKOVÁ Dana	35
FULOVÁ Miriam	39
JANOVIČOVÁ Lubica	43
KAKHNIASHVILI Tamar	47
KÁNTÁS Boglárka	51
KÁNTOCH Anna	54
KOUCKÝ Vladimír	57
KOVÁCS Ákos László	61
NADAREISHVILI Ilia	66
NOVÁ Zuzana	70
OBERMAYER Georg	73
PÁLEK Richard	76
PRAŠNICKÁ Alena	80
REJLOVÁ Kateřina	81
RICKETT Natasha	84
RIEDEL Kristin	87
ROSENDORF Jáchym	91
SKOŘEPA Pavel	94
STOJKOVÁ Pavla	96
ŠILHÁN David	100
ŠKROTT Zdeněk	104
ŠTARK Tibor	108
ÜBACHS Jorne	114
van der KROFT Gregory	116
WENZINA Judith	118
WILKINSON Holly	121

Vydala: Univerzita Karlova, Lékařská fakulta v Hradci Králové
Miroslav Červinka
Sazba: TAH reklamní agentura, s.r.o., Hradec Králové

2018



ISBN 978-80-906595-7-5